2002

Aspects of age, growth, demographics and thermal biology of two lamniform shark species

Kenneth J. Goldman
College of William and Mary - Virginia Institute of Marine Science

Follow this and additional works at: https://scholarworks.wm.edu/etd

Part of the Ecology and Evolutionary Biology Commons, and the Zoology Commons

ASPECTS OF AGE, GROWTH, DEMOGRAPHICS AND THERMAL BIOLOGY

OF TWO LAMNIFORM SHARK SPECIES

By:

Kenneth J. Goldman

August 2002

APPROVAL SHEET

This dissertation is submitted in partial fulfillment of

the requirements for the degree of

Doctor of Philosophy

Kenneth James Goldman

Approved, August 2002

John A. Musick, Ph.D.
Committee Chairman/Advisor

John M. Hoenig, Ph.D.

David Evans, Ph.D.

Enric Cortes, Ph.D.
National Marine Fisheries Service
Panama City, Florida

Steven Branstetter, Ph.D.
National Marine Fisheries Service
St. Petersburg, Florida

ii

Dedicated to my mother, Shirlee Goldman, for standing by me for all of these years, and to the life and memory of my father, Philip Goldman: compassionate human being and dedicated father.

iii

TABLE OF CONTENTS

iv

ACKNOWLEDGEMENTS

LIST OF TABLES

CHAPTER 3

CHAPTER 4

CHAPTER 5

CHAPTER 6

LIST OF FIGURES

CHAPTER 2

CHAPTER 3

CHAPTER 4

CHAPTER 5

CHAPTER 6

ABSTRACT

The Order Lamniformes consists of seven families and 15 species. This remarkably varied morphological and ecological group of sharks includes filter feeders, deep-waters species, open-ocean and coastal species, as well as eight endothermic species.

Age and growth rates for salmon sharks (*Lamna ditropis*) in the eastern North Pacific (ENP) were estimated from seasonally formed bands in the vertebrae, and compared to previously published life history parameters for this species from the western North Pacific (WNP). von Bertalanffy growth parameter estimates from back-calculated length-at-age data were: $L_\infty = 210.0$ cm PCL, $k = 0.17$ yr^{-1}, and $t_0 = -2.1$ years for females, and $L_\infty = 183.9$ cm PCL, $k = 0.20$ yr^{-1}, and $t_0 = -2.3$ years for males. Results from this study show that salmon sharks in the ENP achieve their maximum length at a faster rate, reach sexual maturity at an earlier age and achieve a greater weight-at-length than those in the WNP. Additionally, salmon sharks are known to be endothermic. This dissertation shows that adult salmon sharks maintain a specific body temperature independent of changes in ambient temperature through a combination of physical and physiological means, and essentially function as homeotherms.

Due to uncertainty in previous life history parameter estimates for sand tiger sharks (*Carcharias taurus*) in the western North Atlantic, age and growth rates were re-estimated based on seasonally formed bands in the vertebrae using a larger sample size. Additionally, captive individuals were injected with oxytetracycline (OTC), a fluorescent skeletal marker annually over a three-year period. The results support a hypothesis that this species forms one pair of growth bands annually in the vertebral centra, whereas previous growth rate estimates were based on the formation of two bands per year. von Bertalanffy growth parameter estimates from back-calculated length-at-age data were: $L_\infty = 308.3$ cm TL, $k = 0.09$ yr^{-1}, and $t_0 = -4.8$ years for females, and $L_\infty = 247.5$ cm TL, $k = 0.13$ yr^{-1}, and $t_0 = -4.2$ years for males. The growth rate of this species is shown to be considerably slower than previously predicted meaning the population is more susceptible to fishing mortality.

Demographic analyses were conducted for salmon sharks in the ENP and WNP, and for sand tiger sharks with uncertainty in vital rates incorporated via Monte Carlo simulation. Density-dependent compensation was included in models where fishing mortality was imposed by increasing sub-adult survivorship from output values generated by a previously published "Intrinsic Rebound Potential" model. The results indicate that both species are extremely vulnerable to fishing mortality and that no fishery should be implemented for sand tiger sharks or salmon sharks in the WNP. Salmon sharks in the ENP were the only population examined that indicated the potential to tolerate any fishing mortality.

A comparison of growth completion rates and other life history parameters of ectothermic and endothermic sharks did not indicate that endothermic sharks achieve their maximum length at a faster rate than ectothermic sharks. Endothermy may, instead, have played an evolutionary role in maintaining growth completion rates as these species moved into new niches in temperate and boreal seas as global circulation developed during the past 60 million years.

ASPECTS OF AGE, GROWTH, DEMOGRAPHICS AND THERMAL BIOLOGY

OF TWO LAMNIFORM SHARK SPECIES

GENERAL INTRODUCTION

The Order Lamniformes

The Order Lamniformes consists of seven families and 15 species (Compagno 2001). This remarkably varied morphological and ecological group of sharks includes filter feeders (*Cetorhinus maximum* and *Megachasma pelagios*), deep-waters species (*Odontaspis noronhai* and *Mitsukurina owstoni*), open-ocean (*Isurus paucus* and *Psuedocarcharias kamoharai*) and coastal species (*Carcharias taurus*), as well as high speed predators (*Isurus oxyrinchus*) and the well-known white shark (*Carcharodon carcharias*). While Compagno (1973, 1990) lists a number of tooth and skeletal aspects defining this taxonomic group, many questions regarding the interrelationships of sharks in this group remain unanswered. Additionally, Naylor et al. (1997) posed a new hypothesis on the interrelationships of this group based on DNA sequence data. A group consisting of experts in systematics, meristics, morphology and genetics are currently working to better establish the interrelationships of these species (L.J.V.Compagno and S. Applegate pers. comm.).

Members of the Order Lamniformes have a "typical" shark body form with a fairly large mouth extending well behind the eyes. They possess two dorsal fins without spines and an anal fin. They have five gill slits situated on each side of the head, either with all five completely forward of the pectoral fins or with the last two above the pectoral bases. Their nostrils have no barbels, circumnarial grooves or nasoral grooves. Eyes are laterally or slightly dorsolaterally located on head, and lack lower nictitating

2

eyelids. Members of this group possess a ring type intestinal valve. All lamniform species have aplacental viviparity, with unborn young being oophagous, and adelphophagous in at least one species (Gilmore et al. 1983, Compagno et al. 1989, Gilmore 1993). Males possess testis type termed 'radial' by Pratt (1993) that is seen in no other elasmobranch, except the batoid order Myliobatiformes, and females possess a single functional right ovary anterior to the epigonal organ and connected by a mesovarium to the dorsal abdomen (Gilmore 1993). Additionally, lamniform females appear to be incapable of sperm retention (Pratt 1993). Differential fecundity in lamniform sharks may be representative of their varying life history strategies.

In addition to the characters stated above, eight species in two families (Lamnidae and Alopiidae) of the Order Lamniformes have unique vascular systems, possessing counter-current heat exchangers known as *retia mirabilia*. The evolution of endothermy through this type of vascular system in elasmobranchs is convergent to that of the endothermic tunas (Block et al. 1993, Block and Finnerty 1994, Bernal et al. 2001). Interestingly, if the Naylor et al. (1997) hypothesis that the Alopiidae and Lamnidae do not constitute a monophyletic group is correct, then this feature (*retia* and elevated body temperatures) would also be convergent in these two elasmobranch families. Additionally, the possession of *retia* in mobulid rays (Order Myliobatiformes: Family Mobulidae) indicates that they may have independently evolved this feature as well (Martin pers. comm.). However, the *retial* function in the mobulid rays has not been confirmed as elevated body temperatures have yet to be documented for this group.

Focus and importance of this Dissertation

This dissertation research focuses on aspects of age, growth, demographics and thermal biology in two species of lamniform shark: the salmon shark, *Lamna ditropis* (Family Lamnidae), and the sand tiger shark, *Carcharias taurus* (Family Odontaspididae).

Salmon sharks, *Lamna ditropis*

Over the past 10 years, Alaska state and federal fisheries managers have seen, and taken, an increased interest in salmon sharks. This growing interest is reflected in an increasing annual catch in the sport fishery, and an interest to open commercial fishing. Sharks are currently listed in the Federal Groundfish Management Plans for the Gulf of Alaska (GOA), Bering Sea and Aleutian Islands (BS and AI) as "other species" and are allowed as bycatch. They are included in the commercial bycatch Total Allowable Catch (TAC) for Alaska Federal waters. How much of this bycatch is salmon shark (vs. spiny dogfish, *Squalus acanthias*, and Pacific sleeper shark, *Somniosus pacificus*) is unknown (W. Bechtol pers.comm.). The North Pacific Fishery Management Council (NPFMC) is currently considering closure of commercial fishing for sharks in Federal waters, as the GOA, BS and AI Federal Management Plans do not address directed commercial fishing for sharks in these areas (J. DiCosimo pers.comm). Commercial fishing for sharks in Alaska State waters has been illegal since 1997. Sport fishing regulations in Alaska are two sharks per person per year, with one in possession at any time (one per day). The state extended the sport fishing regulations to include the exclusive economic zone (EEZ, to 200 miles), as the Federal Management Plans do not currently cover sport fishing.

In Chapter 1, life history parameters for salmon sharks in the eastern North Pacific are presented and compared with previously reported life history parameters from the western North Pacific (Tanaka 1980). Age and length of sexual maturity comparisons, and comments on several back-calculation methods, are also made. Chapter 2 presents the first detailed demographic analysis of salmon sharks in both the eastern and western North Pacific, and examines population responses to fishing mortality. Chapter 3 presents the first data ever obtained on salmon shark body temperature from free-swimming individuals, and examines the hypothesis of homeothermy in sharks of the Family Lamnidae proposed by Lowe and Goldman (2001).

Sand tiger sharks, *Carcharias taurus*

The sand tiger shark population in the western North Atlantic has been heavily depleted due to fishing. This has caused them to be placed under legal 'protected' status and to be placed on the endangered species candidate list (Musick et al. 2000). This species is also currently listed as vulnerable by the IUCN in its Red List of Threatened Animals. In Chapter 4, I present a re-examination of the age and growth of this species. Branstetter and Musick (1994) reported von Bertalanffy growth parameters for sand tiger sharks after estimating that bi-annual bands are laid down in the vertebral centra. Having done so, they also stated a caveat about their uncertainty of that estimate. The uncertainty in life history parameters given by Branstetter and Musick (1994) along with the placement of this species on the endangered species candidate list, were the major reason for my re-examination of sand tiger age and growth. A revision of sand tiger shark life history parameters required new demographic analyses to be conducted; this is the focus of Chapter 5 of this dissertation.

The rates of biological functions are affected by temperature (Schmidt-Nielsen 1990). As such, the physiological ecology of any species is instrumental in understanding its environmental niche and may provide clues about species life history parameters such as growth rates and longevity. The fact that one of the species of focus in this dissertation is endothermic and the other ectothermic along with my great interest and fascination with endothermic fishes (Goldman et al. 1996, Goldman 1997, Lowe and Goldman 2001, Anderson and Goldman 2001), prompted me to examine the question: Do endothermic sharks achieve their maximum size at a faster rate than ectothermic sharks of similar size? This question, which has not been examined by anyone to date, is the topic of discussion in Chapter 6.

Overall, this dissertation represents the first examination of age and growth in eastern North Pacific salmon sharks, the first detailed demographic analysis of the species, and the first examination of their physiological ecology. It also provides new life history parameter estimates and revised demographic estimates for the sand tiger shark. The demographic models used in this dissertation represent only the third and fourth times (see Chapters 2 and 5) that uncertainty in estimates of maximum age, age at first reproduction, fecundity and survivorship at age have been incorporated into demographic estimates of elasmobranch fishes. Monte Carlo simulations were used to incorporate this uncertainty into the models. This dissertation also presents a new method for incorporating density-dependent compensation into age structured life table models. Lastly, Chapter 6 provides the first inference as to whether endothermy plays a role in the growth rates of lamniform sharks.

Chapter 1

Growth and maturity of salmon sharks in the eastern and western North Pacific, with comments on back-calculation methods

INTRODUCTION

The salmon shark, *Lamna ditropis*, is a large apex predator inhabiting the coastal

and oceanic waters of the North Pacific Ocean, most commonly ranging from 65°N

latitude to 35°N in the west and to 30°N in the east (Strasburg 1958, Neave and Hanavan

1960, Campagno 1984, Blagaderov 1994, Nagasawa 1998). It occurs individually and in

large aggregations, is found in sea-surface temperatures of 5°C to 18°C, and has a depth

distribution ranging from the surface to at least 150 m (Compagno 1984). The salmon

shark is a highly opportunistic predator, feeding on a wide variety of prey and sharing the

highest trophic level of the food web in boreal and temperate North Pacific waters with

marine mammals and seabirds (Brodeur 1988, Nagasawa 1998). Adult salmon sharks

typically range in size from 200-260 cm total length (TL) and can weigh upwards of 220

kg (Tanaka 1980, JAMARC 1980, Nagasawa 1998). Reported lengths of 300 cm TL and

greater with weights exceeding 450 kg are unsubstantiated.

Salmon sharks are migratory in nature. North-south migrations have been

documented on both sides of the North Pacific with northern movements occurring in

spring and southern movements in autumn (Iino 1939, Kosugi and Tsuchisaki 1950,

Gorbatenko and Cheblukova 1990, Balgaderov 1994, Nakano and Nagasawa 1994,

Hulbert 2001). However, this species is present in boreal waters throughout the year

(Goldman and Human 2002). Very little is known about trans-Pacific movements, but

they are suspected to occur (Nakano and Nagasawa 1996, Goldman and Musick in press).

Sexual segregation is relatively common in sharks, however an extremely large

8

sex ratio difference exists in salmon sharks across the North Pacific basin (Sano 1962, Nagasawa 1998, Goldman and Musick in press). The western North Pacific (WNP) is male dominated while the eastern North Pacific (ENP) is female dominated. Male dominance in the WNP and female dominance in the ENP increase with increasing latitude. Larger sharks range farther north than smaller individuals, and southern catches generally occur in deeper waters (Nagasawa 1998, Goldman and Musick unpub. data).

Shark catches in Alaska waters have been reported to be as high as those from Washington, Oregon and California combined (Camhi 1999), and there is concern over the amount of shark bycatch being taken (S. Gaichas NMFS and pers. comm.). In 1997, state managers closed commercial shark fishing in state waters and imposed conservative sport-fishing limits (1 shark per person per day, 2 per year) that legally encompass federal waters too. Federal managers are currently addressing elasmobranch management issues (Goldman 2001, Goldman and Musick in press).

With the ever-increasing importance of providing accurate, timely life history parameters to foster responsible management efforts, this study had two main objectives. The first was to estimate growth parameters and the age and length at sexual maturity of salmon sharks in the ENP. The second was to compare my results to those previously published on salmon sharks from the WNP to elucidate any existing variability in the life history parameters of this highly sexually segregated population.

MATERIALS AND METHODS

Salmon shark vertebrae were obtained from numerous sources and locations ranging geographically from southern California to Kodiak Island (n=182). The majority of samples came from research cruises in the Gulf of Alaska (GOA) and Prince William

Sound (PWS), by accompanying sport-fishing vessels on salmon shark trips in the GOA

and PWS, and from Alaska Department of Fish and Game (ADF&G) port samplers.

Vertebral samples collected from British Columbia to southern California came from

incidental catches and recently beached animals (see acknowledgements for sources).

Salmon sharks were captured on research cruises using purse seines and hook and

line gear. Precaudal, fork, and total length (PCL, FL, and TL) were measured on a

straight line and recorded along with sex (and clasper length in males). A 20 to 25 cm

section of vertebrae was removed from directly in front of the first dorsal fin (above the

gills) and stored frozen. Samples provided by additional sources included at least one of

the necessary straight-line measurements, date and location of capture or wash-up, and

sex. I use PCL measurements throughout this Chapter to make direct comparisons with

previously published salmon shark data from the WNP. Linear regression equations,

based on my samples, were developed for converting PCL to FL and TL.

Vertebral samples were thawed, cleaned of excess tissue, separated into individual

centra and stored in 70% ethyl alcohol for at least 24 h. Centra were sagittally sectioned

through the focus and then cut again approximately 1.5 mm off-center using an Isomet

rotary diamond saw (Buehler, 41, Lake Bluff, IL). The sections were pressed between 2

pieces of Plexiglas (to prevent warping), air-dried for 24 h under a ventilation hood, and

then mounted onto microscope slides. After drying, sections were polished with wet fine

grit sand paper (320, 400 and 600) to approximately 0.5 mm and air-dried. Sections were

viewed using a binocular dissecting microscope with transmitted light.

A banding pattern was readily distinguishable in sectioned centra, with wide

bands separated by distinct narrow opaque bands. This pattern occurred on both arms of

the corpus calcareum and extended across the intermedialia. Each pair of wide-narrow bands was considered a growth cycle; the narrow bands, hereafter referred to as "rings", were counted (Figure 1.1a). An angle change in the intermedialia and a ring on the corpus calcareum were present approximately 5 to 6 mm from the focus of each centrum and considered to represent a birthmark. The "pre-birth ring" reported by Nagasawa (1998) was present in most specimens just prior to the birthmark, but was not counted nor measured (Figure 1.1a)[1]. A distinct notch was usually present along the inside edge of the corpus calcareum at each ring providing an additional ageing feature, particularly in sections where the cut excluded the radials of the intermedialia (Figure 1.1b).

Two readers independently aged all centra two times in blind, randomized trials. This allowed the calculation of within-reader precision, and between-reader precision twice. When there was a disagreement between readers, a final age determination was made by the two readers viewing the centrum together. Percent agreement (PA=[No. agreed/No. read]•100), and percent agreement plus or minus one year (PA +/- 1 yr) were calculated for length groups of 10 cm to test for precision. Additionally, Chi-square tests of symmetry were conducted using Bowker's, McNemar's, and Evans-Hoenig tests to determine whether differences between and within readers were systematic (biased) or attributable to random error (Hoenig et al. 1995, Evans and Hoenig 1998).

Centrum radius (CR) and distance to each ring were measured to the nearest 0.001 mm as a straight line from the central focus to the outer margin of the corpus calcareum (Figure 1.1a) using a compound video microscope with the Optimus image analysis

---

[1] My ageing protocol was independently developed by my co-reader and I, and later found to be identical to that used for salmon sharks in the WNP (H. Nakano pers. comm.).

Figure 1.1: (a) Sagittal section of a 10 yr old salmon shark's vertebral centrum showing typical banding pattern. CR=centrum radius. (b) Portion of a sagital section from a salmon shark vertebral centrum without intermedialia showing the distinct notching pattern (white arrows) that accompanied the banding pattern used to aid in assessing ages. The 1.0 mm bar applies to both a) and b). PB = prebirth ring, B = birth ring and numbers indicate rings or age.

system (Media Cybernetics 1999). PCL was plotted against CR to determine the proportional relationship between somatic and vertebral growth.

Back-calculation is a method for describing the growth history of each individual sampled, and numerous variations in methodology exist (see Francis 1990 for a thorough review). The relationship between CR and PCL for ENP salmon sharks was investigated to determine the most appropriate method for back-calculating previous length-at-age. This is critical for obtaining accurate life history parameter estimates from the von Bertalanffy growth function. Four different proportions methods were used and compared with my sample length-at-age data. First, I used the standard Dahl-Lea direct proportions method (Carlander 1969):

$$L_i = (L_c/CR_c) \cdot CR_i \qquad (1)$$

where L_i = length at ring 'i', L_c = length at capture, CR_c = centrum radius at capture, and CR_i = centrum radius at ring 'i'. Next, I applied two modified versions of the Dahl-Lea method that use parameter estimates from the specific linear and quadratic fits that described the PCL-CR relationship. The linear-modified Dahl-Lea method (Francis 1990) is:

$$L_i = L_c \cdot [(a+bCR_i)/(a+bCR_c)] \qquad (2)$$

where 'a' and 'b' are the linear fit parameter estimates. The quadratic-modified Dahl-Lea method (Francis 1990) is:

$$L_i = L_c \cdot [(a+bCR_i+cCR_i^2)/(a+bCR_c+cCR_c^2)] \qquad (3)$$

where 'a', 'b', and 'c' are the quadratic fit parameter estimates.

Ricker (1992) applauded Francis' (1990) back-calculation review paper, but like Campana (1990) suggested that the point of origin of proportional back-calculations

should be related to a biologically derived intercept (i.e., length at birth). I, therefore, also applied Campana's (1990) "size-at-birth-modified" Fraser-Lee equation:

$$L_i = L_c + [(CR_i - CR_c) \cdot (L_c - L_{Birth})/(CR_c - CR_{Birth})] \qquad (4)$$

where L_{Birth} = length at birth and CR_{Birth} = centrum radius at birth. (Based on Tanaka (1980), 62.5 cm PCL was used for L_{Birth}.)

A relative marginal increment (RMI) analysis was used to verify the temporal periodicity of ring formation in the vertebrae. This is a standardized marginal increment analysis whereby the margin, or growth area of a centrum from the last narrow growth ring to the centrum edge, is divided by the width of the last fully formed growth increment (Branstetter and Musick 1994). Resulting RMI values were compared to the month of capture. Age-zero animals were not included (as they have no fully formed increments).

The von Bertalanffy growth function was fit to the vertebral age-at-length data for salmon sharks from the ENP with a nonlinear least squares regression algorithm ('nls' in S-Plus, Mathsoft Inc., 2000) to estimate parameters. The von Bertalanffy growth function is:

$$L_t = L_\infty \cdot [1 - exp(-k(t-t_0))] \qquad (5)$$

where L_t = length at age 't', L_∞ = asymptotic or maximum length, k = the growth coefficient, and t_0 = age or time when length theoretically equals zero. Growth parameters were estimated for the sexes separately and combined. Because smaller size classes were not well represented in my female sample and my male sample size was small, lengths at previous ages were back-calculated from centra measurements for both sexes and fitted with the von Bertalanffy growth function. von Bertalanffy growth

parameter estimates were then obtained from mean back-calculated length-at-age, and from a combination of back-calculated lengths-at-age and my sample data. A likelihood ratio test was used to determine whether differences between female and male growth parameters were significant or if a single set of growth parameters better described the data (Kimura 1980, Quinn and Deriso, 1999, Haddon 2001) (SAS Institute Inc. 1999).

The reproductive tracts of 64 female and 14 male salmon sharks were examined to assess their reproductive status. Females ranged in size from 71 to 209 cm PCL, and males ranged from 63 to 187 cm PCL. Clasper lengths were obtained from 12 of the males (from 91 to 187 cm PCL). Reproductive and maturity determinations follow Pratt (1988), Gilmore (1993), Pratt and Tanaka (1994), Hamlett (1999) and Hamlett and Koob (1999).

Median precaudal length-at-maturity (MPCL) was determined by first coding my female (n=64) and male (n=14) maturity data into binary form, with 0=immature and 1=mature. The binary data were fitted with a logistic regression model ('GLM' in S-Plus, Mathsoft Inc. 2000). The median precaudal length-at-maturity was then estimated as: MPCL = - a/b (a = intercept, b = slope). To estimate percent maturity by length for the ENP salmon shark population, the 'a' and 'b' estimates (from the 'GLM' model) were substituted into the equation; percent mature = $100 \cdot [(e^{(a+b \cdot length)})/(1+e^{(a+b \cdot length)})]$, and plotted against PCL. A non-parametric bootstrap (n = 1000 replications) was conducted using S-Plus (Mathsoft Inc. 2000) and 95% confidence limits were obtained from the 2.5th and 97.5th empirical percentiles.

Sperm storage in the oviducal gland has been documented in several shark species (Pratt 1993). Oviducal glands were taken from 6 mature females, ranging in size from

180 to 192 cm PCL, caught in PWS waters in late July and late August to determine the

presence or absence of sperm. Samples were initially fixed in 10% formalin. Samples

were extensively rinsed to remove fixative then stored in 70% ethanol. Cross-sections

along the entire length of each gland were trimmed (Figure 1.2), dehydrated in a graded

series of ethanol, cleared in a limonene-based solvent, infiltrated with paraffin and

embedded in paraffin blocks. Serial sections (5 um) were prepared using a rotary

microtome, mounted onto poly-L-lysine-coated slides, dried, deparaffinized, re-hydrated

and stained using standard Harris hemotoxylin and eosin protocol for examining general

cellular detail (Hinton 1990). Sections were examined for the presence of sperm using a

compound microscope at magnifications ranging from 100x to 1000x.

Weights were obtained from 20 females ranging from 67.1 to 213.4 cm PCL, and

7 males ranging from 69.5 to 187 cm PCL. The power function, $W = a \cdot L^b$, was fitted to

the data (using SigmaPlot, SPSS Inc.), where W = weight (kg) and L = length (cm PCL).

Specimens weighed ranged geographically from southern California to Alaska. A

likelihood ratio test was used to determine whether differences between female and male

weight-length parameters were significant or if a single set of parameters better described

the data (Kimura 1980, Quinn and Deriso 1999, Haddon 2001) (SAS Institute Inc. 1999).

RESULTS

Length Equations

One hundred sixty-six of the 182 salmon sharks in this study were female,

resulting in a F:M sex ratio of 10.4/1. Although females dominated my sample, the

following equations for converting PCL into FL and TL appear to work equally well for

both sexes.

Figure 1.2: Diagram of an oviducal gland showing where cross-section cuts were made

(#'s 1, 2 and 3) for histological examination.

$$FL = 1.0813 \cdot PCL + 6.9137 \qquad (r^2 = 0.99; n = 138)$$

$$TL = 1.1529 \cdot PCL + 15.186 \qquad (r^2 = 0.97; n = 133).$$

ENP Age-Length Composition

The mean age and length composition of ENP salmon sharks was latitude dependent (Table 1.1). Sharks between 0 and 7 yrs old ranging from 62.2 to 153 cm PCL were collected from southern California to southeast Alaska, with smaller individuals found in the southern part of that range. Sharks between 5 and 20 yrs old ranging from 144.8 to 213.4 cm PCL were collected from southeast Alaska up into the Gulf of Alaska, Prince William Sound, and the Bering Sea.

Vertebral Analysis

Percent agreement (PA) among readers was 68.1% for the first set of blind reads and 72.0% for the second set, and the within-reader PA was 79.7% for reader one (the lead author) and 75.3% for reader two. Percent agreement +/- one yr was >95% for all reader comparisons. Agreement between and within reader age assessments was 100% until age 7 or 8, depending on the reader comparison. When grouped by 10 cm length increments, agreement was 100 % for sharks $\leq$ 160 cm PCL, and 100 % +/- 1 yr for sharks $\leq$ 180 cm PCL (Table 1.2). (PA and PA +/- 1 for length groups were the same for both sets of between-reader comparisons – differences occurred above 160 and 180 cm PCL respectively.) The Bowker, McNamara, and Evans-Hoenig Chi-square tests of symmetry gave no indication that differences between and within readers were systematic rather than due to random error (X^2 test, $P > 0.05$ in all cases).

There was a slight curvilinear relationship between centrum radius (CR) and shark PCL (Figure 1.3). A linear regression gave a significant fit to the data (PCL =

Table 1.1: Mean ages and precaudal lengths (PCL) for eastern North Pacific salmon sharks by location. CA = California; seAK = southeast Alaska.

AGE (yrs)	Females CA to seAK	Alaska	Combined	Males CA to seAK	Alaska	Combined
Mean	2	11	10	3	12	9
Range	0 - 5	5 - 20	0 - 20	0 - 7	6 - 17	0 - 17
PCL (cm)						
Mean	103.6	184.7	175.0	113.5	171.9	153.7
Range	62.2 - 153	144.8 - 213.4	62.2 - 213.4	63 - 150.5	155.4 - 187	63 - 187
n	20	146	166	5	11	16

Table 1.2: Percent agreement (PA) and PA +/- one year, from the second set of 'reads', for eastern North Pacific salmon sharks when placed into 10 cm precaudal length (PCL) groups.

PCL (cm)	Total Read	# Agree	# Agree +/- 1	PA	PA +/- 1
60 - 70	5	5	5	100	100
70.1 - 80	2	2	2	100	100
80.1 - 90	0	-	-	-	-
90.1 - 100	4	4	4	100	100
100.1 - 110	1	1	1	100	100
110.1 - 120	5	5	5	100	100
120.1 - 130	3	3	3	100	100
130.1 - 140	1	1	1	100	100
140.1 - 150	6	6	6	100	100
150.1 - 160	9	9	9	100	100
160.1 - 170	11	8	11	72.7	100
170.1 - 180	30	22	30	73.3	100
180.1 - 190	55	38	53	69.1	96.4
190.1 - 200	34	22	32	64.7	94.1
200.1 - 210	12	4	10	33.3	83.3
>210	4	1	3	25.0	75.0
n =	182	131	175	-	-
Percent Agreed	-	-	-	72.0	96.2

Figure 1.3: Relationship between centrum radius and precaudal length for eastern North Pacific salmon sharks showing significant fits given by linear and quadratic equations (sexes combined, n=182). PCL = precaudal length, CR = centrum radius.

Quadratic Fit :
$$PCL = -0.583 \cdot CR^2 + 25.189 \cdot CR - 63.944$$
$$r^2 = 0.94$$

Linear Fit:
$$PCL = 10.553 \cdot CR + 20.964$$
$$r^2 = 0.90$$

Precaudal length (cm)

Centrum radius (mm)

10.553•CR + 20.964; r^2 = 0.90; P < 0.0001); however, a quadratic equation produced a

slightly better fit (PCL = -63.944 + 25.189•CR -0.583•CR^2; r^2 = 0.94; P < 0.0001) and a

t-test showed the third parameter to be statistically significantly different from zero (t =

10.32; df = 181, P <0.0001). However, it was necessary to compare the mean back-

calculated results from equations 1 through 4 with the mean sample PCL data to see if the

slightly better statistical fit of the quadratic equation translated into better biological

accuracy for modeling growth.

The quadratic-modified Dahl-Lea method (equation 3) most accurately

represented the mean sample precaudal length-at-age data. It produced mean back-

calculated lengths-at-age within 4.2 cm of mean sample lengths-at-age for female salmon

sharks >120 cm PCL and within 8.8 cm for females <120 cm PCL (Figure 1.4a). When

applied to males, equation 3 produced mean back-calculated lengths-at-age within 10 cm

of mean sample lengths-at-age for sharks <120 cm PCL and >150 cm PCL. In between

those lengths, however, the deviation from mean sample length-at-age increased to 16.5

cm (Figure 1.4b). (The larger deviations for males are likely the result of small sample

size.) Lee's phenomenon did not occur in either sex using the quadratic-modified Dahl-

Lea method (Tables 1.3 and 1.4).

Vertebral age-at-length data from 166 female salmon sharks provided von

Bertalanffy parameters of L∞ = 207.4 cm PCL, k = 0.17 yr^{-1}, and t₀ = -2.3 years (Figure

1.5). When the von Bertalanffy growth function was fit to the quadratic-modified Dahl-

Lea back-calculations for females, the life history parameters were similar to those

produced from the sample length data (Table 1.5). Vertebral age data from 16 males

Figure 1.4: Mean deviation, from mean sampled precaudal length, of four proportional

back-calculation methods for (**a**) female, and for (**b**) male eastern North Pacific salmon

sharks. Data points represent mean back-calculated lengths-at-age. A point on the x-axis

would represent zero deviation from the sample mean length-at-age.

a

Deviation from sample mean (cm) — y-axis (30, 25, 20, 15, 10, 5, 0, -5, -10, -15, -20, -25, -30)

Legend:
- ○ Dahl-Lea
- □ Dahl-Lea linear-modified
- ● Dahl-Lea quadratic-modified
- ◇ Fraser-Lee -modified

Sample mean precaudal length-at-age (cm) — x-axis (60, 70, 80, 90, 100, 110, 120, 130, 140, 150, 160, 170, 180, 190, 200, 210, 220)

b

Deviation from sample mean (cm) — y-axis (30, 25, 20, 15, 10, 5, 0, -5, -10, -15, -20, -25, -30)

Legend:
- ○ Dahl-Lea
- □ Dahl-Lea linear-modified
- ● Dahl-Lea quadradtic-modified
- ◇ Fraser-Lee birth-modified

Sample mean precaudal length-at-age (cm) — x-axis (60, 80, 100, 120, 140, 160, 180)

Table 1.3: Back-calculated precaudal length-at-age of eastern North Pacific female salmon sharks. B = birth, n = sample size.

Sample mean is the mean length of sharks captured at a given age. All lengths are in cm.

Back-calculated age

Age	n	B	1	2	3	4	5	6	7	8	9	10	11	12	13	14	15	16	17	18	19	20
0	5	59.6																				
1	5	61.9	85.1																			
2	3	59.8	82.6	101.9																		
3	3	61.3	84.5	104.1	118.6																	
4	2	58.5	83.7	102.3	117.9	130.6																
5	3	58.8	82.3	101.4	118.8	132.4	142.4															
6	5	62.1	85.5	107.1	123.7	137.9	147.2	155.2														
7	7	61.3	85.4	106.2	122.5	135.6	146.3	154.0	161.1													
8	12	61.7	88.3	108.7	126.4	140.4	151.9	161.1	167.9	173.4												
9	22	60.0	85.9	107.2	123.2	137.2	149.2	158.7	166.7	172.6	176.8											
10	26	60.9	90.0	109.8	125.7	139.3	150.5	159.7	167.2	173.7	179.5	183.8										
11	16	59.5	86.7	105.5	122.4	136.1	147.7	157.1	164.9	171.8	177.7	182.2	185.7									
12	16	60.1	85.9	104.4	118.3	132.9	144.4	153.5	161.5	168.2	173.8	178.7	182.4	185.6								
13	8	62.2	87.1	104.6	118.6	131.0	142.8	152.1	160.2	167.4	174.4	179.3	183.7	187.0	189.8							
14	11	61.6	87.0	107.6	124.0	136.4	146.8	155.7	163.8	171.0	176.5	180.9	184.5	187.6	190.3	192.2						
15	9	61.3	85.1	103.0	120.1	133.2	144.6	155.2	163.1	170.4	176.1	181.3	185.8	189.1	191.9	194.1	196.0					
16	6	63.5	86.9	104.0	118.5	131.8	143.2	152.5	160.0	167.3	173.7	179.1	182.6	187.5	191.6	194.8	197.5	199.4				
17	5	70.9	94.1	112.7	128.9	140.6	151.9	160.5	167.6	175.2	181.2	187.2	191.8	195.6	198.8	201.9	204.5	206.4	207.7			
18	0	-	-	-	-	-	-	-	-	-	-	-	-	-	-	-	-	-	-	-		
19	0	-	-	-	-	-	-	-	-	-	-	-	-	-	-	-	-	-	-	-	-	
20	2	66.5	81.0	98.7	112.8	129.1	141.9	152.1	160.8	170.0	174.1	179.0	182.9	187.1	191.5	194.5	196.5	198.6	201.0	203.1	204.0	204.9
Back-Calc Mean		61.2	86.9	106.5	122.4	136.2	147.6	156.9	164.6	171.5	176.8	181.6	184.7	187.6	191.9	194.8	198.4	201.9	205.8	203.1	204.0	204.9
Sample Mean		65.9	92.1	115.3	123.3	134	147.3	158.1	164.1	175.7	178.4	185.4	187	186.7	190.8	192.9	196.7	200.2	208.3	-	-	205.1

Table 1.4: Back-calculated precaudal length-at-age of eastern North Pacific male salmon sharks (n = 16). B = birth, PCL = precaudal length (cm). Sample mean is the mean (or individual) length of sharks captured at a given age.

Age	PCL	B	Back-calculated age																	
			1	2	3	4	5	6	7	8	9	10	11	12	13	14	15	16	17
0	63.0	57.4																	
1	91.0	63.6	88.8																
3	118.0	61.6	78.9	98.3	109.5														
4	145.0	63.8	82.1	101.6	123.0	137.4													
6	157.0	52.7	78.4	101.5	123.6	138.0	147.9	154.2											
6	155.4	62.9	92.8	110.5	128.5	140.9	149.5	153.1											
7	150.5	62.2	83.1	101.4	115.5	129.4	137.4	144.6	148.2										
8	163.0	55.7	70.1	98.1	114.8	127.8	140.4	148.9	155.7	160.1									
11	164.0	58.9	71.7	84.6	95.8	112.1	128.1	138.0	145.1	152.2	157.3	160.5	163.0						
11	167.0	62.5	77.5	100.2	116.8	129.9	134.3	139.0	145.4	152.0	157.0	161.7	165.1						
12	187.0	57.7	88.1	107.5	128.1	140.0	150.8	158.0	165.4	170.2	174.4	178.4	182.1	185.2					
13	176.0	58.0	81.2	96.1	109.4	127.0	140.4	150.2	153.8	157.7	162.8	167.1	170.3	172.8	174.9				
14	177.0	56.2	83.1	100.4	111.8	126.5	141.8	147.8	151.8	155.8	158.9	162.7	166.7	169.7	172.9	175.6			
16	176.0	57.5	81.5	94.0	105.8	118.4	129.2	138.8	145.5	149.8	153.4	156.2	159.6	163.3	166.8	169.8	172.4	174.9	
16	182.0	61.9	82.5	98.6	110.0	121.9	131.1	140.0	148.2	153.5	159.9	163.7	166.8	170.3	173.9	176.3	178.3	180.7	
17	187.0	61.1	75.5	97.5	110.7	121.0	132.8	146.4	155.1	162.6	165.9	169.2	173.6	177.0	180.6	182.6	184.3	185.8	186.6
Back-Calc Mean		59.6	81.0	99.3	114.5	128.5	138.6	146.6	151.4	157.1	161.0	164.9	168.4	173.1	173.8	176.1	178.4	180.5	186.6
Sample Mean		63.0	91.0	-	118.0	145.0	-	156.2	150.5	163.0	-	-	165.5	187.0	176.0	177.0	-	179.0	187.0

Figure 1.5: von Bertalanffy growth curves fitted to female and male vertebral sample data for eastern North Pacific salmon sharks. Estimates for parameters of the von Bertalanffy growth function are summarized.

Females (o)	Males (x)
$L_\infty = 207.4$	$L_\infty = 182.8$
$k = 0.17$	$k = 0.23$
$t_0 = -2.3$	$t_0 = -1.9$

Table 1.5: von Bertalanffy growth parameters of female, male and sexes combined for salmon sharks in the eastern North Pacific. Numbers in parentheses are standard errors.

Females	L_∞	k	t_0
Sample data (n=166)	207.4 (2.5)	0.17 (0.01)	-2.3 (0.2)
Back-calculations (n=1814*)	205.3 (0.9)	0.18 (0.002)	-2.0 (0.03)
Mean back-calculation (n=21*)	210.0 (1.1)	0.17 (0.004)	-2.1 (0.09)
Back-calculations w/ sample data (n=1980*)	206.0 (0.8)	0.18 (0.002)	-2.0 (0.03)
Males			
Sample data (n=16)	182.8 (3.7)	0.23 (0.03)	-1.9 (0.3)
Back-calculations (n=161*)	183.9 (2.0)	0.20 (0.008)	-2.0 (0.1)
Back-calculations w/ sample data (n=177*)	184.2 (1.9)	0.20 (0.008)	-2.0 (0.1)
Combined			
Sample data (n=182)	204.5 (2.4)	0.18 (0.01)	-2.2 (0.2)

*Not independent

provided von Bertalanffy parameters of L_∞ = 182.8 cm PCL, k = 0.23 yr^{-1}, and t_0 = -1.9

years (Figure 1.5). Back-calculated lengths-at-age for male salmon sharks, either with or

without sample data included, provided slightly lower k coefficients (= 0.20), but similar

L_∞ and t_0 parameters (Table 1.5). Vertebral age data for the sexes combined (n=182)

provided von Bertalanffy parameters of L_∞ = 204.5 cm PCL, k = 0.18 yr^{-1}, and t_0 = -2.2

years. A likelihood ratio test showed that separate von Bertalanffy growth models better

describe the data for each sex than one model with the sexes combined (X^2 = 29.1; df = 3;

P <0.001).

Relative marginal increment (RMI) analysis showed that postnatal rings form

annually between January and March. The smallest relative margins occurred in

February and March, followed by a consistent increase in RMI with the largest relative

margins occurring in December and January (Figure 1.6).

I assessed the reproductive status of 64 female salmon sharks and found 55 of

them to be fully mature. Out of the 14 males examined, 11 were mature. Mature female

reproductive tracts consisted of a well-developed right ovary (the only functional ovary in

lamniform sharks) with various sized ova, large oviducts and oviducal glands, and

expanded, heavily striated uteri with thickened walls. By contrast, the right ovary from

immature female reproductive tracts was small and had no signs of developing ova, the

oviducal gland was virtually indistinguishable from the oviduct, and the uteri were

extremely small, thin-walled, flaccid and completely smooth. Additionally, the epigonal

organ in mature females was large and extended ⅔ the length of the uteri, whereas in

immature females it was small and generally did not extend much past the anterior end of

Figure 1.6: Results of relative marginal increment analysis showing annuli formation occurs between January and March.

the uteri. No females examined were of an 'intermediate' nature. Mature male

reproductive tracts consisted of large well-developed testes, a thick epididymis leading to

a coiled ductus deferens, rigid (fully calcified) claspers and well-developed siphon sacs.

Immature male reproductive tracts consisted of small testes that were partially embedded

in the epigonal organ, thin epididymis and straight ductus deferens, non-rigid claspers

and poorly developed siphon sacs.

Median precaudal length-at-maturity (MPCL) for ENP female and male salmon

sharks were 164.7 cm PCL and 124.0 cm PCL respectively (Figure 1.7). The smallest

mature female observed was 164.0 cm PCL, and the largest immature female observed

was 176.5 cm PCL (however, all other immature females were $\leq$ 163 cm PCL). None of

the oviducal glands sampled from mature females contained spermatozoa. The smallest

mature male observed was 155.4 cm PCL, and the largest immature male was 91.0 cm

PCL. Based on age estimates from vertebral sample data, ages at MPCL ranges from 6 to

9 yrs for females and from 3 to 5 yrs for males. Ninety-five percent confidence limits

(for percent mature) were very narrow for females < 155 cm PCL and >172.5 cm PCL

and for males < 107.5 cm PCL and > 132.5 cm PCL. The wide vertical confidence

intervals around my calculated estimates of MPCL (Figure 1.7) are caused by not having

many observations for lengths around the estimated MPCL in the sample.

Weight-length relationships for female and male salmon sharks I sampled in the

ENP were $W = 8.2 \times 10^{-05} \cdot L^{2.759}$ ($r^2 = 0.99$) and $W = 3.2 \times 10^{-06} \cdot L^{3.383}$ ($r^2 = 0.99$)

respectively, and $4.4 \times 10^{-05} \cdot L^{2.875}$ ($r^2 = 0.99$) for the sexes combined (Figure 1.8). A

likelihood ratio test showed that separate equations for each sex better describe the data

than a single equation for the sexes combined ($X^2 = 12.1$; $df = 3$; $P < 0.01$).

Figure 1.7: Percent mature vs. precaudal length curves for eastern North Pacific female

(heavy lines) and male (light lines) salmon sharks, with 95 % confidence bands on

percent mature. Diamond and circle show estimates of median precaudal length at

maturity (MPCL) for females and males respectively. Confidence bands are 2.5th and

97.5th empirical percentiles obtained by bootstrapping.

Figure 1.8: Weight-to-precaudal length relationship for eastern North Pacific salmon

sharks. W = weight (kg); PCL = precaudal length (cm).

Males (triangles):
$$W = 3.2 \times 10^{-6} \cdot PCL^{3.383}; \; r^2 = 0.99$$

Females (open circles):
$$W = 8.2 \times 10^{-05} \cdot PCL^{2.759}; \; r^2 = 0.99$$

Sexes Combined w/ 95% CL
$$W = 4.4 \times 10^{-05} \cdot PCL^{2.875}; \; r^2 = 0.99$$

Weight (kg) (y-axis: 0, 20, 40, 60, 80, 100, 120, 140, 160, 180, 200, 220, 240)

Precaudal length (cm) (x-axis: 60, 80, 100, 120, 140, 160, 180, 200, 220)

DISCUSSION

A high degree of variability exists in the periodicity of ring and growth band formation within and among taxonomic groups of elasmobranch fishes, and much of the variation observed in several lamniform sharks has not yet been explained (Branstetter 1990, Branstetter and Musick 1994, Wintner and Cliff 1999). For example, Cailliet et al. (1983) stated that shortfin mako sharks from the Pacific appear to have annual ring formation while Pratt and Casey (1983) stated that Atlantic specimens appeared to produce two rings per year. However, a new technique using bomb radiocarbon to validate ages in long-lived sharks was applied to a single shortfin mako and indicated that they form a single ring annually (Campana et al. 2002).

Tanaka (1980) and Nagasawa (1998) state that salmon sharks produce one ring per year, but a RMI analysis does not appear to have been conducted. The RMI analysis verifies an annual periodicity of banding patterns for salmon sharks ranging from 73 cm to 213.4 cm PCL encompassing ages 1 to 20 for females and ages 1 to 17 for males. The major period of growth occurs from May through November, slowing some as January approaches (Figure 1.6). A brief cessation, or extreme slowing, of growth (ring formation) occurs between January and March, with growth increasing again in April-May. While we were able to examine specimens from every month of the year, additional samples from December through April would enhance RMI precision.

Vertebral growth significantly increased with somatic growth (Figure 1.3) which, along with the reliability of the RMI analysis (Figure 1.6), demonstrates vertebral growth patterns are a reliable indicator of age in salmon sharks. Precision was high between and within readers with limited differences (Table 1.2) that were attributable to random error.

These results provided a high degree of confidence in the accuracy and precision of the age assessments (from sample data) used in the von Bertalanffy growth model, and hence in the resulting life history parameter estimates.

The error associated with back-calculated length vs. the actual length at a given age has been a focal point of papers by Campana (1990), Francis (1990) and Ricker (1992) and prompted my evaluation of several proportional back-calculation methods. There was a statistically valid reason for using the quadratic-modified Dahl-Lea (equation 3) over the linear-modified Dahl-Lea (equation 2) (see results), however, the only way to cross-compare all four back-calculation methods in a biologically meaningful way was to apply all of them to the vertebral sample data. Both modified Dahl-Lea equations were more accurate in representing the mean sample length-at-age data than the standard Dahl-Lea or the size-at-birth-modified Fraser-Lee equations (Figures 1.4a and b). However, the quadratic-modified Dahl-Lea was the best predictor of prior length-at-age. While these back-calculation results are, of course, dependent on the assumption that growth has not significantly changed over time, and are applicable only to salmon sharks, they demonstrate the importance of choosing the appropriate method to minimize error, which results in a greater ability to accurately model growth. Even greater confidence could be had if animals collected in the past were available as this would enable a direct comparison of size-at-age then and now to be made to verify that growth has not changed.

The similar von Bertalanffy growth parameter estimates generated from the female sample data, back-calculated data and the combination of the two indicate that sample size was sufficiently large and encompassed the known size range of the species.

von Bertalanffy parameters for males would be improved with a larger sample size that would be expected to reduce the difference between values of 'k' from sample and back-calculated data (Table 1.5). More samples would probably have little influence on L_∞ and t_0 for either sex since salmon sharks close to maximum size were examined in this study. It is possible that the discrepancy between male and female sample sizes may have influenced the outcome of the likelihood ratio test. However, with the differences in observed maximum length (and L_∞) between the sexes and the small standard errors associated with the male von Bertalanffy estimates (Table 1.5), it is unlikely that an increased male sample size would alter the test result.

My results show that salmon sharks in the ENP attain their maximum size at a faster rate (k) than those from the WNP (Table 1.6). I was unable to test the statistical significance of these differences as neither Tanaka (1980) nor Nagasawa (1998) provided point estimates and standard error values for WNP data. There were, however, significant resultant biological differences present. Both female and male salmon sharks reach first age at sexual maturity upwards of 2 years earlier in the ENP than in the WNP. Female salmon sharks in the WNP mature between 8 and 10 years of age (Tanaka 1980, Nagasawa 1998). Based on reproductive tracts examined, we found that female salmon sharks in the ENP reach sexual maturity between ages 6 and 9. Although age at first maturity was earlier in the ENP, length at maturity appears to be similar; 160-180 cm PCL in the WNP, and a MPCL = 164.7 cm PCL in the ENP (Figure 1.7). Male salmon sharks in the WNP mature at approximately 5 years of age and 140 cm PCL (Tanaka 1980, Nagasawa 1998). From my small sample size, the logistic method enabled me to

Table 1.6: Growth parameters for salmon sharks in the eastern and western North Pacific.

	Eastern North Pacific	Western North Pacific
Females		
L_∞	207.4	203.8
K	0.17	0.14
t_0	-2.3	-3.9
Males		
L_∞	182.8	180.0
K	0.23	0.17
t_0	-1.9	-3.6

estimate that male salmon sharks in the ENP mature between the ages of 3 and 5, and MPCL = 124.0 cm PCL (Figure 1.7). Clasper lengths did not enhance the ability to determine length at sexual maturity in males because males around the calculated MPCL were not sampled. Although the MPCL for males indicates a smaller length at maturity, my confidence in the accuracy of the male MPCL estimate (due to sample size) is low (Figure 1.7).

The lack of spermatozoa in any of the oviducal gland samples analyzed is not surprising considering no lamniform shark examined to date has shown evidence of sperm storage (Pratt 1993). However, specimens I examined were specifically chosen from the time period of late July through late August when mating may be taking place (Goldman and Human 2002). A larger sample size taken through that time period and extending through September might better resolve the question regarding the suspected residence time of sperm in the oviducal gland of lamniform sharks, which is probably only a few days that are timed with actual mating activity (Pratt 1993). The large number of eggs produced to feed oophagous young (Gilmore 1993, Gilmore et al. 1983, Worms 1977) is thought to "flush" any stored sperm out of the oviducal gland (Pratt 1993).

In the WNP, salmon sharks are born in the spring of the year with pups ranging in length from 60 to 70 cm PCL (Tanaka 1980, JAMARC 1980, Nagasawa 1998). Litter size in the WNP is up to 5 pups, with a ratio of male to female of 2.2:1 (Tanaka 1980). My data support a similar timing for pupping and for length at birth in the ENP, but no pregnant females were taken during the course of my research so information on litter size and pup sex ratio is not available for the ENP.

Nagasawa (1998) characterized salmon shark growth through age ten as follows; after birth, "they grow to between 90 and 105 cm PCL by the next spring...subsequent annual growth is 10-15 cm per year up to age-4 fish". He additionally stated that females and males attain an average length of 173 cm PCL and 163 cm PCL, respectively, by age 10. My data indicate that the average growth (cm per year) for salmon sharks in the ENP is very similar to those in the WNP through age 4. By age 5, ENP females are growing at a considerably faster rate than WNP females, reaching an average of 185.4 cm PCL by age 10 (Table 1.7). Male salmon sharks in the ENP appear to begin outgrowing their WNP counterparts by age 4 (Table 1.7). Salmon shark longevity appears to be similar in the ENP and WNP. Maximum observed age for females in my study was 20 vs. 17 in the WNP (Tanaka 1980); however, maximum observed age for males was only 17, vs. 25 for the WNP. My small sample size of male salmon sharks probably prevented me from attaining samples at or near maximum age.

Salmon sharks in the ENP and WNP attain the same maximum length (about 215cm PCL for females and about 190 cm PCL for males). However, WNP salmon sharks take longer to reach a given length than those in the ENP (Table 1.7). Differences also exist between ENP males and females; the weights for the same length animals are considerably different except at male maximum length, which appears to be equivalent to the same size females (Figure 1.8). My data indicate that the weight-at-length differences between ENP and WNP salmon sharks begin at approximately 110 cm PCL for females, and at 140 cm PCL for males (Figure 1.9a and b). While a greater sample size would enhance precision and may alter the equations presented here to some degree, the data

Table 1.7: Mean precaudal length-at-age of salmon sharks in the eastern and western North Pacific. Ranges (or individual lengths for some males) are given for sharks from this study.

| | FEMALES | | | MALES | |
| | WNP* | ENP | ENP | WNP* | ENP |
Age	mean PCL	mean PCL	range	mean	Individual or range
0	62.5	65.9	62.2 - 71.1	62.5	63.0
1	97.5	92.1	73.0 - 105.0	97.5	91.0
2	110.0	115.3	112.0 - 119.0	110.0	-
3	122.5	123.3	118.0 - 128.0	122.5	118.0
4	135.0	134.0	128.0 - 140.0	135.0	145.0
5	141.3	147.3	144.0 - 153.0	139.7	-
6	147.7	158.1	149.7 -164.0	144.3	155.4 - 157.0
7	154.0	164.1	145.9 - 183.0	149.0	150.5
8	160.3	175.7	164.0 - 185.4	153.7	163.0
9	166.7	178.4	164.0 - 192.0	158.3	-
10	173.0	185.4	168.0 - 198.0	163.0	-
11	177.4	187.0	173.0 - 200.0	164.2	164.0 - 176.0
12	181.8	186.7	180.0 - 193.0	165.3	187.0
13	186.2	190.8	159.0 - 213.0	166.5	176.0
14	190.6	192.9	183.0 - 208.0	167.6	177.0
15	195.0	196.7	175.0 - 207.1	168.8	-
16	199.4	200.1	193.0 - 208.3	169.9	176.0 - 182.0
17	203.8	208.3	203.0 - 213.4	171.1	187.0
18	-	-	-	172.2	-
19	-	-	-	173.4	-
20	-	205.1	200.0 - 210.2	174.5	-
21	-	-	-	175.7	-
22	-	-	-	176.8	-
23	-	-	-	178.0	-
24	-	-	-	179.1	-
25	-	-	-	180.3	-

*Mean length-at-age for WNP calculated from information in Nagasawa (1998). Linf was used as mean length at age 17 for females and as mean length at age 25 for males.

Figure 1.9: Comparison of weight-length relationships of eastern and western North

Pacific salmon sharks, **(a)** females, and **(b)** males. (Western North Pacific data from

Tanaka (1980) and Nagasawa (1998).)

a

Weight (kg)

240
220
200
180
160
140
120
100
80
60
40
20
0

Present study

$$W = 8.2 \times 10^{-5} \cdot L^{2.759}$$

$$r^2 = 0.99$$

Tanaka 1980

$$W = 1.04 \times 10^{-4} \cdot L^{2.679}$$

60   80   100   120   140   160   180   200   220   240

Precaudal length (cm)

b

Weight (kg)

180
160
140
120
100
80
60
40
20
0

Present study

$$W = 3.2 \times 10^{-6} \cdot L^{3.383}$$

$$r^2 = 0.99$$

Tanaka 1980

$$W = 1.17 \times 10^{-4} \cdot L^{2.652}$$

60   80   100   120   140   160   180   200

Precaudal length (cm)

show that weight-at-length is particularly greater for adult salmon sharks in the ENP than in the WNP. As with the von Bertalanffy growth models, it is possible that the discrepancy between female and male sample sizes may have influenced the outcome of the likelihood ratio test. However, the sample size discrepancy is not as large and standard errors were small for both sexes, so it is unlikely that an increased male sample size would alter the test result.

While season and size at birth appear to be similar for salmon sharks in the ENP and WNP, the locations where females pup are different. A salmon shark pupping and nursery ground exists along the transitional boundary of the subarctic and central Pacific currents (Nakano and Nagasawa 1996). My data suggest that a second pupping and nursery ground exists, ranging from southeast Alaska to the northern end of Baja California, Mexico, with central California being the most common area for ages zero and one (see Table 1). Ages zero through 5 were only caught between southern California to southeast Alaska, and ages 5 and above were only caught in Alaska waters. The latitudinal size segregation observed in the ENP indicates that pregnant females may move south along the California coast to give birth in the spring.

The high degree of sexual segregation across the Pacific Basin (Nagasawa 1998, Goldman and Musick in press), along with the age and length dependent latitudinal distribution are important factors in pursuing responsible management and conservation of this species. While latitudinal migrations and movements are documented in this species (Iino 1939, Kosugi and Tsuchisaki 1950, Tanaka 1980, Balgaderov 1994, Nakano and Nagasawa 1994, Hulbert 2001), they are still poorly understood. Similarly, while trans-Pacific movements have been inferred from fisheries bycatch data (Goldman and

Musick in press), there has yet to be documentation of individuals moving across the North Pacific. However, the degree of the sexual segregation by itself (in regards to finding a mate) would seem to indicate that movements across the Pacific are likely.

Another critical element for successful management of salmon sharks is stock structure, which is not well understood at this time, however a population genetics study is currently underway. Current information from the western and central North Pacific implies that salmon sharks constitute a single stock, but there is no current information for the Japan Sea or the eastern North Pacific (Sano 1962, Tanaka 1980, Blagaderov 1994, Nagasawa 1998). New technologies such as archival and pop-up satellite transmitters should provide documentation of movements and migrations and key information as to whether regional or international conservation and management plans are needed.

Stock structure may be an important factor in the differential growth rates between ENP and WNP salmon sharks. However, ecological differences between the ENP and WNP could also be responsible for the observed differences. Young salmon sharks appear to move from temperate waters of the U.S. west coast into the Alaska Gyre and the Gulf of Alaska as they approach adulthood, which is when their growth rate begins to exceed that of their WNP counterparts. These waters are extremely productive -- some of the most productive in the world. Food resources and availability may be the key factor in growth rate, age-at-maturity and weight-at-length differences observed between ENP and WNP salmon sharks.

Lamniform sharks possess fairly high growth rates (k) relative to other sharks, particularly for sharks that grow to a large size (Musick 1999). Salmon sharks are among

a small group of lamniform sharks that are endothermic (Smith and Rhodes 1983,

Anderson and Goldman 2001, also see Chapter 3 of this dissertation). This uncommon

physiological trait, combined with the salmon sharks diet that includes many lipid-rich

species, may be an influencing factor in the growth rate of this species. With current

research on mako, white, and thresher shark age and growth, we may soon learn whether

endothermy plays a role in the growth rates of lamniform sharks. Chapter 6 of this

dissertation presents the first written discussion on this topic.

Chapter 2

Demography of salmon sharks in the eastern and western North Pacific

INTRODUCTION

In Chapter 1, I presented the results of my study on salmon shark age and growth

in the eastern North Pacific (ENP) and compared them to previously published life

history parameters in the western North Pacific (WNP) (Tanaka 1980, Nagasawa 1998).

While possessing a moderately fast growth completion rate (k) for an elasmobranch (0.17

yr^{-1} for females, 0.20 yr^{-1} for males), salmon sharks appear to have a very low fecundity

and are relatively slow to mature and, as such, may be extremely vulnerable to fishing

mortality. In addition to the fact that no stock assessments have been conducted on this

species, the differential growth rates between salmon sharks in the ENP and WNP along

with our lack of knowledge of trans-Pacific migrations and stock structure compound

management issues.

The majority of previous demographic analyses on elasmobranch fishes have used

deterministic life-tables (or Leslie matrix models) to calculate intrinsic rates of

population increase and other vital rate parameters to estimate their 'potential' for

exploitation. Incorporating the effect of uncertainty in vital rates into demographic

analyses is a relatively new and extremely useful approach in fisheries ecology, yet so far

only two published studies have incorporated uncertainty or known variation in

elasmobranch vital rates (Cortés 1999, 2002). In a recent paper by Mollet and Cailliet

(2002), comparing the demography of four elasmobranch species using different

modeling approaches, they stated that a "flaw" in their study was the "lack of confidence

bands for our population growth estimates" which can be generated by incorporating

54

uncertainty with Monte Carlo simulation. They strongly recommended that Monte Carlo

"uncertainty analysis" be carried out. This is important because model input parameters

such as survivorship are difficult (at best) to obtain for elasmobranchs, and because

gaining a better understanding of how life histories and population dynamics respond to

exploitation (with uncertainty included) would benefit fishery managers.

Cortés (2002) showed that uncertainty could be incorporated into life-table

analysis via Monte Carlo simulation to generate population growth rates (λ and r) and

other population statistics with confidence bands. His results, from 38 shark species,

show that these types of life-tables produce "nearly identical results" to pre-breeding

census, age-structured Leslie matrix models (which he also presented). I used this life-

table approach in modeling the demography of salmon sharks in the ENP and WNP.

Elasticity (proportional sensitivity) analysis is becoming a standard tool in

demographic analysis (Heppell et al. 2000a). Elasticity is a perturbation measure that

quantifies the proportional change in population growth rate as a function of a

proportional change in other vital rates such as survival, fecundity or growth (Heppell

1998, Heppell et al. 1999, De Kroon et al. 2000). Elasticity analysis from single,

deterministic approaches can lead to inappropriate management decisions (Heppell

2000a, Cortés 2002). As such, I calculated elasticities (with uncertainty incorporated via

Monte Carlo simulation) in my models in order to more accurately gauge the relative

importance of proportional changes in fertility, juvenile survival and adult survival on the

intrinsic rate of population increase (r, where $r = ln\lambda$; λ = finite population growth rate)

(Heppell 1998, Heppell et al. 2000b, De Kroon et al 2000, Caswell 2001).

Density-dependent compensation is a standard concept in ecology and fisheries biology (Krebbs 1985, Holden 1974 and 1977). Potential compensatory mechanisms in fishes include: increased survivorship in pups, juveniles and adults, an increase in fecundity or size at birth, an increase in growth rate leading to earlier age at maturity, decreasing (shortening) reproductive periodicity and immigration of animals from other areas. In sharks, a decrease in the reproductive periodicity may be possible in some species, but there is no evidence to support its occurrence, and no species has been shown to increase its fecundity due to exploitation. Sminkey and Musick (1995) found an increase in juvenile sandbar shark (*Carcharhinus plumbeus*) growth rate after heavy exploitation, but this was not accompanied by a change in age at maturity. Cortés and Parsons (1996) proposed an increase in offspring size for the bonnethead shark (*Sphyrna tiburo*) as a possible compensatory mechanism in that species. There are no available data on salmon shark immigration and emigration between the ENP and WNP, so no inferences can be made about this type of compensation. The best evidence points towards an increase in the survivorship of pups and juveniles (Walker 1992,Walker 1998, Hoenig and Gruber 1990, Musick et al. 1993).

Direct evidence of increased survivorship in pups and juveniles due to exploitation has been obtained for lemon sharks (*Negaprion brevirostris*) ≤ 53 cm PCL (Gruber et al. 2001). The survival rate of young of the year (YOY) and juvenile lemon sharks was made from a mark-depletion experiment and were negatively correlated with estimated initial abundance, demonstrating density-dependent survival rates in that species. The results of Gruber et al (2001) also support the assumption that first year survival can be adequately determined through life-table (or Leslie matrix) methods.

A shortcoming of life-table models is that they assume density-independence, so I consequently incorporated density-dependent compensation in the present model when imposing fishing mortality. I increased survivorship of YOY and juvenile age classes (up to age at first reproduction) based on output from the 'intrinsic rebound potential' model of Au and Smith (1997, also see Smith et al. 1998), which provides a prediction of the net increase in sub-adult survivorship (I_α) at a given level of F along with a prediction of the 'intrinsic rebound potential' (r at maximum sustainable yield = r_{MSY}) of a species.

Demographic analyses are often used for management and conservation purposes. As such, it is important that biologists be able to more accurately describe the variability in estimates of vital rates in marine populations. Incorporating uncertainty into modeling techniques adds one more tool for biologists to use to provide fishery managers the ability to make responsible decisions. The goals of this part of my dissertation research were to: 1) provide the first estimates of demographic parameters for salmon sharks, 2) investigate the 'commercial fishing potential' of this species, 3) provide results that could be used for comparative purposes with other recent demographic studies on sharks (e.g. Cortés 2002, Smith et al. 1998), and 4) see if the Au and Smith (1997) model would adequately predict the necessary compensation to keep population parameter estimtates stable (i.e. attempt to 'connect' the life-table and intrinsic rebound potential models in a manner that would lead to biologically reasonable conclusions).

MATERIALS AND METHODS

The Life-table Model

I used age-structured life-tables based on a yearly time step and a 2-year reproductive cycle (applied to only females) to model the demography of salmon sharks

in the ENP and WNP. Monte Carlo simulation (n = 5,000) was used to incorporate uncertainty in demographic parameters and generate population growth rates (λ and r), generation time ($\bar{A}$), net reproductive rate (R_0), reproductive value (v_x), stable age distribution (c_x), fertility, juvenile and adult elasticity, mean life expectancy, and population doubling or halving time. Due to differences in salmon shark life history parameter estimates and weight-at-length relationships (see Chapter 1) between the ENP and WNP, separate demographic models were run for each area. I use the term "population" throughout this Chapter when referring to each area. This is not meant to infer that they are distinct populations or sub-populations (as this has not been demonstrated), but rather to distinguish between areas and models. Salmon shark life history parameters used for the ENP models are from Chapter 1, and those used for the WNP models are from Tanaka (1980) and Nagasawa (1998).

To include uncertainty in parameter estimates, I established probability distributions for maximum age (ω), age at first reproduction (α), fecundity (m_x = number of female pups per female per year) and survivorship at age (S_x). The maximum age of salmon sharks appears to be very similar in the ENP and WNP (Chapter 1), so 20 to 30 years of age was used for both areas and was represented by a linearly decreasing distribution scaled to a total relative probability of 1 (Figure 2.1a). Female salmon shark age at first maturity has been estimated at 6 to 9 years in the ENP (Chapter 1) and 8 to 10 years in the WNP (Tanaka 1980, Nagasawa 1998). Age at first reproduction is required for the model, hence 7 to 10 years of age was used for the ENP, and 9 to 11 years was used for the WNP. With no available information to specify any given age at first

reproduction as the "most likely", uniform probability distributions were used for this

parameter (Figure 2.1b).

Salmon sharks are thought to mate in late summer and early fall and have roughly

a 9-month gestation period (Tanaka 1980, Goldman and Human 2002). The functional

ovary in all mature females I examined (n = 55) in late summer and early fall in Prince

William Sound, Alaska, appeared to be in a resting stage with small ovarian follicles (or

in a postpartum condition). This suggests that salmon sharks, like several of the other

lamniform sharks, possess a 2-year reproductive cycle.

Litter size of WNP salmon sharks has been reported to be between three and five,

with a sex ratio at birth of 2.2 males per female (Tanaka 1980). (Males are also the

dominant sex in the WNP, whereas females are the dominant sex in the ENP – see

Chapter 1). There are no data on the litter size of ENP salmon sharks or the sex ratio of

litters. However, females on both sides of the Pacific reach similar maximum lengths,

therefore I assumed total fecundity (number of sharks per litter) to be the same. I did not,

however, assume the same sex ratio for ENP salmon sharks. With no data available on

the sex ratio of ENP salmon shark litters, I chose to use a 1:1 ratio. A 1:1 ratio tends to

be more common in vertebrates, and ENP salmon sharks pup in a different location than

those in the WNP (Goldman and Musick in press, also see Chapter 1) giving less reason

to assume the same sex ratio amongst litters. I represented total fecundity for the ENP

and WNP as normal distributions ranging between three and five with a standard

deviation set arbitrarily at 30% of the mean, and used the minimum and maximum

reported litter size to bound the distribution. This decision was in accordance with

Figure 2.1: (a) Probability distribution for longevity used in model simulations for ENP

and WNP salmon sharks; (b) Probability distribution for age at first reproduction for

salmon sharks in the eastern North Pacific (distribution for western North Pacific was

also uniform, but ranged from 9 to 11).

a)

Longevity

b)

Age at first reproduction

Cortés' (2002) observations that the standard deviation of the mean litter size in elasmobranch fishes generally ranged between 20 and 40% and, as such, he used a standard deviation of 30% when the value was not reported in the literature. Female-specific fecundity (m_x; number of females per female per year) was obtained by dividing the total number of offspring in a litter by the reproductive cycle in years accounting for the sex ratio of litters. For the ENP, this meant simply dividing by 4 (2-year cycle x 2 offspring per female = 4) to obtain the number of females per female per year, whereas for WNP it meant dividing by 6.4 to account for the 2.2:1 sex ratio of pups in a litter.

There are several methods available for estimating natural mortality (M), and hence survivorship in the absence of fishing ($S = e^{-M}$). I estimated the probability of annual survival at the beginning of each age using the following six life-history methods following Cortés (2002) (see Appendix 1 for equations): 1) Hoenig (1983), 2) Pauly (1980), 3) Chen and Watanabe (1989), 4) Peterson and Wroblewski (1984), and 5 and 6) Jensen (1996). Although method 4 uses dry weight, wet weight seems to yield more realistic estimates of survival for sharks (Cortés 2002 and pers. comm.).

I used a relatively cautious approach when setting probability distributions for survivorship. I used the lowest and highest values from the six methods as lower and upper bounds for setting survivorship probability distributions. The first five age classes (ages 0 to 4; < 1.5 m PCL) were represented by uniform distributions (Figure 2.2a), as there are no data that would give reason to suspect that one estimate is more realistic than another. For salmon sharks ages five to 30 (> 1.5 m PCL), I assumed that survivorship would more likely be at the higher end of the distribution rather than the lower end because of their larger size, so I used a linearly ascending distribution scaled to a total

relative probability of 1 (Figure 2.2b), with the highest estimate of survivorship twice as likely to occur in model simulations as the lowest.

Annual population growth rates ($\lambda=e^r$) were obtained by iteratively solving the discrete form of the Lotka-Euler equation (Goodman, 1982, Roff 1982):

$$1 = \sum_{x=1}^{\omega} e^{-rx} l_x m_x$$

where l_x is the probability of an individual being alive at the beginning of age x, m_x is the number of female offspring produced annually by a female at age x, and ω is maximum age. Generation time ($\overline{A}$) was calculated as

$$\overline{A} = \sum_{x=1}^{\omega} e^{-rx} x l_x m_x$$

which is the mean age of the parents of the offspring produced by a population at the stable age distribution (Caswell 2001).

The reproductive value distribution (v_x) was obtained through

$$\frac{v_x}{v_o} = \frac{e^{r(x-1)}}{l_x} \sum_{j=x}^{\omega} e^{-rx} l_x m_x$$

where v_o is the reproductive value at birth (which is equal to one), and j denotes all the ages a female will pass through from x to ω (Goodman 1982, Ebert 1999, Cortés 2002).

Figure 2.2: Examples of survivorship distributions for (a) age-zero and (b) age five

salmon sharks. Values shown are for the eastern North Pacific models.

a)

Age zero survivorship

Probability

0.785   0.809   0.833   0.857   0.881

b)

Age five survivorship

Relative probability

20

15

10

5

0

0.785   0.809   0.833   0.857   0.881

The stable age distribution (c_x) was obtained through

$$c_x = \frac{e^{-rx}l_x}{\sum\limits_{x=1}^{\omega} e^{-rx}l_x}$$

The reproductive value and stable age distribution columns were used to calculate elasticities following Caswell (2001) and Cortés (2002) as

$$e_{ij} = \frac{a_{ij}}{\lambda} \frac{v_i \ w_j}{\langle w, v \rangle}$$

where a_{ij} is the element corresponding to row i of column j (survivorship), v_i is the value of row i in the reproductive value column (v_x), w_j is the value of row j in the stable age distribution column (c_x), and $\langle w, v \rangle$ is the scalar product of row elements in the w (c_x) and v (v_x) distributions. I calculated elasticities for age zero survival (fertility), juvenile survival and adult survival by summation of elasticity elements across relevant age classes, which may present viable management options.

The mean life expectancy was obtained by

$$\overline{X}_{Life \ Expectancy} = \frac{1}{-\ln(\sum\limits_{x=0}^{\omega} P_x)}$$

where P_x is the mean survivorship of the probability distribution for age x (Lawless 1982).

The net reproductive rate (R_O) was obtained by

$$R_O = \sum\limits_{x=0}^{\omega} l_x m_x$$

Population halving ($t_{0.5} = \dfrac{\ln 0.5}{r}$) and doubling ($t_2 = \dfrac{\ln 2}{r}$) times were calculated

from the mean instantaneous rate of population growth (r) from model simulations.

The uncertainty in demographic traits (age specific survival and fecundity, age at

first reproduction and maximum age) was randomly selected from each trait's probability

distribution during Monte Carlo simulation. Ninety-five percent confidence intervals for

each parameter were obtained from the 2.5th and 97.5th percentiles.

Density-Dependent Compensation

The above model is a density-independent model. To allow for density-dependent

compensation (for a given level of F) due to the changes in mortality of fished ages, I

used the predicted net increase in sub-adult survivorship from Au and Smith's (1997 –

also see Smith et al. 1998) 'intrinsic rebound potential' model. This model provides, as

output, a prediction of the net increase in pre-adult survivorship needed for a population

to 'rebound' back to stationary equilibrium ($r = 0$) when a given level of F is imposed

(and assumes $r = 0$ before F begins and that Z [= $M+F$] is sustainable).

The Au and Smith (1997) model solves for 'r' using a variant of the Lotka-Euler

equation (See Au and Smith 1997 or Smith et al. 1998 for details of converting the Lotka-

Euler equation given above to):

$$e^{-(M+r)} + l_\alpha b\, e^{-(r\alpha)} [1 - e^{-(M+r)(\omega - \alpha + 1)}] = 1$$

where l_α = the net increase in sub-adult survivorship (from age 0 to age at first

reproduction, α), and b = fecundity (females per female per year). Setting $r = 0$,

changing M to the total level of mortality Z with $l_\alpha = l_{\alpha.z}$ and solving for l_α, the

solution to the above equation is:

$$l_{\alpha,z} = \frac{1-e^{-z}}{b[1-e^{-(z)(\omega - \alpha + 1)}]}$$

where $l_{\alpha,z}$ = the predicted net increase in sub-adult survivorship at a given level of Z.

I used Monte Carlo simulation (n = 5,000) to incorporate uncertainty in

demographic parameters and generate estimates of l_α. I then evenly distributed the net

increase in l_α, between when F = 0 and when a given level of F was present, amongst

the sub-adult age classes in the life-table model and ran Monte Carlo simulations with F

and the l_α 'factor' included. The method of calculating the amount of increased

survivorship for each age class and evenly distributing it (l_α) among sub-adults is given

in Appendix 2. Survivorship was accordingly increased (compensation included) for

ages zero through six in the ENP life-table model and for ages zero through eight in the

WNP life-table model.

All simulations (life-table and intrinsic rebound potential) were implemented with

Microsoft Excel spreadsheet software equipped with proprietary add-in risk assessment

software (Crystal Ball, Decisioneering Inc., Denver, CO) and Microsoft Visual Basic for

Application macros.

Fishing Mortality Scenarios

I examined the effect of fishing mortality (F) on salmon sharks in the ENP and

WNP considering only scenarios that would be the most likely to occur if a sizeable

commercial fishery began in either area. I started models that incorporated fishing

mortality at F = 0.025 and increased F in steps of 0.025, stopping when the population

could no longer remain at a stable or near-stable equilibrium (i.e. when compensation

predicted by the Au and Smith (1997) model would no longer keep population parameter

estimates stable).

Eastern North Pacific

Salmon sharks are taken in U.S. waters (particularly Alaska) as bycatch in trawl,

gillnet, and seine fisheries, but this bycatch has been poorly documented (Camhi, 1999).

There is currently no directed commercial fishery for salmon sharks in the ENP, but a

small recreational fishery exists along Alaska's central coastline (the Gulf of Alaska,

GOA, and in Prince William Sound, PWS). If commercial fishing began for salmon

sharks in the ENP it would be in the central GOA and in PWS where large aggregations

are commonly found, particularly during the summer months. Salmon sharks younger

than five years of age have not been taken from GOA or PWS waters (Chapter 1), as

small salmon sharks (< 5 years of age) range between northern Baja, Mexico, and

southeast Alaska. Additionally, small salmon sharks are not commonly taken as bycatch

in other fisheries, so it is unlikely that a fishery could be developed for them. The large

overlap in length-at-age (see Chapter 1, Table 7) along with the fact that the purse seines

and surface long-lines would probably be the primary gear of a fishery, makes it highly

unlikely that a size-selective fishery could be developed in Alaska waters. Therefore, the

fishing scenarios I used for the ENP included ages 5 to 30.

Western North Pacific

Japanese commercial salmon shark catch between 1952 and 1965 was reported at

110.4 thousand metric tons (mt), with a high of 40.1 thousand mt in 1954, but more

recent landing data are unavailable (Compagno 1990). Salmon sharks were commonly

caught in gillnets set for salmon (*Oncorhynchus*) and flying squid (*Ommastrephes*)

primarily by Canadian, Japanese and Russian fisheries, with smaller interests from

Taiwanese and North Korean fisheries (Blagoderov 1994, McKinnell and Waddell 1993,

Nakano and Nagasawa 1996, Robinson and Jamieson 1984). Currently, a small directed

fishery occurs each summer off Japan taking between 1,000 and 3,000 individuals (H.

Nakano pers. comm.), but the bycatch from other fisheries may still be quite large.

Goldman and Human (2002) estimated the Japanese flying squid fishery catches over

105,000 salmon sharks each year.

Salmon sharks taken as bycatch in the WNP generally range between 70 cm and

190 cm PCL (Nakano and Nagasawa 1994, Nakano and Nagasawa 1996, McKinnell and

Seki 1998), but larger adults are also taken and are the major catch in the current directed

fishery. As such, the main fishing scenario I used for the WNP included F at all ages.

For comparative purposes, I also ran four additional scenarios for WNP salmon sharks:

1) $F_{0.025}$ began at age five, 2) the sex ratio of pups per litter was 1:1 (instead of 2.2:1

male dominated) with F = 0, 3) the sex ratio of pups per litter was 1:1 and $F_{0.025}$

included all ages, 4) the sex ratio of pups per litter was 1:1 and $F_{0.025}$ began at age 5.

RESULTS

Instantaneous natural mortality rate estimates from the six methods used ranged

from 0.255 to 0.091 for salmon sharks in the ENP and from 0.209 to 0.097 for the WNP.

Minimum and maximum age-specific survivorships (P_x) are given in Tables 2.1 and 2.2.

The Hoeing (1983) method predicts the average natural mortality for the whole

Table 2.1: Minimum and maximum survivorship estimates for salmon sharks in the eastern North Pacific used in life-table model simulations. Double dashed line is where fishing mortality begins. Density-dependent compensation included for all age classes before single dashed line.

Age x	F=0 Survivorship (S)		F=0.025 starting at 5 a=1.013 up to age 7 Survivorship (S)		F=0.05 starting at 5 a=1.026 up to age 7 Survivorship (S)	
	Minimum	Maximum	Minimum	Maximum	Minimum	Maximum
0	0.775	0.870	0.785	0.881	0.795	0.893
1	0.775	0.870	0.785	0.881	0.795	0.901
2	0.775	0.870	0.785	0.881	0.795	0.909
3	0.775	0.878	0.785	0.889	0.795	0.913*
4	0.775	0.886	0.785	0.897	0.795	0.913**
5	0.775	0.892	0.765	0.881	0.756	0.870
6	0.775	0.896	0.765	0.885	0.756	0.874
7	0.775	0.899	0.756	0.877	0.737	0.855
8	0.775	0.902	0.756	0.880	0.737	0.858
9	0.775	0.904	0.756	0.882	0.737	0.860
10	0.775	0.906	0.756	0.883	0.737	0.861
11	0.775	0.907	0.756	0.885	0.737	0.863
12	0.775	0.908	0.756	0.886	0.737	0.864
13	0.775	0.909	0.756	0.886	0.737	0.865
14	0.775	0.910	0.756	0.887	0.737	0.865
15	0.775	0.910	0.756	0.888	0.737	0.866
16	0.775	0.911	0.756	0.888	0.737	0.866
17	0.775	0.911	0.756	0.889	0.737	0.867
18	0.775	0.912	0.756	0.889	0.737	0.867
19	0.775	0.912	0.756	0.889	0.737	0.867
20	0.775	0.912	0.756	0.890	0.737	0.868
21	0.775	0.912	0.756	0.890	0.737	0.868
22	0.775	0.913	0.756	0.890	0.737	0.868
23	0.775	0.913	0.756	0.890	0.737	0.868
24	0.775	0.913	0.756	0.890	0.737	0.868
25	0.775	0.913	0.756	0.890	0.737	0.868
26	0.775	0.913	0.756	0.890	0.737	0.868
27	0.775	0.913	0.756	0.891	0.737	0.869
28	0.775	0.913	0.756	0.891	0.737	0.869
29	0.775	0.913	0.756	0.891	0.737	0.869
30	0.775	0.913	0.756	0.891	0.737	0.869

*Calculated value = 0.9151   **Calculated value = 0.9192

Table 2.2: Minimum and maximum survivorship estimates for salmon sharks in the western North Pacific used in life-table model simulations. Double dashed line is where fishing mortality begins. Density-dependent compensation included for all age classes before single dashed line.

Age x	F=0 Survivorship (S) Minimum	Maximum	F=0.025 starting at 0 a=1.011 up to age 9 Survivorship (S) Minimum	Maximum	F=0.025 starting at 5 a=1.011 up to age 9 Survivorship (S) Minimum	Maximum
0	0.811	0.870	0.800 ≡≡≡≡≡ 0.858		0.820	0.880
1	0.811	0.870	0.800	0.858	0.820	0.880
2	0.811	0.870	0.800	0.858	0.820	0.880
3	0.811	0.875	0.800	0.862	0.820	0.885
4	0.811	0.881	0.800	0.868	0.820	0.891
5	0.811	0.885	0.800	0.872	0.800	0.872
6	0.811	0.889	0.800	0.876	0.800	0.876
7	0.811	0.892	0.800	0.880	0.800	0.880
8	0.811	0.895	0.800	0.882	0.800	0.882
9	0.811	0.897	0.791	0.874	0.791	0.874
10	0.811	0.898	0.791	0.876	0.791	0.876
11	0.811	0.900	0.791	0.878	0.791	0.878
12	0.811	0.901	0.791	0.879	0.791	0.879
13	0.811	0.902	0.791	0.880	0.791	0.880
14	0.811	0.903	0.791	0.881	0.791	0.881
15	0.811	0.904	0.791	0.881	0.791	0.881
16	0.811	0.904	0.791	0.882	0.791	0.882
17	0.811	0.905	0.791	0.882	0.791	0.882
18	0.811	0.905	0.791	0.883	0.791	0.883
19	0.811	0.906	0.791	0.883	0.791	0.883
20	0.811	0.906	0.791	0.884	0.791	0.884
21	0.811	0.906	0.791	0.884	0.791	0.884
22	0.811	0.907	0.791	0.884	0.791	0.884
23	0.811	0.907	0.791	0.884	0.791	0.884
24	0.811	0.907	0.791	0.885	0.791	0.885
25	0.811	0.907	0.791	0.885	0.791	0.885
26	0.811	0.907	0.791	0.885	0.791	0.885
27	0.811	0.908	0.791	0.885	0.791	0.885
28	0.811	0.908	0.791	0.885	0.791	0.885
29	0.811	0.908	0.791	0.885	0.791	0.885
30	0.811	0.908	0.791	0.885	0.791	0.885

Survivorship does not change when you have mx=1:1

population (relative to ω) and, as such, consistently provided the highest survivorship values for ages zero through two in all models. The Peterson and Wroblewski (1984) method, which is weight-length based, consistently produced the highest survivorship values for ages three through 30 in all models. For ENP salmon sharks, the Jensen 'k' (1996) method produced the lowest estimates of survivorship, while the Hoeing (1983) method produced the lowest survivorship estimates for the WNP population.

The results of initial life-table model simulations (with F = 0) indicate that the salmon shark population in the ENP is slowly increasing at a rate of almost 1.2 % per year with a doubling time of 59.2 years (Table 2.3). In contrast, the results for the WNP population indicate it is decreasing at a rate of just over 2 % per year with a halving time of 29.6 years. While the mean results of the models indicate the ENP population is growing, the 95 % confidence bands show the variability (from uncertainty) of parameter inputs and indicate that under the conditions used in the model, this range might be as high as 4.1 % per year or that the population could be slightly decreasing at a rate of 1.5 % per year (Table 2.3). Confidence bands for 'r' in the WNP indicate that this population may be decreasing between 0.65 % and 3.8 % per year (Table 2.3). Deterministic estimates of 'r' conducted with the Solver minimization function in Microsoft Excel show that age at first reproduction accounted for a greater amount of variation in 'r' than maximum age (Table 2.4). Mean generation time and life expectancy were slightly higher for the WNP population (Table 2.3). Summed elasticites were highest for juvenile survival (followed by adult survival and fertility) indicating that an increase in their mortality would have the largest effect on population growth rates

Table 2.3: Estimates of eastern and western North Pacific (ENP and WNP) salmon shark demographic parameters and elasticities (population growth rates, λ and r, generation times, $\overline{A}$; net reproductive rate, R_o).

F (starts at age) ENP	λ	r	$\overline{A}$	Ro	Mean Life Expectancy
0	1.012 (0.985-1.042)	0.0117 ([-0.0151]-0.0412)	13.1 (11.4-15.0)	1.2 (0.8-1.6)	5.9 (5.4-6.5)
0.025 (5)	1.003 (0.975-1.035)	0.0033 ([-0.0251]-0.0342)	12.9 (11.2-14.7)	1.0 (0.7-1.5)	5.4 (4.9-5.8)
0.05 (5)	0.995 (0.966-1.029)	-0.0047 ([-0.0052]-0.0282)	12.6 (10.9-14.4)	0.9 (0.6-1.4)	4.9 (4.6-5.3)
WNP					
0	0.977 (0.962-0.994)	-0.0234 ([-0.0385]-[-0.0065])	14.9 (13.0-16.7)	0.7 (0.6-0.9)	6.6 (6.1-7.0)
0.025 (0)	0.959 (0.945-0.975)	-0.0416 ([-0.0568]-[-0.0255])	14.8 (12.9-16.5)	0.5 (0.4-0.7)	5.7 (5.4-6.1)
0.025 (5)	0.967 (0.952-0.984)	-0.0331 ([-0.488]-[0.0161])	14.7 (12.8-16.3)	0.6 (0.4-0.8)	5.9 (5.5-6.2)
WNP if m_x=1:1					
0	1.009 (0.992-1.027)	0.0088 ([-0.0084]-0.0271)	14.5 (12.5-16.0)	1.1 (0.9-1.5)	6.6 (6.1-7.0)
0.025 (0)	0.991 (0.975-1.009)	-0.0093 ([-0.0258]-0.0091)	14.4 (12.5-15.9)	0.9 (0.7-1.1)	5.7 (5.4-6.1)
0.025 (5)	1.000** (0.982-1.020)	-0.0005 ([-0.179]-0.195)	14.3 (12.4-15.7)	1.0* (0.8-1.3)	5.9 (5.5-6.2)
	** = 0.9995			* = 0.997	

ENP	Elasticities			Population doubling time
	Fertility	Juvenile	Adult	
0	7.1 (6.2-8.1)	56.8 (53.4-60.2)	36.1 (33.1-39.1)	59.2
0.025 (5)	7.3 (6.4-8.2)	57.7 (54.4-61.0)	35.0 (32.0-38.0)	210.0
0.05 (5)	7.4 (6.5-8.3)	58.6 (55.3-61.8)	34.0 (31.1-36.9)	-147.5
WNP				
0	6.3 (5.6-7.1)	59.3 (56.3-62.3)	34.4 (31.3-37.7)	-29.6
0.025 (0)	6.3 (5.7-7.2)	59.6 (56.7-62.5)	34.1 (31.0-37.3)	-16.7
0.025 (5)	6.4 (5.8-7.3)	60.0 (57.1-62.8)	33.6 (30.7-36.7)	-20.9
WNP if m_x=1:1				
0	6.5 (5.9-7.4)	60.9 (58.2-63.5)	32.6 (29.9-35.6)	78.8
0.025 (0)	6.5 (5.9-7.4)	61.2 (58.5-63.9)	32.3 (29.5-35.1)	-74.5
0.025 (5)	6.6 (5.9-7.4)	61.6 (59.0-64.1)	31.8 (29.2-34.5)	-1,386.6

Table 2.4: Influence of maximum age and age at first reproduction on the intrinsic rate of population growth for salmon sharks in the eastern and western North Pacific (ENP and WNP) with F = 0. Sex ratio of pups per litter used in ENP model = 1:1. Parentheses indicate sex ratio of pups per litter used in WNP models.

		Age at first reproduction (α)				
Maximum age (ω)		7	8	9	10	11
ENP	20	0.0432	0.0239	0.0072	-0.0076	-
	25	0.0467	0.0286	0.0134	0.0003	-
	30	0.0478	0.0302	0.0157	0.0032	-
WNP (2.2:1)	20	-	-	-0.013	-0.025	-0.037
	25	-	-	-0.005	-0.015	-0.025
	30	-	-	-0.001	-0.011	-0.020
WNP (1:1)	20	-	-	0.024	0.009	-0.005
	25	-	-	0.030	0.017	0.005
	30	-	-	0.032	0.020	0.009

in both populations (Table 2.3).

The predicted stable age distributions in the ENP and WNP were dominated by the first six age classes (Figure 2.3). The young-of-the-year comprised approximately 21 % of the ENP population and 15 % of the WNP population with the next five age classes comprising another 58 % of the ENP population and 52 % of the WNP population. The older age classes appear to contribute slightly more to the stable age distribution in the WNP than in the ENP. An examination of the stable age distributions when F was imposed showed minimal changes in the predicted stable age distributions (for both populations). In reality, however, whenever there is exploitation, the age distribution is likely to have shifted from stability.

Fishing for salmon sharks in the ENP

The Au and Smith (1997) model predicted that a 1.3 % increase in the survivorship of each sub-adult age class would compensate for an F = 0.025 (Table 2.5). Results from the life-table simulation indicated that while a fishery at $F_{0.025}$ may be sustainable in the ENP, the predicted compensation was not sufficient to keep 'r' at the pre-fishing level (Table 2.3). Along with the decrease in the population growth rate, there was a decrease in generation time, the net reproductive rate and mean life expectancy (Table 2.3). The predicted population doubling time increased dramatically, however, from 59.2 years (when F = 0) to 210 years (Table 2.3). Fishing at $F_{0.025}$ brought about subtle, but predictable, changes in elasticities. The importance of juvenile survival to the population growth rate increased the most, while a slight increase was seen in fertility elasticity and adult survival elasticity decreased slightly (Table 2.3).

Figure 2.3: Predicted female stable age distribution for salmon sharks in the eastern and

western North Pacific (ENP and WNP) with no fishing mortality.

Table 2.5: Sub-adult survivorship compensation values from Monte Carlo simulations of

the Au and Smith (1997) density-dependent model for estimating the 'intrinsic rebound

potential' of fish populations. F = fishing mortality, l_α = net increase in sub-adult

survivorship, r_F = "intrinsic rebound potential" (predicted intrinsic rate of population

increase in response to F), l_α ratio = predicted proportional difference in sub-adult

survivorship between different levels of F, a = predicted proportional increase in

survivorship per sub-adult age class.

	F	l_α	r_F	l_α ratio	a
ENP	0.00	0.1695	0.00	-	-
	0.025	0.1857	0.008	1.096	1.013
	0.05	0.2035	0.015	1.201	1.026
WNP	0.00	0.2551	0.00	-	-
	0.025	0.2827	0.007	1.108	1.011

The value for increased sub-adult survivorship (a) from the Au and Smith (1997) model doubled when F was doubled to 0.05 (Table 2.5). Results from the subsequent life-table model, not surprisingly, follow the same trend as when $F_{0.025}$ was applied. However, unlike $F_{0.025}$, $F_{0.05}$ resulted in a negative population growth rate with declines in all estimated parameters, and a population halving time of 147.4 years (Table 2.3). The trend in changes in elasticities continued with juvenile survival elasticity further increasing in its importance relative to population growth.

Fishing for salmon sharks in the WNP

The Au and Smith (1997) model predicted that a 1.1 % increase in the survivorship of each sub-adult age class would compensate for an F = 0.025 (Table 2.5). Results from the life-table simulation indicated that the predicted compensation was not enough to keep the WNP population from further decline with a fishery at $F_{0.025}$, and the halving time increased from 29.6 to 16.7 years. As with the ENP population, all population statistics declined, juvenile survival elasticity increased slightly while adult survival elasticity slightly decreased and fertility elasticity remained the same (Table 2.3).

WNP - Additional Scenario #1 ($F_{0.025}$ begins at age 5)

This life-table model was run to see if the combination of decreased mortality (due to a lack of F) at ages zero through four along with the predicted increase in sub-adult survivorship could compensate for a fishery at $F_{0.025}$. As suspected, population statistics did not decline by as much as when all ages are fished, however the compensation was still not enough to keep the population from further decline relative to when F = 0 (Table 2.3). Trends in elasticities were again similar to other model

predictions with juvenile survival elasticity gaining in its importance relative to the population growth rate, adult survival elasticity decreasing slightly and fertility elasticity increasing slightly.

WNP - Additional Scenario #2 (1:1 sex ratio for pups per litter and F = 0)

Changing the fecundity (number of females per female per year) does not change the compensation value generated by the Au and Smith (1997) model. While their model does have a function (*b*) that can be used to increase fecundity, I chose to be consistent in my use of their model and incorporated the change in fecundity into the life-table model.

Results from the life-table simulation were very similar to those for the ENP when F = 0 (Table 2.3). Under these conditions of fecundity, the model indicates that the WNP population would be slowly increasing at approximately 0.9 % per year with a longer generation time and population doubling time than in the ENP. Mean life expectancy under these conditions was, as expected, the same as when fecundity was 2.2:1 (male dominated). Elasticity values were, again, consistent in showing the importance of juvenile survival to the population growth rate (Table 2.3).

WNP - Additional Scenario #3 (1:1 sex ratio for pups per litter and $F_{0.025}$ begins at age 0)

The results of this model simulation indicate that, on average, these conditions would cause population growth rate to decline at almost 1 % per year (Table 2.3). The predicted compensation was not enough to keep population statistics from decreasing. This scenario caused an increase in juvenile survival elasticity while adult survival elasticity slightly decreased and fertility elasticity remained the same (Table 2.3). Along with the decline in population statistics, this scenario also caused the population doubling time to become a population halving time of 74.5 years.

WNP - Additional Scenario #4 (1:1 sex ratio for pups per litter and $F_{0.025}$ begins at age 5)

Results from this life-table simulation indicated that while a fishery at $F_{0.025}$ may be sustainable in the WNP, the predicted compensation was not quite enough to keep 'r' at the pre-fishing level (Table 2.3). Along with the decrease in the population growth rate (relative to $F = 0$), there was a slight decrease in generation time, net reproductive rate and mean life expectancy (Table 2.3). The predicted population halving time under these conditions would be 1,386.6 years (Table 2.3).

DISCUSSION

Salmon shark population status

Demographic analysis is a useful tool in evaluating potential population changes under various conditions of fishing mortality (Caughley 1977, Hoenig and Gruber 1990), and continuing advances in modeling vital rates of long-lived fishes are beginning to provide us with more insight into their productivity.

The results of my demographic analyses indicate that salmon sharks are extremely vulnerable to fishing mortality. In the ENP, indications are that the population is fairly stable, growing at a nominal rate of about 1.2 % per year on average. The best-case scenario for a fishery in the ENP would be to keep F at a level below 0.025, as even that level fishing mortality could push population parameter estimates below levels of stability (Table 2.3). $F_{0.05}$ is clearly not sustainable according to my results.

The large aggregations of salmon sharks seen each summer in Alaska have been documented for over 40 years (Paust and Smith 1989, S. Meyer pers. comm.), however, some believe that salmon sharks are dramatically increasing in number (Gallucci et al. 2002a, 2002b). This appears to be completely anecdotal as no stock assessments of

salmon sharks have been conducted in Alaska or the ENP, and there are no historical data

on abundance from which to make such claims. It is highly unlikely that the density of

salmon sharks in one or two fjords in Prince William Sound, Alaska, is a reliable (or

reasonable) gauge of the overall salmon shark abundance in Alaska or the ENP. Bycatch

of salmon sharks in Alaska state waters (from research surveys and NMFS Observer

Program data) has been estimated to be relatively consistent over the past 10-12 years

(Goldman 2001), however many discards-at-sea are not reported by commercial fishers.

Without a stock assessment there is no way to know whether the total bycatch is

sustainable. Additionally, the current sport fishery in Alaska is very small, catching

between 200 and 500 individuals per summer (S. Meyer and C. Stock pers. comm.), and

probably has little to no impact on the population.

My results for salmon sharks in the WNP indicate that this population is declining

at just over 2 % per year (Table 2.3). These results, obviously, suggest that no fishery

should be implemented at this time. There may be several reasons for this outcome. We

do not know the fishing mortality that that population has been exposed to over the past

50-60 years. However, with the elimination of open ocean driftnet fishing and the

cessation of the Japanese open ocean salmon fishery, it is likely that there is less salmon

shark bycatch in the open North Pacific. (This could also be a factor in my population

growth estimate for the ENP, depending on immigration and emigration between areas).

The life history parameters I used for the WNP model were published over 20 years ago

and my generation time estimate for this population was 14.9 years. As such, my model

outcome may not reflect the current population status of salmon sharks in the WNP, and

the population could be rebounding if other density-compensatory factors are at play,

such as an increased growth rate (and potentially an earlier age at first reproduction).

Another aspect of the WNP model that is certainly partly responsible for the

outcome is the fecundity estimate I used. Tanaka (1980) stated that the sex ratio of pups

in a WNP litter is 2.2:1, male dominated. However, if the sex ratio of litters were 1:1

(additional scenarios 2, 3, and 4), the WNP population would currently be slowly

increasing, similar to the ENP population (Table 2.3)[1]. These conditions could

potentially allow for a small fishing mortality, but my results indicate that at $F_{0.025}$ age at

entry should be five years or older (Table 2.3). The later the age of entry, the better the

population would be able to maintain itself according to the predictions from elasticity

analysis. Considering that a wide size and age range of salmon sharks is taken in the

WNP, this could prove difficult to accomplish. As with the ENP population, no stock

assessments have been conducted in the WNP, so implementing a fishery before one is

conducted could lead to poor decisions and stock collapse. It seems unlikely that the

small commercial fishery off Japan (1,000 to 3,000 sharks per year) would have a large

impact on the population, but this is unknown.

Model simulation assumptions and limitations

Monte Carlo simulation was used because this probabilistic approach allows the

inclusion of a range of values that reflect the uncertainty in estimates of demographic

traits (maximum age, age at first reproduction, fecundity and age-specific survivorship).

I used distributions for these traits that I thought would reasonably approximate the

---

[1] A model was run for the ENP population with $m_x = 2.2$:1 male dominated ($F = 0$). The results were similar to those for the WNP under the same conditions (i.e. decreasing population status).

biology of salmon sharks. I also thought my estimate for reproductive periodicity, and the sex ratio of pups (in the ENP) were biologically realistic for this species. Further research on salmon shark reproductive biology may enable modification of the statistical distributions used to describe the demographic traits of salmon sharks.

Salmon sharks on both sides of the Pacific have been exploited to varying degrees (either through bycatch or directed fishing), which may have violated the assumption of a stable age distribution. If exploitation rates were consistent over the years, however, it is less likely that the assumption of a stable age distribution was violated.

Overall, the statistical distributions I used to describe survivorship seemed reasonable, although the lower bounds used may not be realistic for larger individuals (Tables 2.1 and 2.2). I dealt with this by setting the distributions for sharks greater than 1.5 m as shown in Figure 2.2b, instead of discarding the lowest estimate as was done by Cortés (2002). By doing so, I felt I used a slightly more cautious approach. Cortés (2002) assigned a higher probability to estimates of natural mortality obtained from the Peterson and Wroblewski (1984) method since its results are based on empirical, rather than estimated, parameters. In this study, the Peterson and Wroblewski (1984) method provided the highest estimates in all model scenarios for sharks above three years of age. The manner in which my survivorship probability distributions were set for sharks five years of age and greater, gave the highest estimated survivorship value twice the probability of occurring in model simulations relative to the lowest value (Figure 2.2b). Since young animals are likely to have lower survivorship than older animals and are potentially the most difficult to estimate natural mortality for, I felt it was a more conservative approach to use uniform distributions for ages zero through four (< 1.5 m).

Density-independent models assume invariability in vital rates over time. While we know that vital rates do vary over time, it is extremely difficult to collect and continue to update the biological information required for most shark species. In his examination of the demography of 38 shark species, Cortés (2002) felt that the life-table models he used were "robust" to deviations of the assumptions of traditional density-independent population and fisheries models (e.g. invariance of vital rates over time).

Elasticities and density-dependent compensation

Elasticity analysis for sharks has shown that population growth rates are generally much more sensitive to perturbations of juvenile and adult survival than to the survival of age-zero individuals or fecundity (Heppel et al. 1999, Cortés 2002). This is a more typical pattern for long-lived animals in general whether marine or terrestrial (Heppell et al. 1999, Hepell et al. 2000b, Cortés 2000), and suggests that the protection of age-zero animals would be insufficient to aid in the recovery of declining shark populations. Therefore, management efforts need to focus on juvenile and adult portions of the population to effectively aid in the recovery of shark species. While in some cases examined, juvenile and adult sharks appear to be equally susceptible to increased mortality (Cortés 2002), my results for salmon sharks indicate that juveniles would be the most important stage, followed by adults, on which to focus management to focus in both the ENP and WNP (Table 2.3). Cortés (2002) produced an elasticity continuum for 38 shark species, which corresponds with the well know r-K continuum (Musick 1999). My elasticity calculations for salmon sharks place them near the middle of that continuum.

Elasticity analysis provides useful insight into the effects of decreasing the survival of one or more ages or stages of a population. However, increases in fecundity

or a change in the age at first reproduction could offset the effect of reduced survival of adult ages. The ultimate benefit of elasticity analysis is in its predictive ability - one does not have to wait for a population response (or lack of one) to understand the potential effects of increased mortality on particular ages or groups of ages in the population. This is critical as recovery times of shark populations are likely to be long due to their general life-history characteristics.

Heppell et al. (1999) and Cortés (2002) evaluated the potential for density-dependent compensation by calculating the ratios of mean adult survival elasticity to mean fertility elasticity and of mean juvenile survival elasticity to mean fertility elasticity. For example, a ratio of juvenile survival to fertility elasticities of 2.0 indicates that a 10 % decrease in juvenile survival would have to be compensated for by a 20 % increase in fertility to return to its original r. They deemed that the required compensatory response was not possible if its magnitude exceeded the biological limits of age zero survival (= 1) or fecundity of a given population. Using salmon sharks in the ENP as an example, the ratio of mean adult survival elasticity to mean fertility elasticity was 5.1, and the ratio of mean juvenile survival elasticity to mean fertility elasticity was 8.2. The adult survival to fertility ratio might be feasible for salmon sharks - a 51 % increase in fecundity would be required, taking the maximum known pups per litter from five to 7.5 (or the mean of four to around six pups per litter), but more information needs to be obtained on salmon shark litter size to know if this is indeed possible. The juvenile survival to fertility ratio, however, vastly exceeds the potential for this species (i.e. an 82 % increase in survivorship of age-zero individuals is simply not possible). Similar results occur with the elasticity values for the WNP population.

My inclusion of density-dependent compensation in life-table model simulations where fishing mortality was imposed by using the I_α (net increase in sub-adult survivorship) value generated by the Au and Smith (1997) model, provided reasonable results. The amount of predicted compensation in sub-adult survivorship was not sufficient to keep population growth rates stable when F was imposed, which may be a result of using the rebound potential model in this manner, or due to the biological parameter inputs for salmon sharks used in my models. Additionally, I_α predictions may have fallen short of keeping population parameter estimates stable due to assumptions of that model (e.g. it assumes $r = 0$ and Z is sustainable). Future investigation of the use of the intrinsic rebound potential model in the manner presented here should focus on this aspect. If the I_α predictions are correct, this would mean that salmon sharks possess an extremely low 'rebound potential' and may be even more susceptible to exploitation than predicted here. It appears that 'connecting' the life-table models used by Cortés (2002) and the intrinsic rebound potential model of Au and Smith (1997) is useful and should be applied to other elasmobranch species to better evaluate the performance of the method. Initial indications (from this study) are that this could become a useful tool for future modeling of elasmobranch demographics.

Conclusion

The use of Monte Carlo simulation does not eliminate the need for further data gathering or sensitivity tests (Cortés 2002). Important additional data to gather to enhance predictive power of the models and elasticity analysis used herein include better information on fecundity, litter size, sex ratio of pups and longevity. The ability to obtain

refined estimates of natural mortality (M) would be useful for model simulations; possibly through increasing the precision of the weight-length relationship (e.g. n = 20 for my females length-weight relationship in Chapter 1) or tag-recapture data. However, empirical data is needed on the current level of F (both directed fishing and from bycatch) and catch per unit effort time series data on trends in abundance in order to test the hypotheses generated by the model. Much of the information required to enhance the demographic modeling of salmon sharks will be difficult to gather, but the pursuit of better data is a necessity if we are to better model the demography of all elasmobranch fishes.

The present demographic analysis has provided information useful for better understanding the life history strategy of salmon sharks and in giving fishery managers an idea of the population sensitivity of salmon sharks to fishing mortality. Elasmobranchs tend to have low productivities relative to other marine fishes (Musick 1999), however there is a wide range among species. My estimates of salmon shark vital rates fell in the middle of the continuum Cortés (2002) generated for vital rates of 38 other species. This research has shown that salmon sharks are likely to be extremely sensitive to fishing mortality. Models should be used to generate testable hypotheses, not give conclusion regarding demographic questions. As such, a stock assessment of the ENP and WNP populations should be a mandatory pre-requisite to the institution of any directed fishery for salmon sharks in the ENP and WNP or another collapsing shark population will likely be the result.

Chapter 3

Homeothermy in adult salmon sharks

INTRODUCTION

The salmon shark, *Lamna ditropis* (Family Lamnidae), occurs in the boreal and cool temperate coastal and oceanic waters of the North Pacific Ocean (Strasburg 1958, Campagno 1984, Blagaderov 1994, Nakano and Nagasawa 1994). It is a large apex predator that can reach 260 cm total length (TL) and weigh 220 kg (Tanaka 1980, Goldman and Musick in press).

As with all other lamnids, salmon sharks are known to be endothermic based on their possession of vascular counter-current heat exchangers (*retia mirabilia*) that allow the retention of heat created by their own oxidative metabolism (Hochachka et al. 1978, Carey et al. 1985, Fudge & Stevens 1996, Bernal et al. 2001a). The first descriptions of *retia* in lamnid sharks were by Eschricht & Müller (1835a and b), and Burne (1923) provided a detailed description of the *retia* in the porbeagle shark, *Lamna nasus* (as *Lamna cornubica*). *Retia* in salmon sharks are located in the cranium near the eyes (orbital *retia*), in locomotor musculature (lateral cutaneous *retia*), and viscera (suprahepatic and kidney *retia*). Temperature probe data (from moribund and recently dead animals) has shown temperature elevations of 15.6 °C over sea surface temperature (Smith and Rhodes 1983, Anderson and Goldman 2001).

Due to the inevitable linkage of aerobic heat production and heat loss via the gills and body surface, the steady state body temperature (T_b) of most fishes is virtually identical to ambient water temperature (T_a) (Brill et al. 1994). However, lamnid sharks (Family Lamnidae) and tunas (Family Scombridae, tribe Thunnini) show a convergent

91

evolution in their capacity to conserve metabolic heat thereby maintaining a steady state

$T_b > T_a$ (Brill et al. 1994, Bernal et al. 2001a). Perhaps the major (and most intriguing)

physiological questions surrounding fishes that have elevated body temperatures are: Are

they able to control rates of heat gain and heat loss? And, if so, to what degree?

Studies with captive juvenile mako sharks (*Isurus oxyrinchus*) and several species

of tunas have demonstrated that these fishes regulate rates of heat transfer with the

environment (Neill et al. 1976, Dewar et al. 1994, Bernal et al. 2001b). Free-swimming

juvenile bigeye (*Thunnus obesus*) and bluefin tunas (*Thunnus thynnus*) have also been

shown to possess this ability (Holland et al. 1992, Holland and Sibert 1994, Kitagawa et

al. 2001). However, when subjected to changes in T_a, small mako sharks and tunas (even

large bluefin) are unable to defend a specific body temperature (Carey and Lawson 1973,

Brill et al. 1994, Bernal et al. 2001b, Block et al. 2001). At a given T_a, small mako

sharks and tunas all possess an equilibrium body temperature (T_e) that is several degrees

above T_a. Rapid changes in T_a result in a shift in T_b, and ultimately a new T_e. Their

excess body temperature (T_x, where $T_x = T_e - T_a$) before and after changes in T_a is,

however, generally maintained within a fairly narrow range (i.e., T_x is constant with

respect to T_a) (Neill and Stevens 1974). Alternatively, data from adult lamnid sharks has

shown that their T_x is not constant with respect to T_a (Carey et al 1981, Goldman 1997,

Lowe and Goldman 2001).

Although they possess elevated body temperatures (Carey et al. 1985, Lowe and

Goldman 2001), the capacity of free-swimming lamnid sharks to regulate rates of heat

gain and loss has not been demonstrated. This is due to a number of factors including their size, logistical difficulties in studying them, and the serendipity involved in obtaining field data that can serve as a surrogate for a laboratory experiment. I present results from 47.7 hours of stomach temperature telemetry data obtained from four free-swimming salmon sharks, and data from a 'control' experiment with a dead salmon shark which was necessary in order to examine the rate of heat loss. Herein, I provide evidence that adult salmon sharks regulate rates of heat gain and loss in order to defend a specific body temperature, and that this is achieved through a combination of physiological thermoregulation and thermal inertia. I examine my data relative to the physiological ecology of salmon sharks and address the 'homeothermy hypothesis' presented by Lowe and Goldman (2001).

MATERIALS AND METHODS

Stomach temperature data were obtained via acoustic telemetry from four free-swimming salmon sharks in Prince William Sound, Alaska, during July 1999 and July and August 2000. Sharks #1and #4 were tracked in the 'Port Gravina' fjord (60°40.0' N; 146°20.0' W). Sharks #2 and #3 were tracked near Windy Bay on the north side of Hawkins Island (60°34.5' N; 145°59.8' W). Length was measured and sex determined at time of capture (shark #1), or by repeated observations of the shark from a small tracking vessel and using underwater videos obtained when the transmitter was fed to the individual (shark #2). Based on the high degree of sexual segregation in this species and documented lengths in Alaska waters, it is highly likely that sharks #3 and #4 were also female and approximately 180 cm precaudal length (PCL), the mean PCL of salmon sharks in Alaska (Goldman and Musick in press).

Acoustic transmitters were manufactured by VEMCO Ltd. (Halifax, Nova Scotia, Canada - model V22-TP) and by Sonotronics (Tucson AZ – model CHP-87-LT). Transmitters operated at frequencies of 34.0, 42.5 or 50.0 kHz . VEMCO transmitters were 'multiplexed' possessing both a thermistor and depth sensor with ranges of 0-30 °C and 0-200 m respectively. They had a life of 9-10 days, and a range of approximately 1 km at the study sites (based on manufacturers estimates and a single range test). Sonotronics transmitters possessed thermistors, with a range of 0-30 °C. They had a life of approximately 60 days and were audible from about one-half the distance of the VEMCO transmitters.

Manufacturers made initial temperature calibrations on all transmitters. Temperature calibrations were verified in a digital readout water bath, using a Fluke K/J 51 thermometer as a backup. These two devices were always within 0.1 °C of each other. Transmitter readings were always within 0.2 °C of the manufacturer's calibrations. The accuracy (and precision) of the two VEMCO transmitter calibrations were verified a final time as they were regurgitated after 28.3 and 22.4 hours by sharks # 2 and #4 respectively. (Water temperature readings at the depth where transmitters settled on the bottom were identical to temperature calibrations made in the lab).

Transmitters were fed to sharks by catching them in a purse seine and inserting the transmitter in a herring bait into the stomach via a small PVC tube (shark #1) or by lowering the transmitter in a bait into the water column via rod and reel for a shark to consume (sharks # 2, 3, and 4). Sharks #1 and #3 were fed Sonotronics temperature transmitters. Sharks #2 and #4 were fed multiplex (temperature and depth) VEMCO

transmitters allowing swimming depth data to be obtained. No swimming depth data were obtained from shark #3.

Immediately upon ingestion of a transmitter, sharks were monitored using a directional hydrophone (Dukane Corporation, St. Charles, Illinois, model N3OA5A with an analog to digital converter from Ultrasonic Telemetry Systems, Brea, California, or a VEMCO model VR-10 with VR-60 receiver). Three tracks were conducted from small (approximately 3 m) skiffs while one was conducted from the Alaska Department of Fish and Game's (17.7 m) R/V Montague. A member of the tracking crew constantly monitored the acoustic signal, and data values were recorded every 5 minutes. Each telemetered shark was tracked until the signal was permanently lost or until the transmitter was regurgitated.

Temperature-depth profiles have been shown to provide valid estimates of T_a at swimming depth (Goldman 1997). Profiling the water column with a temperature-depth transmitter prior to, during, and-or after tracks and comparing the profile to the swimming depth of the shark provided estimates of T_a for sharks #2 and #4. Ambient water temperature and swimming depth data were obtained from shark #1 via a National Geographic 'Critter Cam" camera attached to its first dorsal fin. The camera came off (prematurely) after 2.4 hours after which sea surface temperature (SST) was used for comparison with stomach temperature. I compared T_b for shark #3 to T_a at 25 m, which was obtained from a transmitter regurgitated by shark #2.

Stomach temperature is an excellent indicator of body core temperature (T_b) (Goldman 1997, Lowe and Goldman 2001), and the terms are used interchangeably in

this paper. However, the ingestion of seawater while feeding has been shown to cause a temporary reduction in stomach temperature that may significantly affect the statistical analysis of stomach temperature for use as an index of T_b (McCosker 1987, Goldman 1997, Lowe and Goldman 2001). In addition to consuming the baited transmitters, sharks #2 and #3 each fed during the time period tracked. Those temperature data are reported here, but were not used in any calculation or statistical analysis presented. Paired t-tests were used to compare T_b with T_a (and estimates of T_a at swimming depth), and cross-correlations were calculated to see if T_a had a lag-time effect on T_b.

Heat loss (or gain) in fishes with counter-current heat exchangers is proportional to the difference between T_e and T_b, not between T_a and T_b, because $T_b > T_a$ (i.e., a T_x is present therefore T_b will not reach T_a) (Brill et al. 1994, Neill et al. 1976, Neill and Stevens 1974). The equation describing the rate of change in body temperature is:

$$dT_b/dt = k(T_e - T_b) + Hp \qquad (3.1)$$

where dT_b/dt = rate of change of T_b with time, k is the thermal rate coefficient ($^\circ$C min^{-1} $^\circ$C thermal gradient^{-1}) – an empirically determined descriptor of heat transfer from the body to the environment, and Hp = internal heat production ($^\circ$C per minute). Equation 1 and its solution (Brill et al. 1994, Neill et al. 1976, Bernal et al. 2001b) are appropriate to use for tuna and small mako sharks because changes in T_a result in a new T_e. However, equation 3.1 is unable to provide realistic estimates of k when a specific body temperature is defended (i.e., because $T_e \cong T_b$ for all observed T_a values), and is therefore inappropriate for my salmon shark data (see results).

On 9 September 2001, I conducted a control experiment in order to examine the rate

of heat loss from the body core of an adult salmon shark (through the body surface) in 5.5

°C water, thus allowing estimation of a minimum cooling k (no estimation of a warming

k was made). A 187 cm PCL, 157 kg salmon shark (similar to the size of the tracked

sharks) was caught hook and line and sacrificed using buffered MS222. To ensure no

heart activity (i.e. no residual heat production), the shark was injected with 50 cc of

potassium chloride via a cardiac puncture. A VEMCO V22-TP acoustic transmitter was

inserted into the stomach to measure temperature and pressure. The shark was then

lowered to a depth of 85 m where ambient temperature was 5.5 °C, and T_b was monitored

for 3.92 h. The equation describing the rate of change in body temperature in the dead

shark is:

$$dT_b/dt = -kT_b \qquad (3.2)$$

which when solved yields:

$$T_b(t) = T_b(0) \cdot e^{(-kt)} \qquad (3.3)$$

where $T_b(t)$ = body temperature at time t, $T_b(0)$ = initial body temperature (prior to

change in T_a), and t = time.

RESULTS

A total of 4.03 continuous hours of temperature data were obtained from shark #1

on 25 July 1999 (Figure 3.1a). The track was terminated as the research cruise time

ended. Stomach temperature ranged from 22.8 to 26.2 °C with a mean of 25.2 °C.

Stomach temperature became stable 35 minutes after ingesting the transmitter (Figure

3.1a), and a mean stomach temperature of 25.7 °C was subsequently maintained. The

maximum difference observed between stomach and ambient temperatures was 21.2 °C

(Table 3.1). Ambient water temperature ranged from approximately 5.0 to 15.9 °C, and

was 12.4 °C at the shark's mean swimming depth. Sea surface temperature during the

time tracked was 15.0 to 15.9 °C.

Temperature data were obtained for 19.2 hours from shark #2 over a 28.3 hour

time period on 25 and 26 July 2000 (Figure 3.1b). The track was terminated due to the

regurgitation of the transmitter. Stomach temperature ranged from 20.1 to 26.0 °C with a

mean of 25.0 °C. Stomach temperature became stable 56 minutes after ingesting the

transmitter (Figure 3.1b). Aside from the reduction in stomach temperature associated

with feeding at 2045 hours, the shark maintained a constant body temperature with a

mean of 25.1 °C. The maximum difference observed between stomach and ambient

temperatures was 19.5 °C (Table 3.1). Ambient water temperature ranged from 5.7 to

14.1 °C, and was 9.2 °C at the shark's mean swimming depth. Sea surface temperature

during the time tracked was 13.8 to 14.1 °C.

Temperature data were obtained for 3.8 continuous hours from shark #3 on 28

July 2000 (Figure 3.1c). The track was terminated after losing the signal and not

relocating it during two days of searching. Stomach temperature ranged from 20.8 to

25.9 °C with a mean of 24.4 °C. Stomach temperature became stable 22 minutes after

ingesting the transmitter (Figure 3.1c). Aside from the reduction in stomach temperature

associated with feeding at 2100 hours, the shark maintained a constant body temperature

with a mean of 25.4 °C. The maximum difference observed between stomach

temperature and ambient temperature at 25 m was 17.8 °C (Table 3.1). Ambient water

Table 3.1: Salmon shark body temperature (T_b) ranges and means (w/ standard deviations), ambient water temperature (T_a) ranges and means (in parentheses), and the maximum difference observed (X_d) between T_b and T_a. All temperatures are in °C.

Shark #	T_b range	Mean T_b*	T_a range	X_d	Hours tracked
1	22.8 - 26.2	25.7 ± 0.5	< 5.0 - 15.9 (12.4)	21.2	4.03
2	20.1 - 26.0	25.1 ± 0.5	5.7 - 14.1 (9.2)	19.5	19.2
3	20.8 - 25.9	25.4 ± 0.4	8.1 - 13.9 (11.0)	17.8[†]	3.8
4	17.4 - 25.8	25.0 ± 0.5	< 5.7 − 14.9 (9.3)	19.7	20.7

*Does not include initial rise to stable T_s or decreases and subsequent rise back to stable T_s due to feeding; † = T_a at 25 m used in calculations.

temperature at 25 m was 8.1 °C and SST was 13.9 °C.

Temperature data were obtained for 20.7 hours from shark #4 over a 22.4 hour time period on 30 and 31 August 2000 (Figure 3.1d). The track was terminated due to the regurgitation of the transmitter. Stomach temperature ranged from 17.4 to 25.8 °C with a mean of 24.1 °C. Stomach temperature became stable 60 minutes after the transmitter was ingested (Figure 3.1d), and a mean stomach temperature was 25.0 °C was subsequently maintained. The maximum difference observed between stomach and ambient temperatures was 19.7 °C (Table 3.1). Ambient temperature ranged from 5.7 to 14.9 °C, and was 9.3 °C at the shark's mean swimming depth. Sea surface temperature during the time tracked was 14.8 to 15.1 °C.

Stomach temperature elevations over water temperature for all four sharks were considerable (max. = 21.2 °C), and mean stomach temperatures differed among the four individuals by only 0.7 °C. Body temperature elevations over ambient temperature, estimates of ambient temperature or SST were all statistically significant (paired t-tests, all P values < 0.0005). Changes in T_a (< 5.0 - 15.9 °C) had no apparent effect on T_b -- they were uncorrelated (maximum individual $r^2 = 0.25$), and lag effects from T_a on T_b were not present (maximum cross-correlation value for an individual, $r^2 = 0.39$).

The k coefficient for cooling in the control shark (equation 3.3) was 0.037 min^{-1}. This value represents a minimum k when applied to a living shark because I am unable to include heat loss via the gills in a free-swimming salmon shark. Additionally, heat lost through the body wall is likely greater when the animal is alive and producing heat, than when the animal is dead.

Figure 3.1: Temperature data for four salmon sharks tracked in Prince William Sound,

Alaska. (a) = shark #1, (b) = shark #2, (c) = shark #3, and (d) = shark #4. Open circles =

stomach temperature; solid circles = sea surface temperature (SST); solid triangles =

ambient water temperature (or estimated ambient water temperature via temperature-

depth profiles); solid diamonds = water temperature at 25 m. Small vertical arrows

indicate the time when stomach temperature became stable. Vertically dashed lines

separate days.

DISCUSSION

All four salmon sharks maintained elevated stomach temperatures within a very narrow range, while measured ambient temperatures ranged from below 5.0 to 15.9 °C (Figure 3.2). Each individual showed an increase in stomach temperature after ingesting a transmitter, and two individuals showed decreases followed by similar increases after either consuming either a bait or a natural prey item during the course of the track (Figures 1b and 1c). These observations are virtually identical to those observed in white sharks and are likely caused by ingestion of small amounts of seawater with either cold bait and/or prey (McCosker 1987, Goldman 1997). Interestingly, white shark stomach temperature becomes fairly stable after 3 to 6 minutes, but then takes several hours to reach a stable stomach temperature (Goldman 1997) while salmon shark stomach temperature reached equilibrium in 22 to 60 minutes. This may be due to differences in heat production and conservation ability (e.g. salmon sharks possess a kidney *rete*, white sharks do not), differences in body size between the two species, temperature of the seawater ingested, temperature of the prey ingested or a combination of these factors.

Salmon sharks made regular vertical movements in the water column, sometimes exceeding 140 m. Shark #4 exhibited this behavior in a manner that enabled us to test for the occurrence of physiological thermoregulation. Over 30 min (beginning at 2005 hours – Figure 3.1d), this shark dove from 9.6 m, where T_a was 13.2 °C, to 123.8 m where T_a was ≤ 5.7 °C. The shark remained at T_a ≤ 5.7 °C (between 56 and 124 m) for 3.3 h

Figure 3.2: Mean body temperature with standard deviation for four salmon sharks

tracked in Prince William Sound, Alaska. Mean (*or median) water temperatures and

ranges are shown below body temperature data for each individual.

during which time no decrease in T_b was observed (Figure 3.1d). In fact, instead of decreasing in response to the decrease in T_a, T_b actually increased slightly (from 24.8 to 25.5 °C, mean of 25.0 °C).

In fishes with elevated T_b's, k, HP or both may change as a function of T_a (Neill and Stevens 1974, Dewar et al. 1994). While tracking the salmon sharks, I found they maintained constant horizontal swimming speeds during rapid and long duration changes in T_a, indicating that Hp was relatively constant during these periods (i.e., equivalent to metabolic heat production). Since equation 3.1 does not provide realistic estimates of k when $T_e = T_b$, I used the data from the control shark and from the free-swimming shark's 3.3 h excursion into cold water to investigate whether physiological thermoregulation was occurring or whether T_b was maintained solely due to thermal inertia (Neill and Stevens 1974).

Based on the control shark, the free-swimming shark's T_b should have decreased at a minimum rate of 0.037 °C min^{-1}, yet it was maintained and slightly increased during that time (Figure 3.3). Therefore, thermal inertia alone could not be responsible for my observations. My data demonstrate that adult salmon sharks can regulate heat balance by altering their whole-body thermal rate coefficient (k). Changes in k that are independent of activity indicate physiological thermoregulation (Holland et al. 1992, Dewar et al. 1994), as does the fact that T_x was not constant with respect to T_a (Neill and Stevens 1974).

Salmon sharks can apparently also alter routes of blood flow through vascular shunts

Figure 3.3: Body temperature of shark #4 during 3.3 hour excursion into water $\leq 5.7\ ^\circ C$

(solid circles and line) compared to the predicted temperature loss, at $k = 0.037\ min^{-1}$,

based on the control shark (dashed line).

(Carey et al. 1981, Bernal et al. 2002a). This would provide a mechanism for regulating rates of heat gain and loss. A hepatic sinus bypasses the suprahepatic *rete* (at the forefront of the liver). The anatomy of the sinus suggests that it can be opened and closed in the living animal, thereby regulating the amount of heat retained within the system. Additionally, cool blood from the dorsal aorta flows around the suprahepatic *rete* into the viscera (Carey et al. 1981, Bernal et al. 2002a).

An animal that is able to maintain an elevated and uniform body temperature that is regulated independent of changes in ambient temperature is defined as a homeotherm (Hickman et al. 1984). Telemetered temperature data on free-swimming lamnid sharks led Lowe and Goldman (2001) to hypothesize that adult mako and white sharks may be homeotherms. My data demonstrate that adult salmon sharks essentially function as homeotherms, in a way analogous to mammals, through a combination of thermal inertia and physiological thermoregulation. The thermal buffer to the environment created by the combination of physical and physiological thermoregulation is probably the underlying factor in the evolutionary niche expansion of salmon sharks into boreal waters and allows them to range throughout the water column in search of prey.

Circadian cycles of body temperature are an additional feature of homeotherms. My data do not indicate the presence of a circadian body temperature cycle, which is present in birds and mammals, but more diel tracking data may reveal such a cycle.

Based on temperature measurements, known geographical distribution and a small amount of comparative anatomical data from the viscera and musculature of lamnid sharks, Carey et al. (1985) predicted that salmon sharks should rank atop this endothermic family in their "ability to maintain an elevated temperature". Telemetered

stomach temperature data from shortfin mako, white, and salmon sharks strongly support this ranking. Whereas white sharks possess a slightly higher mean body temperature than other lamnids, the maximum reported elevation of stomach temperature over ambient water temperature is 8.0 °C for shortfin mako sharks (Carey et al. 1981), 14.3 °C for white sharks (Goldman 1997), and 21.2 °C for salmon sharks (this study).

The data presented here support the homeothermy hypothesis of Lowe and Goldman (2001). However, all of the telemetered T_b's reported from free-swimming lamnid sharks to date have been obtained from adult specimens. It is important to obtain similar data from across size classes, particularly small individuals, in order to examine possible ontogenetic changes in thermoregulatory ability and changes in thermal inertia, and thereby define the limits of homeothermy in lamnid sharks. The relationship between body size, heat production, and heat loss in these sharks is almost certainly a key component in addressing and answering these questions.

Chapter 4

A re-examination of the age and growth of sand tiger sharks

in the western North Atlantic

INTRODUCTION

The sand tiger shark, *Carcharias taurus*, is a large coastal species that inhabits subtropical and temperate waters of the Atlantic, Indian and western Pacific Oceans, as well as the Mediterranean Sea (Gilmore et al. 1983, Compagno 1984, Pollard et al. 1996). This is a slow moving species, most frequently swimming near or at the bottom (usually around 30-60 m, but as deep as 191 m). However they are also found swimming in the mid-water and near the surface (Compagno 1984). They are often found in aggregations while migrating, feeding, and mating, as well as during courtship and pupping (Compagno 1984, Gilmore 1993). Sand tiger sharks feed on a wide variety of teleost fishes as well as smaller elasmobranchs and invertebrates such as squids, crabs and lobsters (Compagno 1984, Gelsleichter et al. 1999).

Seasonal movements of sand tiger sharks are well known in the western North Atlantic. They migrate north along the coast each spring from Florida to as far as the Gulf of Maine, and return south in the fall (Bigelow and Schroeder 1953, Gilmore et al. 1983, Musick et al. 1993). Juvenile sand tiger sharks occupy summer nurseries typically ranges from North Carolina to Cape Cod, MA, and in winter they occur from North Carolina to northern Florida (Gilmore et al. 1983, Gilmore 1993). Mating occurs in relatively shallow waters from February to April off Florida's east coast and in April and May off North Carolina, while parturition takes place off Florida and in the northern Gulf of Mexico between December and March (Gilmore et al. 1983, Gilmore 1993).

112

Adult female sand tiger sharks typically range in size from 270-290 cm total length (TL), but can reach a maximum size of 318 cm TL (Springer 1939). They mature between 220 cm and 230 cm TL (Gilmore et al. 1983). Adult males can reach 257 cm TL, but are generally less than 250 cm TL (Compagno 1984) and mature between 190 cm and 195 cm TL (Gilmore et al. 1983). The maximum length of this species does not seem to vary with differences in geographic location (Bass et al. 1975, Branstetter and Musick 1994).

The reproductive mode for sand tiger sharks is aplacental viviparity and includes both adelphophagous and oophagous stages (Springer 1948, Bass et al. 1975, Gilmore et al. 1983). Seven different nutritional phases have been shown to occur during embryonic growth (Gilmore et al. 1983, Gilmore 1993). Adelphophagy results in a maximum fecundity of two pups per litter that range from 95-105 cm TL, which does not appear to vary geographically (Gilmore et al. 1983, Branstetter and Musick 1994, Last and Stevens 1994). Whereas gestation and embryonic growth are well documented in sand tiger sharks, their reproductive periodicity has been a source of some contention. Gilmore (1993) stated that sand tiger sharks reproduce annually in the western North Atlantic, and Gordon (1983) believed they may mate annually in Australian waters. Alternatively, Cliff (1989), and Branstetter and Musick (1994) presented evidence supporting a two-year reproductive cycle for sand tiger sharks in South African waters and the western North Atlantic, respectively. Successful captive reproduction over the past 10 years lends strong support to a two-year reproductive cycle hypothesis (Henningsen et al, in review).

The sand tiger shark is fished or caught as bycatch in all areas it is found, but is of variable importance regionally (Compagno 1984). In the western North Atlantic, sand

tiger sharks are exposed to several fisheries due to their highly migratory nature (Casey and Kohler 1990, Musick et al. 1993, Anonymous 1999). As a result, the population has been depleted by an estimated 80-90 % since the mid 1970's (Musick et al. 1993, Musick et al. 2000). Because their low fecundity makes them particularly susceptible to almost any fishing exploitation, bycatch still poses a realistic threat to their survival. To prevent further decline of sand tiger sharks in the western North Atlantic, they were put on the protected species list, amended to the NMFS Fishery Management Plan for Atlantic sharks in 1997 (NMFS 1999). They also have fully protected status in Australian waters and their capture in South African waters is being phased out (Pollard et al. 1996, Anonymous 2002). Although the western North Atlantic population may have stabilized since given "prohibited possession" status, recovery is not yet apparent (Musick et al 2000).

Branstetter and Musick (1994) stated that sand tiger sharks may reach an age of 30 to 35 years and gave the following von Bertalanffy growth parameters for in the western North Atlantic: $L_\infty = 323.0$ cm TL, $k = 0.14$ yr^{-1}, and $t_0 = -2.6$ yrs for females; $L_\infty = 301.0$ cm TL, $k = 0.17$ yr^{-1}, and $t_0 = -2.3$ yrs for males; and $L_\infty = 321.0$ cm TL, $k = 0.14$ yr^{-1}, and $t_0 = -2.6$ for sexes combined. This was based on their estimation that this species forms two pairs of growth bands annually in the vertebral centra. They also stated a caveat about their uncertainty of that estimation. A re-calculation of the life history parameters from Branstetter and Musick's (1994) mean back-calculated lengths-at-age was conducted assuming annual formation of a single pair of growth bands (Goldman 1998), which gave the following von Bertalanffy growth parameters: $L_\infty = 323.0$ cm TL, $k = 0.07$ yr^{-1}, and $t_0 = -5.1$ for females; and $L_\infty = 302.0$ cm TL, $k = 0.08$ yr$^-$

[1], and $t_0 = -4.5$ for males; and $L_\infty = 322.0$ cm TL, $k = 0.07$ yr^{-1}, and $t_0 = -5.2$ for sexes combined. The difference in these life history parameter estimations, and their ramifications for management and conservation of this species (Musick et al. 1993, Musick et al. 2000), was the major reason for my re-examination of sand tiger age and growth. I aged 96 sand tiger sharks from bands formed seasonally in the vertebrae, and administered oxytetracycline (OTC) to three wild-caught sand tiger sharks that were held in aquaria for 2-3 yrs during which OTC was re-administered annually. I report my findings herein and briefly discuss the reproductive periodicity of this species.

MATERIALS AND METHODS

Sand tiger shark vertebrae (n=96) were obtained by the Virginia Institute of Marine Science (VIMS) (n=55) and from the National Marine Fisheries Service (NMFS) Narragansett, RI, laboratory (n=41). (Some samples from each institute were tournament or sport caught.) Twenty-five samples (from the VIMS survey) previously used for analysis by Branstetter and Musick (1994) were re-examined for this study. Vertebral samples and weights of sand tiger sharks used in this study from the VIMS survey were taken between 1980 and 2001; those obtained from NMFS were taken between 1963 and 1991. Vertebral samples were not obtained from all animals that were measured and weighed (over this nearly 40-year period), hence the discrepancy in sample sizes.

Sand tiger sharks taken by VIMS were measured on a straight line, and precaudal, fork, and total length (PCL, FL, and TL) were recorded along with sex and weight (when possible). A 20 to 25 cm section of vertebrae was removed from the area midway between the first dorsal fin and the gills, and stored frozen. Samples provided by NMFS included at least one of the necessary measurements and the date and location of capture.

I use TL measurements throughout this paper in order to make direct comparisons with previously published data on sand tiger shark growth parameters (Branstetter and Musick 1994). Linear regression equations based on measurements taken by VIMS and the NMFS lab, were developed for converting TL to FL and PCL.

Vertebral samples were thawed, cleaned of excess tissue, separated into individual centra and stored in 70% ethyl alcohol for at least 24 h. Centra were sagittally sectioned through the focus and then cut again approximately 1.5 mm off-center using an Isomet rotary diamond saw (Buehler, 41, Lake Bluff, IL). The sections were pressed between 2 pieces of Plexiglas (to prevent warping), air-dried for 24 h under a ventilation hood, and then mounted onto microscope slides. After drying, sections were polished with wet fine grit sand paper (320, 400 and 600) to approximately 0.5 mm and air-dried. Sections were viewed using a binocular dissecting microscope with transmitted light.

A banding pattern was readily distinguishable in sectioned centra, with wide bands separated by distinct narrow opaque bands. This pattern occurred on both arms of the corpus calcareum and the narrow bands extended across the intermedialia. A notch occurring on the outside edge of the corpus calcareum accompanied the distinct narrow bands (Figure 4.1) providing an additional ageing feature, particularly in sections where the cut excluded the radials of the intermedialia. Each pair of wide-narrow bands was considered a growth cycle; the narrow bands, hereafter referred to as "rings", were counted (Figure 4.1). An angle change in the intermedialia and a ring on the corpus calcareum were present approximately 6 to 7 mm from the focus of each centrum and considered to represent a birthmark. The "pre-birth rings" reported by Branstetter and

Figure 4.1: Sagittal section of a 11 yr old sand tiger shark's vertebral centrum showing

typical banding pattern. CR=centrum radius. Arrows represent ages.

Labels visible in figure: B, CR, Intermedialia, Corpus calcareum

Musick (1994) were present in most specimens, but were not counted nor measured.

Two readers independently aged all centra two times in blind, randomized trials.

This allowed the calculation of within-reader precision, and between-reader precision

twice. Percent agreement (PA=[No. agreed/No. read]•100), and percent agreement plus

or minus one year (PA +/- 1 yr) were calculated for length groups of 10 cm to test for

precision. Additionally, Chi-square tests of symmetry were conducted using Bowker's,

McNemar's, and Evans-Hoenig tests to determine whether differences between and

within readers were systematic (biased) or attributable to random error (Hoenig et al.,

1995; Evans and Hoenig, 1998).

Centrum radius (CR) and distance to each ring were measured to the nearest 0.001

mm as a straight line from the central focus to the outer margin of the corpus calcareum

(Figure 4.1) using a compound video microscope with the Optimus image analysis

system (Media Cybernetics 1999). TL was plotted against CR to determine the

proportional relationship between somatic and vertebral growth.

Back-calculation is a method for describing the growth history of each individual

sampled, and numerous variations in methodology exist (see Francis 1990 for a thorough

review). The relationship between CR and TL for sand tiger sharks was investigated to

determine the most appropriate method for back-calculating previous length-at-age. This

is critical for obtaining accurate life history parameter estimates from the von Bertalanffy

growth function. Three different proportions methods were used and compared with my

sample length-at-age data. First, I used the standard Dahl-Lea direct proportions method

(Carlander 1969):

$$L_i = (L_c/CR_c) \cdot CR_i \qquad\qquad (1)$$

where L_i = length at ring 'i', L_c = length at capture, CR_c = centrum radius at capture, and CR_i = centrum radius at ring 'i'. Next, I applied a modified version of the Dahl-Lea method that use parameter estimates from the specific linear fit that described the TL-CR relationship. The linear-modified Dahl-Lea method (Francis 1990) is:

$$L_i = L_c \cdot [(a+bCR_i)/(a+bCR_c)] \qquad (2)$$

where 'a' and 'b' are the linear fit parameter estimates.

Ricker (1992) applauded Francis' (1990) back-calculation review paper, but like Campana (1990) suggested that the point of origin of proportional back-calculations should be related to a biologically derived intercept (i.e., length at birth). I, therefore, also applied Campana's (1990) "size-at-birth-modified" Fraser-Lee equation:

$$L_i = L_c + [(CR_i - CR_c) \cdot (L_c - L_{Birth})/(CR_c - CR_{Birth})] \qquad (3)$$

where L_{Birth} = length at birth and CR_{Birth} = centrum radius at birth. (Based on Gilmore et al. 1983, and Branstetter and Musick 1994, 100 cm TL was used for L_{Birth}.)

A relative marginal increment (RMI) analysis was used to verify the temporal periodicity of ring formation in the vertebrae. This is a standardized marginal increment analysis whereby the margin, or growth area of a centrum from the last narrow growth ring to the centrum edge, is divided by the width of the last fully formed growth increment (Branstetter and Musick 1994). Resulting RMI values were compared to the month of capture. Age-zero animals were not included (as they have no fully formed increments).

The von Bertalanffy growth function was fit to the vertebral age-at-length data for sand tiger sharks with a nonlinear least squares regression algorithm ('nls' in S-Plus, Mathsoft Inc. 2000) to estimate parameters. The von Bertalanffy growth function is:

$$L_t = L_\infty \cdot [1 - \exp(-k(t - t_0))] \qquad (4)$$

where L_t = length at age 't', L_∞ = asymptotic or maximum length, k = the growth

coefficient, and t_0 = age or time when length theoretically equals zero. Growth

parameters were estimated for the sexes separately and combined. Because my sample

size was small, lengths at previous ages were back-calculated from centra measurements

for both sexes and fitted with the von Bertalanffy growth function. von Bertalanffy

growth parameter estimates were then obtained from mean back-calculated length-at-age,

and from a combination of back-calculated lengths-at-age and my sample data. A

likelihood ratio test was used to determine whether differences between female and male

growth parameters were significant or if a single set of growth parameters better

described the data (Kimura 1980, Quinn and Deriso 1999, Haddon 2001) (SAS Institute

Inc. 1999).

Two male sand tiger sharks (152.5 cm and 157 cm TL) captured off of Cape May,

NJ, USA, in 1998 for public display, were donated to this study. They were injected with

oxytetracycline (OTC) at a dose of 25 mg/kg body weight (Tanaka 1990, Glesleichter et

al. 1998); one was kept at Ripley's Aquarium, Myrtle Beach, SC, and the other at New

England Aquarium, Boston, MA. In 1999, an additional sand tiger (estimated at 164 cm

TL) at the New England Aquarium that had a spinal deformity was offered for use in this

study and fed OTC (that was injected into it's food). Each individual was re-

administered (injected or fed) OTC again approximately one year later, and one

individual was administered OTC a third time (Table 4.1). All three sharks were

sacrificed using buffered MS222 in either December 2000 or January 2001.

Table 4.1: Dates, aquarium, sex, lengths and method of administering oxytetracycline (OTC) to three sand tiger sharks, *Carcharias taurus*.

Shark #	Date	Aquarium	Sex	PCL	FL	TL	OTC method
OTC-1	10/15/1998	Ripley's	M	112	127	157	injected
	10/15/1999			138	157	201	injected
	1/18/2001			160	181	218.6	euthanized
OTC-2	10/15/1998	New England	M	110	125	152.5	injected
	11/4/1999			139	156	188	injected
	10/7/2000			-	-	-	fed
	12/13/2000			162	180	219	euthanized
OTC-3	3/3/1999	New England	M	-	-	164	fed
	11/21/1999			-	-	201	fed
	10/13/2000			-	-		fed
	12/13/2000			154	175	210	euthanized

Weights were obtained (by VIMS and NMFS) from 102 sand tiger sharks between 1963 and 1991, including 55 females (95 to 272 cm TL), and 47 males (100.7 to 259 cm TL). Data were fitted to the power equation, $W = a \bullet L^b$, (using SigmaPlot, SPSS Inc.), where W = weight (kg) and L = length (cm TL). A likelihood ratio test was used to determine whether differences between female and male weight-length parameters were significant or if a single set of parameters better described the data (Kimura 1980, Cerrato 1990, Quinn and Deriso 1999, Haddon 2001) (SAS Institute Inc. 1999).

RESULTS

Length Equations

Length measurements from 272 sand tiger sharks (137 female, 135 male) were obtained by VIMS and NMFS between 1963 and 2001. Females ranged from 95 cm TL to 277 cm TL, and males ranged from 98.4 cm TL to 248 cm TL. FL and PCL can be derived from TL by:

FL = 0.8471•TL - 0.592 $\qquad (r^2 = 0.99; n = 138)$

PCL = 0.7736•TL - 5.05 $\qquad (r^2 = 0.97; n = 134)$.

Vertebral Analysis

Percent agreement among readers (PA) was 67.7 % for the first set of blind reads and 75.0% for the second set, and the within-reader PA was 75.0% for reader one (the lead author) and 72.9% for reader two. Percent agreement +/- one yr was > 92 % for all reader comparisons. When grouped by 10 cm length increments, agreement for sharks ≤ 200 cm TL was 100 %, except for a single 1 yr disagreement in each set of readings, and 100 % +/- 1 yr for sharks ≤ 220 cm TL (Table 4.2). The Bowker, McNamara, and Evans-

Table 4.2: Percent agreement (PA) and PA +/- 1 year, for both sets of readings for sand tiger sharks, *Carcharias taurus*, when placed into 10 cm length (TL) groups.

Length Group (cm)	Read	First set of readings				Second set of readings			
		Agree	Agree +/- 1	PA	PA +/- 1	Agree	Agree +/- 1	PA	PA +/- 1
90.1-100	7	7	7	100	100	7	7	100	100
100.1-110	7	7	7	100	100	7	7	100	100
110.1-120	7	7	7	100	100	7	7	100	100
120.1-130	7	7	7	100	100	7	7	100	100
130.1-140	1	1	1	100	100	1	1	100	100
140.1-150	9	9	9	100	100	9	9	100	100
150.1-160	2	1	2	50	100	2	2	100	100
160.1-170	5	5	5	100	100	4	5	80	100
170.1-180	2	2	2	100	100	2	2	100	100
180.1-190	0	0	0	-	-	0	0	-	-
190.1-200	4	4	4	100	100	4	4	100	100
200.1-210	5	2	5	40.0	100	2	4	40	80
210.1-220	7	3	7	42.9	100	3	7	43	100
220.1-230	7	2	5	28.6	71.4	3	6	43	86
230.1-240	9	2	7	22.2	77.8	4	8	44	89
240.1-250	7	4	7	57.1	100	4	7	57	100
250.1-260	3	0	2	0	66.7	2	3	67	100
260.1-270	4	2	4	50	100	3	3	75	75
270.1-280	3	0	1	0	33.3	1	3	33	100
n =	96	65	89			72	92		
Percent Agree				67.7	92.7			75.0	95.8

Hoenig Chi-square tests of symmetry gave no indication that differences between and within readers were systematic rather than due to random error (X^2 test, $P > 0.05$ in all cases).

A linear regression gave a significant fit to the TL-CR data (TL = 10.753•CR + 36.786; $r^2 = 0.97$; $P < 0.0001$) (Figure 4.2). However, it was important to compare the mean back-calculated results from equations 1 through 3 with my mean sample TL data to see which method provided better biological accuracy for modeling growth.

The linear-modified Dahl-Lea method (equation 2) most accurately represented the mean sample length-at-age data. It produced mean back-calculated lengths-at-age within 9.1 cm of mean sample lengths-at-age for female sand tiger sharks, except for lengths of approximately 195 and 250 cm TL (Figure 4.3a). When applied to males, equation 2 produced mean back-calculated lengths-at-age within 9.8 cm of mean sample lengths-at-age for sharks <195 cm TL. At greater lengths, deviation from mean sample length-at-age ranged from 2.7 to 15.1 cm TL (Figure 4.3b). Lee's phenomenon was present with the individual back-calculated data. There was a tendency for some age classes (usually older ones) to underestimate the mean sample length-at-age data after the first few back-calculated ages (Tables 4.3 and 4.4). This is not too surprising considering the time frame over which samples were obtained, and the potential for sampling variation (i.e. where in the spinal column the vertebrae were removed). However, Lee's phenomenon was not apparent in the mean back-calculation values, which were, overall, very similar to the mean age-at-length data.

Figure 4.2: Relationship between centrum radius (CR) and total length (TL) for sand

tiger sharks (n=90).

$$TL = 10.753(CR) + 36.786$$
$$r^2 = 0.97$$

Figure 4.3: Mean deviation, from mean sampled total length, of three proportional back-calculation methods for (a) female, and for (b) male sand tiger sharks. Data points represent mean back-calculated lengths-at-age. A point on the x-axis would represent zero deviation from the sample mean length-at-age.

Table 4.3: Back-calculated total length (cm) of female sand tiger sharks. B = birth, n = sample size. Sample mean is the mean length of sharks captured at a given age. All lengths are in cm TL.

Age	n	B	Back-calculated age																
			1	2	3	4	5	6	7	8	9	10	11	12	13	14	15	16	17
0	14	101.6																	
1	1	104.7	117.3																
2	2	108.0	125.4	138.5															
3	3	102.3	118.0	133.5	145.7														
4	4	110.9	129.5	143.6	158.1	172.2													
5	1	94.5	109.5	130.8	152.7	169.0	185.7												
6	0	-	-	-	-	-	-	-											
7	2	111.1	128.3	142.4	158.3	171.4	182.6	192.7	203.3										
8	0	-	-	-	-	-	-	-	-	-									
9	0	-	-	-	-	-	-	-	-	-	-								
10	1	80.2	99.5	117.0	131.0	146.3	159.6	175.6	187.0	199.0	209.4	217.0							
11	1	85.8	102.5	121.0	139.9	156.0	167.7	181.1	193.2	204.4	217.2	225.7	234.7						
12	5	112.4	130.5	145.6	161.9	176.7	188.9	200.1	210.0	219.7	228.8	235.9	242.3	249.0					
13	4	112.9	129.2	144.3	158.1	171.6	183.7	195.1	205.1	214.9	224.6	232.6	238.6	243.8	248.9				
14	4	106.8	124.3	138.3	151.0	164.2	175.0	186.4	195.5	203.2	211.4	219.0	225.5	231.4	237.0	241.3			
15	1	80.2	91.1	108.0	123.2	143.0	163.3	177.1	193.2	202.5	209.9	215.5	223.4	229.1	236.2	243.6	249.5		
16	2	106.1	118.7	130.7	144.6	156.1	166.9	182.2	191.2	202.7	211.8	219.0	227.5	236.2	241.5	247.6	254.6	260.6	
17	2	107.7	124.1	137.1	149.0	159.4	171.0	181.0	191.2	202.0	210.2	218.5	227.4	235.5	243.1	250.5	257.1	262.8	267.6
Back-calc Mean		106.7	125.2	139.8	154.1	168.5	179.6	190.9	200.8	210.1	219.0	226.4	233.7	240.1	242.4	245.2	254.7	261.7	267.6
Sample Mean		108.5	120.8	141.5	150.7	177.6	194.0	-	208.5	-	-	220.0	240.0	250.2	251.5	243.5	253.0	263.0	270.5

130

Table 4.4: Back-calculated total length (cm) of male sand tiger sharks. B = birth, n = sample size. Sample mean is the mean length of sharks captured at a given age. All lengths are in cm TL.

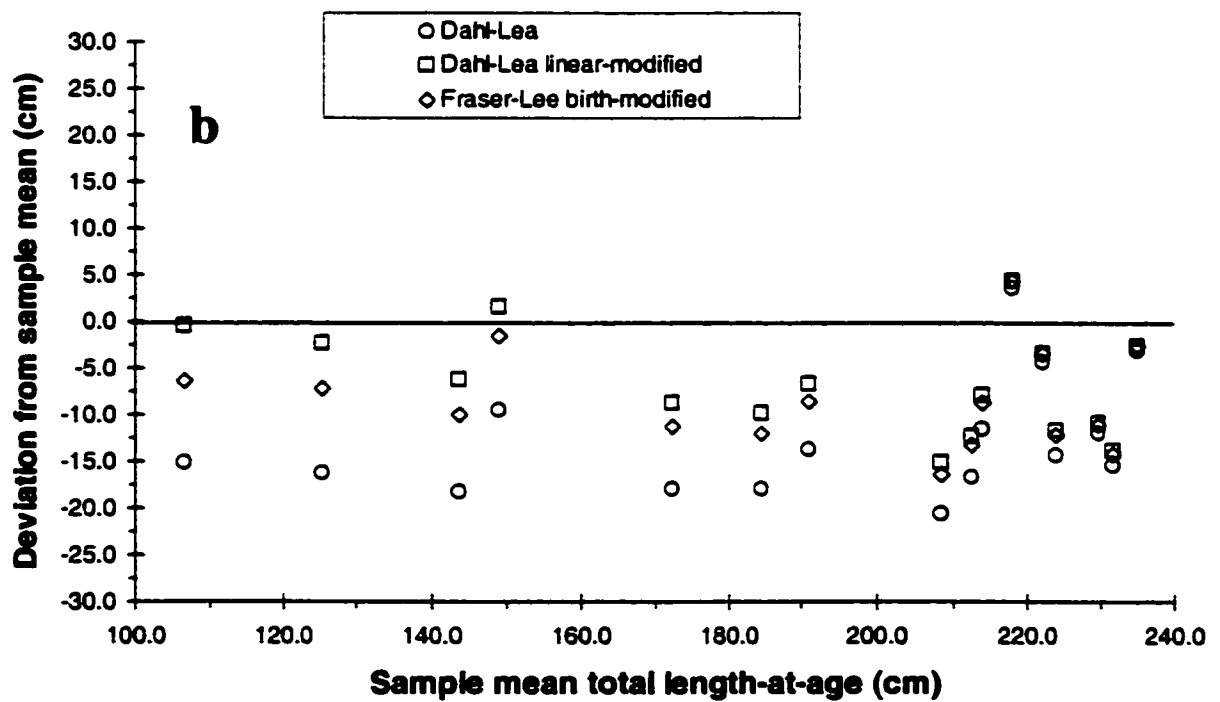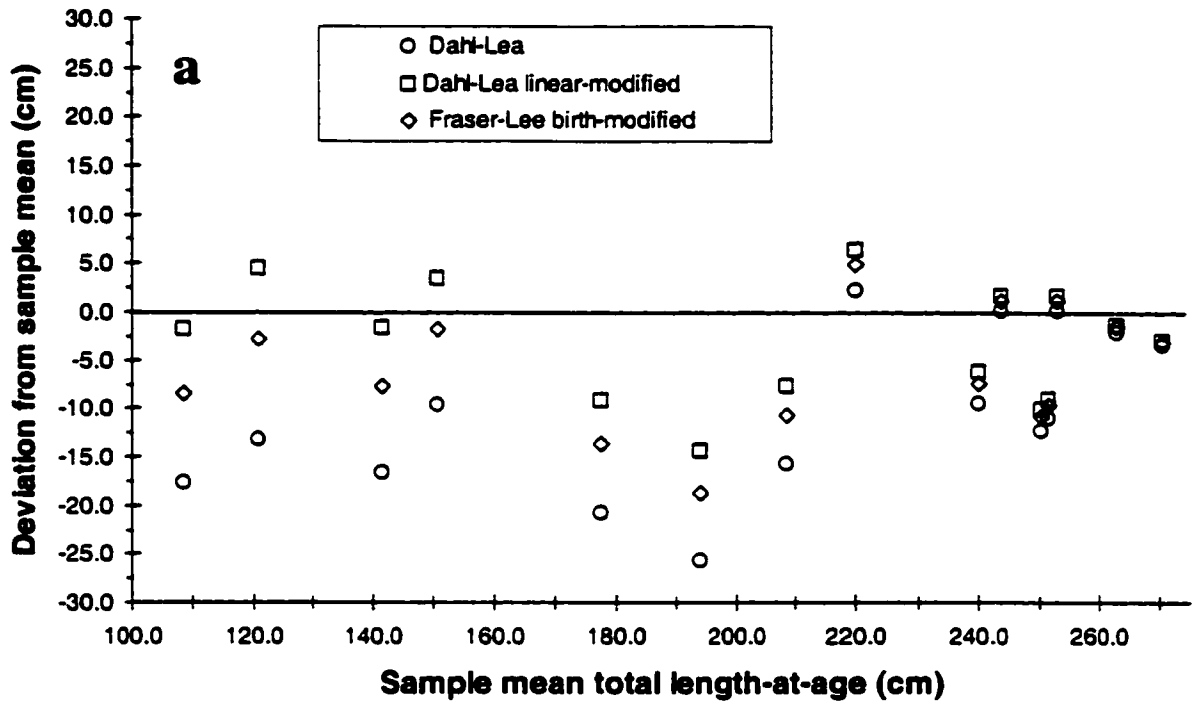	Age	n	B	1	2	3	4	5	6	7	8	9	10	11	12	13	14	15
								Back-calculated age									
0	9	102.1															
1	4	105.9	119.3														
2	5	111.5	128.4	139.8													
3	2	106.1	121.4	134.4	145.8												
4	3	104.4	122.0	137.0	151.9	161.8											
5	2	110.2	126.2	144.0	160.6	173.1	181.2										
6	1	104.1	121.5	134.0	147.1	161.6	174.5	184.3									
7	2	112.6	129.7	145.8	158.1	172.1	183.1	193.0	203.6								
8	2	108.4	126.2	141.5	156.3	169.2	178.9	189.2	198.2	208.0							
9	1	105.7	124.6	136.7	148.8	160.9	172.0	182.0	191.5	200.3	210.2						
10	0	-	-	-	-	-	-	-	-	-	-	-					
11	3	108.6	123.3	136.7	151.6	166.9	179.8	191.5	201.8	210.3	217.5	223.8	228.1				
12	5	104.5	120.2	135.3	148.1	161.3	172.5	182.9	191.8	199.8	206.5	213.0	218.9	223.5			
13	2	107.6	120.9	135.3	146.6	156.3	166.8	177.2	184.9	191.0	197.4	204.3	210.1	212.6	219.3		
14	1	96.1	112.3	128.3	144.1	155.7	166.5	175.1	182.8	189.1	193.0	198.0	203.0	207.5	212.1	215.9	
15	1	101.5	115.5	126.9	137.1	147.2	158.7	166.6	175.7	185.7	196.0	205.0	211.9	218.8	223.8	228.8	232.3
Back-calc Mean		106.0	122.9	137.5	150.5	163.5	174.7	184.2	193.4	200.2	206.1	212.3	217.8	218.8	218.6	222.4	232.3
Sample Mean		106.4	125.3	143.8	149.0	172.3	184.5	191.0	208.5	212.5	214.0	224.0	231.8	229.7	222.0	218.0	235.0

131

Vertebral age-at-length data from 48 female sand tiger sharks provided von

Bertalanffy parameters of L_∞ = 295.8 cm TL, k = 0.11 yr^{-1}, and t_0 = -4.2 years (Figure

4.4). von Bertalanffy parameters from the linear-modified Dahl-Lea back-calculations

(with or without sample data included) gave slightly lower k coefficients and slightly

higher L_∞ and t_0 values (Table 4.5). Results from mean back-calculated data had the

lowest standard error. Vertebral age data from 48 males provided Bertalanffy parameters

of L_∞ = 249.5 cm TL, k = 0.16 yr^{-1}, and t_0 = -3.4 years (Figure 4.4). Back-calculated

lengths-at-age for male sand tiger sharks (with or without sample data included) again

provided slightly lower k coefficients, slightly higher L_∞ and t_0 parameters, and mean

back-calculated data had the lowest standard error (Table 4.5). Vertebral age data for the

sexes combined (n=96) provided von Bertalanffy parameters of; L_∞ = 280.5 cm TL, k =

0.12 yr^{-1}, and t_0 = -4.1 years. Parameters resulting from back-calculated data for the

sexes combined produced results with similar trends as those for females and males

(Table 4.5). A likelihood ratio test showed that separate von Bertalanffy growth models

better describe the data for each sex than one model with the sexes combined (X^2 = 22.8;

df = 3; P = 0.000044).

Although I was missing samples from some winter months, relative marginal

increment (RMI) analysis indicates that the first postnatal and all subsequent rings form

annually between December and February. The smallest relative margins in my sample

occurred in February, followed by a consistent increase in RMI with the largest relative

margins occurring in October (Figure 4.5).

The administration of OTC was successful in marking vertebrae in 2 of the 3 sand

Table 4.5: von Bertalanffy growth parameters of female, male and sexes combined for sandtiger sharks in the western North Atlantic. Numbers in parentheses are standard errors.

Females	L_∞	k	t_0
Sample data (n=48)	295.8 (14.0)	0.11 (0.02)	-4.2 (0.5)
Back-calculations (n=366*)	302.4 (7.4)	0.09 (0.006)	-4.6 (0.22)
Mean back-calculation (n=18*)	308.3 (5.2)	0.09 (0.004)	-4.8 (0.21)
Back-calculations w/ sample data (n=414*)	305.3 (6.9)	0.09 (0.006)	-4.7 (0.20)
Males			
Sample data (n=48)	249.5 (7.2)	0.16 (0.02)	-3.4 (0.4)
Back-calculations (n=278*)	252.7 (6.1)	0.13 (0.009)	-4.1 (0.2)
Mean back-calculation (n=16*)	247.5 (3.6)	0.13 (0.009)	-4.2 (0.2)
Back-calculations w/ sample data (n=326*)	256.1 (5.4)	0.12 (0.008)	-4.3 (0.2)
Combined			
Sample data (n=96)	280.5 (9.4)	0.12 (0.01)	-4.1 (0.4)
Back-calculations (n=644*)	294.7 (6.5)	0.09 (0.005)	-4.8 (0.2)
Mean back-calculation (n=34*)	293.1 (16.0)	0.09 (0.01)	-5.0 (0.7)
Back-calculations w/ sample data (n=740*)	295.2 (5.7)	0.09 (0.004)	-4.8 (0.2)

*Not independent

Figure 4.4: von Bertalanffy growth curves fitted to female (n=48) and male (n=48)

sample data for sand tiger sharks. Estimates for parameters of the von Bertalanffy

growth function are summarized.

Figure 4.5: Results of relative marginal increment analysis indicating annual ring

formation likely occurs between December and February.

tiger sharks. The vertebrae from the animal with the spinal deformity did not mark, possibly due to the diseased nature of the spine or due to low weight estimates and subsequent low doses. The two sharks whose vertebrae were successfully marked by the OTC were both aged at 2 years for their date of capture in 1998. One animal had two OTC marks and the other had three (Table 4.1). The annual OTC marks in both specimens were located near points where rings had formed (Figure 4.6).

Weight-to-length relationships for female and male sand tiger sharks in the western North Atlantic were; $W = 1.3 \times 10^{-04} \cdot L^{2.4}$ ($r^2 = 0.84$, n=55) and $W = 9.0 \times 10^{-05} \cdot L^{2.5}$ ($r^2 = 0.84$, n=47) respectively, and $7.9 \times 10^{-05} \cdot L^{2.5}$ ($r^2 = 0.84$) for the sexes combined (Figure 4.7). A likelihood ratio test showed that a single equation for the sexes combined better describe the data than separate equations for each sex individually ($X^2 = 5.3$; $df = 2$; $P = 0.07$).

DISCUSSION

A high degree of variability exists in the periodicity of ring and growth band formation within and among taxonomic groups of elasmobranch fishes, and much of the variation observed in several lamniform sharks has not yet been explained (Branstetter, 1990; Branstetter and Musick, 1994; Wintner and Cliff, 1999). For example, Cailliet et al (1983) stated that shortfin mako sharks from the Pacific appear to have annual ring formation while Pratt and Casey (1983) stated that Atlantic specimens appeared to produce two rings per year. However, a new technique using bomb radiocarbon to validate ages in long-lived sharks was applied to a single shortfin mako and indicated that they form a single ring annually (Campana et al. 2002). This method requires vertebral

Figure4. 6: Sagittally cut vertebral section of OTC sand tiger shark #OTC-2 (from Table

4.1). Arrows without asterisks represent wild growth. Double asterisk indicates initial

OTC mark shortly after capture. Arrows with single asterisks indicate OTC marks and

captive growth rings. All three OTC marks can clearly be seen.

Figure 4.7: Weight- length relationship for sand tiger sharks. The upper dashed line is for females; the lower dashed line is for males; the solid line in between them is for the sexes combined and best describes the relationship for this species. W = weight (kg); TL = total length (cm).

Males (triangles):
$$W = 3.2 \times 10^{-6} \cdot TL^{3.383}; \; r^2 = 0.99$$

Females (open circles):
$$W = 8.2 \times 10^{-05} \cdot TL^{2.759}; \; r^2 = 0.99$$

Sexes Combined (solid line):
$$W = 4.4 \times 10^{-05} \cdot TL^{2.875}; \; r^2 = 0.99$$

samples from animals born prior to the early 1960's. Although I had some samples from the early 1960's, they were all very young animals, hence I was unable to apply the bomb radiocarbon method in this study.

Branstetter and Musick (1994) suggested that sand tiger sharks form two rings per year in their vertebral centra whereas my results support a hypothesis that only one ring is formed annually. The difference in ageing protocols between the two studies is almost certainly the cause of the different results. I feel it is necessary to state the reasons I did not follow the Branstetter and Musick (1994) protocol in this study, then discuss my results and comment on their ramifications for recovery of the western North Atlantic population.

Branstetter and Musick (1994) "counted and measured rings in the intermedialia". When the intermedialia was damaged, they counted along the corpus calcareum. I found that using the intermedialia as the primary counting surface for ageing sand tiger sharks could lead to errors. In addition to the distinct rings (narrow bands) that extended all the way across the intermedialia and matched up with rings on the corpus calcareum and the presence of notches (at or near the rings) along the outside arm of the corpus calcareum, the intermedialia contained subtle or indistinct bands. These 'indistinct bands' made using the intermedialia as the primary counting (and measuring) surface problematic for the following reasons: 1) they extended completely across the intermedialia, but did not appear on the corpus calcareum (nor were they associated with notches on the corpus calcareum); 2) they did not extend all the way across the intermedialia; 3) part-way across the intermedialia they blended into another indistinct band; 4) part-way across the intermedialia, they blended into a distinct band; 5) the number of indistinct bands

(between distinct bands) was inconsistent ranging from 0-5 in number. Additionally, some indistinct bands were seen on the corpus calcareum, but they did not match up with bands in the intermedialia and did not possess a corresponding notch along the outer arm of the corpus calcareum. These reasons were paramount in my decision to use the corpus calcareum as the primary counting and measuring surface, with the distinct rings in the intermedialia and notches as 'confirmation' of an annulus.

The radials of the intermedialia of carcharhinid sharks are relatively hard, robust and numerous, making it nearly solid. In contrast, the radials of the intermedialia in lamnoid sharks are less numerous, softer and quite fragile, and the large amount of interstitial space often prevents its presence in sectioned vertebrae. When present, the outer edge of the intermedialia in lamniform vertebral sections can become warped in a concave manner. When this occurs, the rings near the outer edge of the intermedialia become "bunched up" and indistinguishable. The bands on the corpus calcareum can also become more tightly grouped at the outer edge, particularly in larger/older animals, however the rings have a tendency to remain distinguishable due to the stronger (more stout) nature of the structure. Based on these observations, I suggest that future studies on the age and growth of lamniform sharks use the corpus calcareum as the primary counting and measuring surface.

I found that vertebral growth significantly increased with somatic growth (Figure 4.2), which along with the reliability of the centrum edge analysis (Figure 4.5) demonstrates vertebral growth patterns are a reliable indicator of age in sand tiger sharks. Precision was high between and within readers with limited differences (Table 4.2) that were attributable to random error. These results provided a high degree of confidence in

the accuracy and precision of my age assessments (from sample data) used in the von

Bertalanffy growth model, and hence in the resulting life history parameter estimates.

The similar von Bertalanffy growth parameter estimates generated from my sample data,

back-calculated data and the combination of the two indicate that my sample size was

sufficiently large and encompassed the known size range of males, and all but the very

upper end of the known size range of females. While my back-calculation results are, of

course, dependent on the assumption that growth has not significantly changed over time,

and are applicable only to sand tiger sharks, they demonstrate the importance of choosing

the appropriate method in order to minimize error (Figure 4.3a and 4.3b), which results in

a greater ability to accurately model growth.

Branstetter and Musick (1994) gave a weight-length equation for sand tiger sharks

of; $W = 1.62 \times 10^{-06} \cdot L^{3.15}$. This equation was later found to have an error in it, which has

not been published. The corrected weight-length equation is: $W = 1.62 \times 10^{-06} \cdot L^{3.24}$. My

data for length conversions and maximum size of sand tiger sharks are similar to those

form the corrected weight-length equation. The increased sample size (particularly for

smaller individuals) enhances the accuracy and precision of these estimates. More

importantly, I was able to determine that a single length-weight curve combined is

adequate for describing that relationship for both sexes.

The RMI conducted by Branstetter and Musick (1994) indicated that specimens

from the first part of the year (January-July) had an even number of bands while

specimens from the second part of the year (August–December). I found no such

relationship – animals from every month of the year from which I had more than a single

sample possessed both even and odd numbers of rings. My RMI analysis indicated that a

single ring is formed annually sometime between December and February (Figure 4.5).

Additionally, the results from the two OTC sharks support the hypothesis that a single

ring is formed annually. The annual OTC marks in both specimens were located near

points where rings had formed (Figure 4.6) even though they were kept under a constant

photoperiod and ambient temperature.

Centrum banding patterns may be related to physiological changes induced by

changes in environmental parameters such as temperature and photoperiod (Cailliet et al.

1986, Branstetter 1987), however, it has been shown not to be the case for some species

such as the little skate, *Raja erinacea* (Natanson 1993), and the Pacific angel shark,

Squatina californica (Natanson and Cailliet 1990, Cailliet et al. 1992). The north-south

migration of sand tiger sharks has been proposed as a possible reason that two rings were

formed in the vertebral centra each year (Branstetter and Musick 1994) with the primary

cue for the migration being either temperature or photoperiod. The primary cue for sand

tiger migration has not been demonstrated, but the fact that captive sand tiger sharks

appear to form a single ring in their vertebral centra each year makes those possibilities

less likely. Vertebral growth is inevitably linked to food intake, and a lack of food for

short periods of time can cause subtle bands to appear in vertebral centra of some species

(J. Gelsleichter pers comm.). This may explain the "indiscrete bands" I saw in sand tiger

vertebrae, and play a role in the annual formation of rings in the centra.

The life history parameters presented by Goldman (1998) resulted in k

coefficients that were ½ of those presented by Branstetter and Musick (1994). This is

because Goldman (1998) simply doubled the age estimates from Branstetter and Musick

(1994) by assuming that one ring was formed annually in the vertebral centra (e.g. a 5

year old would then be considered to be 10 years of age), and not from the examination of any vertebral samples. In contrast, the estimations of sand tiger life history parameters presented herein are the combined result of using an independently developed ageing protocol (applied to vertebral samples from 96 sand tiger sharks), a subsequent RMI analysis and the use of a direct validation method (OTC), all of which support a hypothesis that one ring is formed annually in vertebral centra. As such, I believe my results are a much better indicator of sand tiger shark life history parameters than either (Goldman 1998) or Branstetter and Musick (1994).

Branstetter and Musick (1994) characterized sand tiger growth based on mean back-calculated lengths-at-age as follows; "growth was 25-30 cm per year for ages 0-1, 20-25 cm per year for ages 2-3, and 15-20 cm per year for ages 4-5. Subadults and adults had a growth rate of 10-15 cm per year for ages 6-7, and growth declined to 5-10 cm per year for ages 8 and greater." They also characterized growth in females and males to be nearly identical throughout life. My results indicate that growth is similar up to age 5 at which point-in-time females begin outgrowing males at a significant rate, and that two separate growth curves should be used to describe the rate at which each sex attains their maximum size (Figure 4.4). Mean back-calculated lengths-at-age from this study indicate that growth averaged 14.5-18.5 cm per year for ages 0-1, 13-14.5 cm per year for ages 2-3, and 11 cm per year for age 4. For ages 5 and 6, growth averaged 10-11.2 cm for females and 9.2-9.5 for males; and for age 7 females averaged 9.3 cm per year whereas males averaged 6.8 cm per year. For sand tiger sharks $\geq$ 8 years of age, the growth rates declined to an average of 6.4 cm per year for females and 4.6 cm per year for males.

Female sand tiger sharks become sexually mature at a length of 220-230 cm TL and males mature at 190-195 cm TL (Gilmore et al. 1983). Previous estimates of age at maturity stated that the equivalent ages to those lengths are 6 years for females and about 4 years for males (Branstetter and Musick 1994). My age-at-length results place age at sexual maturity at 9-10 years for female sand tiger sharks, and at 6-7 years for males. Reproduction in captivity (from copulation to parturition) has been documented in South Africa and Australia. A female sand tiger shark born at Underwater World aquarium, Australia, in 1992 became pregnant in 2000 (resulting in two pre-term stillborn pups ~70-80 cm TL) (Henningsen et al. in review). Additionally, a male sand tiger born at the New York aquarium in 1994 has recently (2001-2002) been exhibiting pre-copulatory behavior (H. Walters pers. comm.). These data, although captive, provide corroboration to my estimates of age at sexual maturity.

Gilmore (1990) stated that all female sand tiger sharks he examined from Florida to North Carolina between March and January were impregnated and that no resting stage took place in the reproductive cycle of this species. However, Branstetter and Musick (1994) presented strong evidence that a resting stage did occur and that the reproductive cycle was at least 2 years. They presented VIMS records from 29 mature female sand tiger sharks caught off Virginia (during the 1980's and early 1990's) that were all noted as either postpartum or in a resting state with small ovarian egg follicles. Since then, I have records (from the VIMS survey) for an additional 17 mature females that were in the same postpartum or resting stage condition. The mother of the afore mentioned female born at Underwater World, Australia was captured pregnant in 1992, and while in captivity has given birth two more times; in 1997 and 1999 (Henningsen et al, in review).

A gestation period of 9-12 months leaves little to no energetic "turn-around" time for a female to build-up her reserves and go through another reproductive cycle, unless there is a resting year. If a female carried pups through a 12-month gestation period, she would immediately have to mate again in order to reproduce the following year. Any time delay in mating would "throw off" her timing for parturition, and at some point-in-time she would require a resting period. The current body of evidence strongly supports a two-year reproductive cycle for female sand tiger sharks. However, preliminary evidence from captive male sand tiger sharks indicates that they may mate annually (A. Henningsen pers. comm.).

Maximum observed age for female and male sand tiger sharks in this study was 17 and 16, respectively. These ages are close to the maximum documented ages of sand tiger sharks in captivity. Govender et al. (1991) reported a male that had been in captivity at an aquarium in Durban, South Africa for 16 years, and there is currently a 20 year old female (as of 2002) at the National Aquarium in Baltimore, MD, USA (A. Henningsen pers. comm.). Branstetter and Musick (1994) estimated longevity at 30-35 years by extrapolating their von Bertalanffy curves generated from back-calculated data. Applying the same technique to my data, longevity may be as high as 40 years for females and 30 years for males. Applying the formula $5*ln2/k$ (which determines the time required to reach 95 % of its asymptotic length – see Cailliet et al. 1992, Neer and Cailliet 2001) to my back-calculated and sample data provided longevity estimates of 32-38 for females and 22-27 for males.

My estimates of sand tiger shark life history parameters show that they are much slower growing than previously thought. Since my mean back-calculated lengths-at-age

gave the smallest standard error in von Bertalanffy estimates (Table 4.5), they may better represent the life-history parameters of this species and should probably be used when determining vital rates. Considering the large population depletion suffered by sand tiger sharks in the western North Atlantic over the past 20 years, this information is crucial for accurately assessing the ability of the population to recover, and further justifies the need for this species to be fully protected. The life history parameters presented here also allow for a re-adjustment of previously predicted vital rate estimates that can aid managers in taking appropriate steps for sand tiger shark protection and conservation.

Chapter 5

Demographic analysis of sand tiger sharks, *Carcharias taurus*, in the western North Atlantic, based on new life history parameters

INTRODUCTION

In Chapter 4, I presented the results of my study on sand tiger shark (*Carcharias taurus*) age and growth in the western North Atlantic and compared them to previously published life history parameters for the area (Branstetter and Musick 1994). My results support a hypothesis that only a single ring is formed annually in sand tiger shark's vertebral centra (instead of two) and, as such, this species growth completion rate (*k*) is slower than previously reported. This almost certainly makes them more vulnerable to exploitation and over-fishing. More importantly, new demographic analyses are required to estimate vital rates in order to advise fishery managers about this population's current status and potential recovery time. It is also necessary to re-evaluate the impact on the population from additional mortality due to fishing.

Using life history parameters from Branstetter and Musick (1994), previous demographic analyses have estimated vital rates for sand tiger sharks from age-based life-table and Leslie matrix models (Goldman 1998, Mollet and Cailliet 2002, Cortés 2002), age- and stage-based matrix models (Mollet and Cailliet 2002) and an intrinsic rebound potential model (Smith et al. 1998). Of those studies, however, Cortés (2002) is the only one to have incorporated uncertainty into vital rate estimates. Incorporating the effect of uncertainty in vital rates into demographic analysis of elasmobranchs is a relatively new and important aspect of fisheries ecology, because the results of deterministic models may lead to errors in management decisions (Musick 1999, Heppell 2000a, Cortés 2002). Mollet and Cailliet (2002) stated that a "flaw" in their sand tiger demographic models

152

was the "lack of confidence bands for population growth estimates" which may be generated by incorporating uncertainty with Monte Carlo simulation. They strongly recommended that Monte Carlo "uncertainty analysis" be carried out. This is important because model input parameters such as survivorship are difficult to obtain for elasmobranchs (particularly for young individuals), and because incorporating variability into models may lead to a better understanding of how life history strategies and population dynamics respond to exploitation.

Cortés (2002) showed that uncertainty could be incorporated into life-table analysis via Monte Carlo simulation to generate population growth rates (λ and r) and other population statistics with confidence bands. His results, from 38 shark species, show that these types of life-tables produce "nearly identical results" to pre-breeding census, age-structured Leslie matrix models (which he also presented). I used this life-table approach (along with the life history parameters from Chapter 4) in modeling the demography of sand tiger sharks.

Elasticity (proportional sensitivity) analysis is becoming a standard tool in demographic analysis (Heppell et al. 2000a). Elasticity is a perturbation measure that quantifies the proportional change in population growth rate as a function of a proportional change in other vital rates such as survival, fecundity or growth (Heppell 1998, Heppell et al. 1999, De Kroon et al. 2000). Elasticity analysis from single, deterministic approaches can lead to inappropriate management decisions (Heppell 2000a, Cortés 2002). As such, I calculated elasticities with uncertainty incorporated via Monte Carlo simulation in my models in order to more accurately gauge the relative importance of proportional changes in fertility, juvenile survival and adult survival on the

intrinsic rate of population increase (r, where $r = ln\lambda$; λ = finite population growth rate) (Heppell 1998, Heppell et al. 2000b, De Kroon et al 2000, Caswell 2001).

Density-dependent compensation is a standard concept in ecology and fisheries biology (Holden 1974 and 1977, Krebbs 1985). Potential compensatory mechanisms in fishes include: increased survivorship in pups, juveniles and adults an increase in fecundity or size at birth, an increase in growth rate leading to earlier age at maturity, decreasing (shortening) reproductive periodicity and immigration of animals from other areas. In sharks, a decrease in the reproductive periodicity may be possible in some species, but there is no evidence to support its occurrence, and no species has been shown to increase its fecundity due to exploitation. There is no known immigration to, or emigration from, the western North Atlantic sand tiger population and this should probably not be considered a viable option for compensation in this species. Sminkey and Musick (1995) found a small increase in juvenile sandbar shark (*Carcharhinus plumbeus*) growth rate after heavy exploitation, but this was not accompanied by a change in age at maturity. Cortés and Parsons (1996) proposed an increase in offspring size for the bonnethead shark (*Sphyrna tiburo*) as a possible compensatory mechanism in that species. The best evidence of density-dependent compensation in elasmobranchs points towards an increase in the survivorship of pups and juveniles (Walker 1992,Walker 1998, Hoenig and Gruber 1990, Musick et al. 1993).

Direct evidence of increased survivorship in pups and juveniles due to exploitation has been obtained for lemon sharks (*Negaprion brevirostris*) ≤ 53 cm precaudal length (Gruber et al. 2001). The survival rate of young of the year (YOY) and juvenile lemon sharks was made from a mark-depletion experiment and were negatively

correlated with estimated initial abundance, demonstrating density-dependent survival rates in that species. The results of Gruber et al (2001) also support the assumption that first year survival can be adequately determined through life-table (or Leslie matrix) methods.

A shortcoming of life-table models is that they assume density-independence, so I consequently incorporated density-dependent compensation in the present model when imposing fishing mortality. I increased survivorship of YOY and juvenile age classes (up to age at first reproduction) based on output from the 'intrinsic rebound potential' model of Au and Smith (1997, also see Smith et al. 1998), which provides a prediction of the net increase in sub-adult survivorship (l_α) at a given level of F along with a prediction of the 'intrinsic rebound potential' (r at maximum sustainable yield = r_{MSY}) of a species.

Demographic analyses are often used for management and conservation purposes. However, it is important that the results of any model (such as those presented here) are used to form hypotheses that can be compared to, and tested with, empirical data (e.g. catch per unit effort). The goals of this Chapter of my dissertation research were to: 1) provide new estimates of demographic parameters for sand tiger sharks based on the life history results in Chapter 4; 2) determine if the Au and Smith (1997, also see Smith et al 1998) 'intrinsic rebound potential' model would adequately predict the necessary compensation to keep demographic parameters stable when fishing mortality was imposed (i.e. attempt to 'connect' the life-table and intrinsic rebound potential models in a manner that would lead to biologically reasonable results and conclusions); and 3) provide results that could be used for comparative purposes with future demographic analyses of sand tiger sharks.

MATERIALS AND METHODS

The Life-table Model

I used age-structured life-tables based on a yearly time step and a 2-year reproductive cycle (applied to only females) to model the demography of sand tiger sharks in the western North Atlantic. Monte Carlo simulation (n = 5,000) was used to incorporate uncertainty in demographic parameters and generate population growth rates (λ and r), generation time ($\overline{A}$), net reproductive rate (R_0), reproductive value (v_x), stable age distribution (c_x), fertility, juvenile and adult elasticity, and mean life expectancy. Population doubling or halving times were calculated from the mean intrinsic rate of population growth (r) from model simulations.

To include uncertainty in parameter estimates, I established probability distributions for maximum age (ω), age at first reproduction (α), fecundity (m_x = number of female pups per female per year) and survivorship at age (S_x). The estimated maximum age of female sand tiger sharks (from Chapter 4) is 30 to 40 years, which was represented by a linearly decreasing distribution scaled to a total relative probability of 1 (Figure 5.1a).

Female sand tiger sharks reach sexual maturity between 220 and 230 cm TL (Gilmore et al. 1983), and age at first maturity has previously been estimated to be 6 years of age (Branstetter and Musick 1994). Based on my results from Chapter 4, age at first maturity occurs at 9 to 10 years of age. Age at first reproduction is required for the model, hence 10 to 11 years of age was used. With no available information to specify a

particular age at first reproduction as the "most likely", a uniform probability distribution was used for this parameter (Figure 5.1b).

Sand tiger sharks mate between February and April off Florida's east coast and during April and May off North Carolina, and have a 9-12 month gestation period (Gilmore et al. 1983, Gilmore 1993). While some contention still surrounds the reproductive periodicity of sand tiger sharks, the current evidence (see Chapter 4) supports a two-year reproductive cycle, which was used in my models.

Adelphophagy in sand tiger sharks results in a maximum litter size of two pups, with a sex ratio of 1:1 (Gilmore et al.1983, Last and Stevens 1994). I represented total fecundity as a fixed distribution of 2. Female-specific fecundity (m_x; number of females per female per year) was obtained by dividing the total number of offspring in a litter by the reproductive cycle in years.

There are several methods available for estimating natural mortality (M), and hence survivorship in the absence of fishing ($S = e^{-M}$). I estimated the probability of annual survival at the beginning of each age using the following six life-history methods following Cortés (2002) (see Appendix 1 for equations): 1) Hoenig (1983), 2) Pauly (1980), 3) Chen and Watanabe (1989), 4) Peterson and Wroblewski (1984), and 5 and 6) Jensen (1996). Although method 4 uses dry weight, wet weight seems to yield more realistic estimates of survival for sharks (Cortés 2002 and pers. comm.). The mean water temperature (23.8 °C) from the VIMS long-line survey, from 1974 to 2000, was used in the Pauly (1980) model.

I used a relatively cautious approach when setting probability distributions for

Figure 5.1: Probability distributions for (a) sand tiger shark longevity and (b) age at first reproduction.

a)

Longevity

y-axis: Relative Probability (.000, .044, .088, .132, .176)
x-axis: Age (years) (30.000, 32.500, 35.000, 37.500, 40.000)

b)

Age at first reproduction

y-axis: Probability
x-axis: Age (years) (10.000, 10.500, 11.000)

survivorship. I used the lowest and highest values from the six methods as lower and upper bounds for setting survivorship probability distributions. The first three age classes (ages zero to two; < 1.5 m TL) were represented by uniform distributions (Figure 5.2a), as there are no data that would give reason to suspect that one estimate is more realistic than another. For sand tiger sharks age three to 40 (> 1.5 m TL), I assumed that survivorship would more likely be at the higher end of the distribution rather than the lower end because of their larger size, so I used a linearly ascending distribution scaled to a total relative probability of 1 (Figure 5.2b), with the highest estimate of survivorship twice as likely to occur in model simulations as the lowest.

Annual population growth rates ($\lambda = e^r$) were obtained by iteratively solving the discrete form of the Lotka-Euler equation (Goodman, 1982, Roff 1982):

$$1 = \sum_{x=1}^{\omega} e^{-rx} l_x m_x$$

where l_x is the probability of an individual being alive at the beginning of age x, m_x is the number of female offspring produced annually by a female at age x, and ω is maximum age. Generation time ($\overline{A}$) was calculated as

$$\overline{A} = \sum_{x=1}^{\omega} e^{-rx} x l_x m_x$$

which is the mean age of the parents of the offspring produced by a population at the stable age distribution (Caswell 2001).

The reproductive value distribution (v_x) was obtained through

Figure 5.2: Examples of probability distributions used for age specific survivorship. (a)

Distributions as set for ages zero through two, (b) distributions as set for ages three to 40.

a)

Age zero survivorship

Probability

0.835   0.852   0.868   0.885   0.901

b)

Age five survivorship

Relative probability

0.836   0.852   0.869   0.885   0.901

$$\frac{v_x}{v_o} = \frac{e^{r(x-1)}}{l_x} \sum_{j=x}^{\omega} e^{-rx} l_x m_x$$

where v_o is the reproductive value at birth (which is equal to one), and j denotes all the ages a female will pass through from x to ω (Goodman 1982, Ebert 1999, Cortés 2002).

The stable age distribution (c_x) was obtained through

$$c_x = \frac{e^{-rx} l_x}{\sum_{x=1}^{\omega} e^{-rx} l_x}$$

The reproductive value and stable age distribution columns were used to calculate elasticities following Caswell (2001) and Cortés (2002) as

$$e_{ij} = \frac{a_{ij} \, v_i \, w_j}{\lambda \, \langle w, v \rangle}$$

where a_{ij} is the element corresponding to row i of column j (survivorship), v_i is the value of row i in the reproductive value column (v_x), w_j is the value of row j in the stable age distribution column (c_x), and $\langle w, v \rangle$ is the scalar product of row elements in the w (c_x) and v (v_x) distributions. I calculated elasticities for age zero survival (fertility), juvenile survival and adult survival by summation of elasticity elements across relevant age classes, which may present viable management options.

The mean life expectancy was obtained by

$$\overline{X}_{Life \, Expectancy} = \frac{1}{-\ln(\sum_{x=0}^{\omega} P_x)}$$

where P_x is the mean survivorship of the probability distribution for age x (Lawless 1982).

The net reproductive rate (R_0) was obtained by

$$R_0 = \sum_{x=0}^{\omega} l_x m_x$$

Population halving ($t_{0.5} = \frac{\ln 0.5}{r}$) and doubling ($t_2 = \frac{\ln 2}{r}$) times were calculated from the mean intrinsic rate of population growth (r) from model simulations.

The uncertainty in demographic traits (age specific survival and fecundity, age at first reproduction and maximum age) was randomly selected from each trait's probability distribution during Monte Carlo simulation. Ninety-five percent confidence intervals for each parameter were obtained from the 2.5th and 97.5th percentiles.

Density-Dependent Compensation

As with all life-tables, the model described above is a density-independent model. To allow for density-dependent compensation (for a given level of F) due to the changes in mortality of fished ages, I used the predicted net increase in sub-adult survivorship from Au and Smith's (1997 – also see Smith et al. 1998) 'intrinsic rebound potential' model. This model provides, as output, a prediction of the net increase in pre-adult survivorship needed for a population to 'rebound' back to stationary equilibrium ($r = 0$) when a given level of F is imposed (and assumes $r = 0$ before F begins and that Z [= $M+F$] is sustainable).

The Au and Smith (1997) model solves for 'r' using a variant of the Lotka-Euler equation (See Au and Smith 1997 or Smith et al. 1998 for details of converting the Lotka-Euler equation given above to):

$$e^{-(M+r)} + I_\alpha b \ e^{-(r\alpha)} [1 - e^{-(M+r)(\omega-\alpha+1)}] = 1$$

where I_α = the net increase in sub-adult survivorship (from age 0 to age at first reproduction, α), and b = fecundity (females per female per year). Setting $r = 0$, changing M to the total level of mortality Z with $I_\alpha = I_{\alpha.Z}$ and solving for I_α, the solution to the above equation is:

$$I_{\alpha.Z} = \frac{1 - e^{-Z}}{b[1 - e^{-(Z)(\omega - \alpha + 1)}]}$$

where $I_{\alpha.Z}$ = the predicted net increase in sub-adult survivorship at a given level of Z.

I used Monte Carlo simulation (n = 5,000) to incorporate uncertainty in demographic parameters and generate estimates of I_α. I then evenly distributed the net increase in I_α, between when F = 0 and when F$_{0.025}$ was imposed, amongst the sub-adult age classes in the life-table model and ran Monte Carlo simulations with F and the I_α 'factor' included. The method of calculating the amount of increased survivorship for each age class and evenly distributing it (I_α) among sub-adults is given in Appendix 2. Survivorship was accordingly increased (compensation included) for ages zero through nine.

All simulations (life-table and intrinsic rebound potential) were implemented with Microsoft Excel spreadsheet software equipped with proprietary add-in risk assessment

software (Crystal Ball, Decisioneering Inc., Denver, CO) and Microsoft Visual Basic for Application macros.

Fishing Mortality Scenarios

In 1997, the National Marine Fisheries Service (NMFS) prohibited possession of sand tiger sharks in U.S. Atlantic waters (NMFS 1999). A 1998 NMFS large coastal sharks stock assessment provided historical estimates of fishing mortality (F) for this 'group' from 1974 through 1997 (NMFS 1998). Estimates of F during those years ranged from a minimum of 0.03 (from 1974 to 1976) to a maximum of 0.21 (in 1995 and 1996). These values were all deemed too high, resulting in further depletion of the sand tiger shark population (NMFS 1998, Cortés pers. comm.). Recovery is not yet apparent in the sand tiger shark population (Musick et al. 2000), therefore, instituting any kind of fishery would be unwarranted. However, considering the updated information on life history parameters (Chapter 4) along with the fact that sand tiger sharks are still taken as bycatch in several fisheries (Casey and Kohler 1990, Musick et al. 1993, NMFS 1999), investigating the potential impacts of F on the population for future management purposes is essential. Additionally, it allows further investigation into the use of the Au and Smith (1997) model as a predictor of the required density-compensation necessary to keep vital rates stable when additional mortality is imposed from fishing.

I examined the effect of fishing mortality (F) on sand tiger sharks using $F_{0.025}$ for two reasons. First, this value is less that the minimum estimate from 1974-76 in the 1998 NMFS assessment, making it a reasonable starting place. Second, it allows direct comparison of these results with those obtained in my demographic analysis for salmon sharks in Chapter 2. I examined two fishing scenarios for sandtiger sharks incorporating

density-dependent compensation. Since all age classes are exposed to fishing mortality via bycatch, the main fishing scenario I used for sand tiger sharks included $F_{0.025}$ at all ages. For comparative purposes, I also ran an additional scenario where $F_{0.025}$ began at age five (approximately 180-190 cm TL).

RESULTS

Natural mortality estimates from the six methods used ranged from 0.180 to 0.097. Minimum and maximum age-specific survivorships (P_x) are given in Table 5.1. The Hoeing (1983) method predicts the average natural mortality for the whole population (relative to ω). This method provided the highest survivorship values for ages zero through 17 in all models. The Peterson and Wroblewski (1984) method, which is weight-length based, produced the highest survivorship values for ages 18 through 40 in all models, and the lowest value (by only 0.001) for age zero. The Pauly (1980) method produced the lowest estimates of survivorship for ages two through 40.

The results of initial life-table model simulations (with F = 0) indicate that the western North Atlantic sand tiger shark population would be decreasing at a rate of just over 1 % per year with a population halving time of 62.4 years (Table 5.2). The 95 % confidence values show the variability (from uncertainty) of parameter inputs and indicate that under all combinations from the probability distributions of ω, α, and P_x used in the model, the western North Atlantic sand tiger shark population may still be in decline at a rate between 0.09 and 2.1 % per year (Table 5.2). Deterministic estimates of 'r' conducted with the Solver minimization function in Microsoft Excel show that age at

Table 5.1: Minimum and maximum survivorship estimates for sand tiger sharks used in life-table model simulations. Double dashed line indicates where F begins. Density-dependent compensation included for all age classes before single dashed line.

Age	F=0 Survivorship		F=0.025 @ all ages a=1.014 up to age 10		F=0.025 @ ages 5+ a=1.014 up to age 10	
	Minimum	Maximum	Minimum	Maximum	Minimum	Maximum
0	0.835	0.901	0.826	0.891	0.847	0.908*
1	0.836	0.901	0.827	0.891	0.848	0.908*
2	0.836	0.901	0.827	0.891	0.848	0.908*
3	0.836	0.901	0.827	0.891	0.848	0.908*
4	0.836	0.901	0.827	0.891	0.848	0.908*
5	0.836	0.901	0.827	0.891	0.827	0.891
6	0.836	0.901	0.827	0.891	0.827	0.891
7	0.836	0.901	0.827	0.891	0.827	0.891
8	0.836	0.901	0.827	0.891	0.827	0.891
9	0.836	0.901	0.827	0.891	0.827	0.891
10	0.836	0.901	0.816	0.879	0.816	0.879
11	0.836	0.901	0.816	0.879	0.816	0.879
12	0.836	0.901	0.816	0.879	0.816	0.879
13	0.836	0.901	0.816	0.879	0.816	0.879
14	0.836	0.901	0.816	0.879	0.816	0.879
15	0.836	0.901	0.816	0.879	0.816	0.879
16	0.836	0.901	0.816	0.879	0.816	0.879
17	0.836	0.901	0.816	0.879	0.816	0.879
18	0.836	0.901	0.816	0.879	0.816	0.879
19	0.836	0.902	0.816	0.879	0.816	0.879
20	0.836	0.902	0.816	0.880	0.816	0.880
21	0.836	0.903	0.816	0.881	0.816	0.881
22	0.836	0.903	0.816	0.881	0.816	0.881
23	0.836	0.904	0.816	0.882	0.816	0.882
24	0.836	0.904	0.816	0.882	0.816	0.882
25	0.836	0.905	0.816	0.882	0.816	0.882
26	0.836	0.905	0.816	0.883	0.816	0.883
27	0.836	0.905	0.816	0.883	0.816	0.883
28	0.836	0.906	0.816	0.883	0.816	0.883
29	0.836	0.906	0.816	0.884	0.816	0.884
30	0.836	0.906	0.816	0.884	0.816	0.884
31	0.836	0.906	0.816	0.884	0.816	0.884
32	0.836	0.907	0.816	0.884	0.816	0.884
33	0.836	0.907	0.816	0.884	0.816	0.884
34	0.836	0.907	0.816	0.884	0.816	0.884
35	0.836	0.907	0.816	0.885	0.816	0.885
36	0.836	0.907	0.816	0.885	0.816	0.885
37	0.836	0.907	0.816	0.885	0.816	0.885
38	0.836	0.907	0.816	0.885	0.816	0.885
39	0.836	0.907	0.816	0.885	0.816	0.885
40	0.836	0.908	0.816	0.885	0.816	0.885

*Actual value was 0.913; Increases in sub-adult survivorship was not allowed to surpass maximum adult survivorship when F = 0

Table 5.2: Estimates of demographic parameters and elasticities for sand tiger sharks in the western North Atlantic (population growth rates, λ and r; generation times, $\overline{A}$; net reproductive rate, R_0). Numbers in parentheses are ranges

F (starts at age)	λ	r	$\overline{A}$	R_0
0	0.989 (0.979-0.999)	-0.0111 ([-0.0209]-[-0.0009])	17.1 (15.6-17.8)	0.8 (0.7-1.0)*
0.025 (0)	0.973 (0.963-0.983)	-0.0276 ([-0.0373]-[0.0169])	16.8 (15.4-17.5)	0.6 (0.5-0.8)
0.025 (5)	0.979 (0.970-0.990)	-0.0211 ([-0.0308]-[0.0100])	16.6 (15.2-17.3)	0.7 (0.6-0.9)

Elasticity			Mean Life	Population
Fertility	Juvenile	Adult	Expectancy	doubling time
5.5 (5.3-6.0)	54.9 (53.1-56.7)	39.6 (37.7-41.5)	7.3 (6.9-7.7)	-62.4
5.6 (5.4-6.1)	55.6 (54.0-57.3)	38.8 (36.9-40.6)	6.4 (6.1-6.7)	-25.1
5.7 (5.4-6.2)	56.2 (54.6-57.8)	38.1 (36.4-39.8)	6.5 (6.2-6.9)	-32.8

*Actual value = 0.986

first reproduction accounted for a greater amount of variation in 'r' than maximum age (Table 5.3).

The mean reproductive rate of the population was estimated to be 0.8. Mean generation time was 17.1 years, and mean life expectancy was estimated to be 7.3 years. Summed elasticity values were highest for juvenile survival followed by the adult survival and then fertility, indicating that an increase in juvenile mortality would have the largest effect on the population growth rate, r (Table 5.2).

The predicted stable age distribution (with ω = 40, α = 10, and F = 0) was dominated by the first six age classes (Figure 5.3). The young-of-the-year comprised approximately 12.8 % of the population with the next five age classes comprising another 43.0 % of the population. The predicted stable age distribution indicates that a total of 74.4 % of the population is comprised of individuals that are younger than the age at first reproduction (9 years of age or less). An examination of the stable age distribution when $F_{0.025}$ was imposed showed minimal changes. In reality, however, whenever there is exploitation, the age distribution is likely to have shifted from stability.

Fishing for sand tiger sharks

The Au and Smith (1997) model predicted that a 1.4 % increase in the survivorship of each sub-adult age class would compensate for $F_{0.025}$ (Table 5.4). Results from the life-table simulation indicated that the predicted compensation was not sufficient to keep 'r' from decreasing. Along with the decrease in the population growth rate, there was a decrease in generation time, the net reproductive rate and mean life expectancy (Table 5.2). The predicted population halving time was shortened to 25.1

Table 5.3: Influence of maximum age and age at first reproduction on the intrinsic rate of population growth for sand tiger sharks in the western North Atlantic.

	Age at first reproduction (α)	
Maximum age (ω)	9	10
30	-0.005	-0.013
35	-0.003	-0.011
40	-0.002	-0.010

Figure 5.3: Predicted female stable age distribution for sand tiger sharks in the western

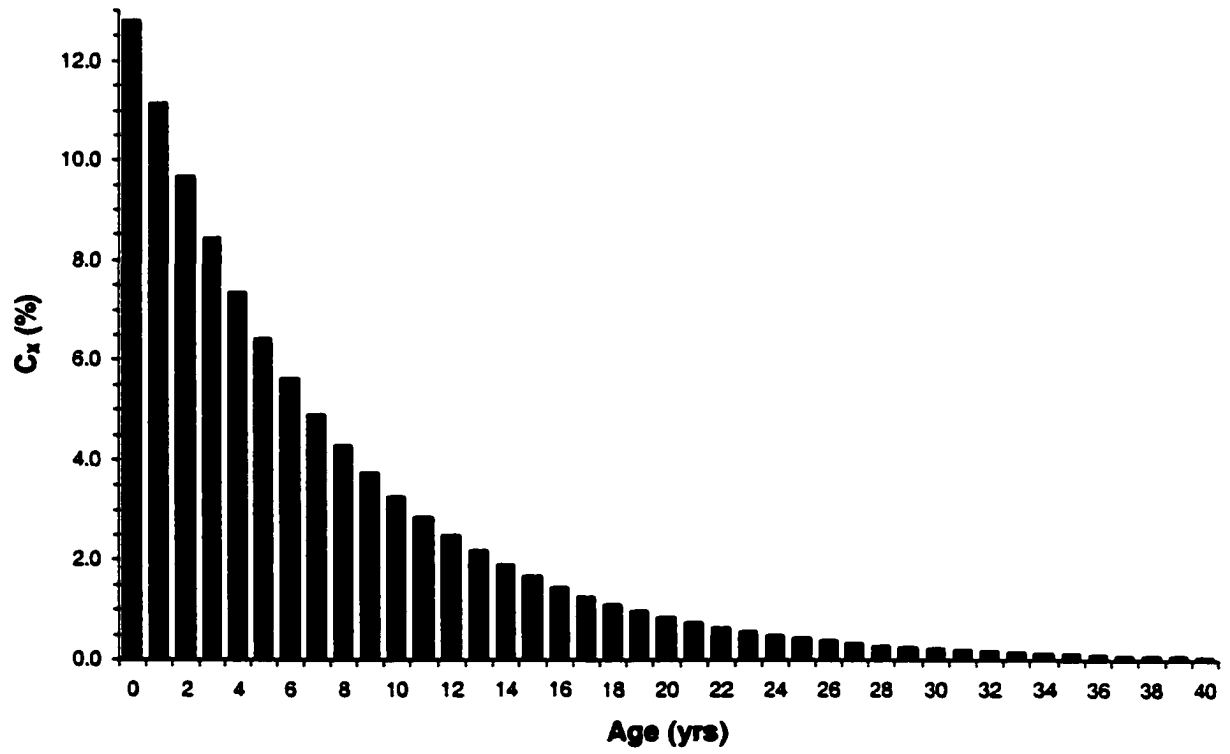North Atlantic (ω = 40 yrs, α = 10, and F = 0).

Table 5.4: Sub-adult survivorship compensation values from Monte Carlo simulations of the Au and Smith (1997) density-dependent model for estimating the 'intrinsic rebound potential' of fish populations. F = fishing mortality, l_α = net increase in sub-adult survivorship, r_F = "intrinsic rebound potential" (predicted intrinsic rate of population increase in response to F), l_α ratio = predicted proportional difference in sub-adult survivorship between different levels of F, a = predicted proportional increase in survivorship per sub-adult age class.

F=	l_α	r_F =	l_α ratio	a=
0.00	0.2618	0.00	-	-
0.025	0.3010	0.0085	1.150	1.014

years. Fishing at $F_{0.025}$ brought about subtle, but predictable, changes in elasticities. The importance of juvenile survivorship to the population growth rate increased the most, while a smaller increase was seen in fertility elasticity and adult survival elasticity decreased slightly (Table 5.2).

Additional Scenario ($F_{0.025}$ begins at age 5)

This life-table model was run to see if the combination of decreased fishing mortality at ages zero through four along with the predicted increase in sub-adult survivorship could compensate for a fishing mortality of $F_{0.025}$. Population statistics did not decline by as much as when all ages are fished (which is what would be expected), however, the combination of no fishing mortality on ages zero through four and compensation (up to age at first maturity) were still not enough to keep the population from a greater rate of decline relative to when F = 0 (Table 5.2). Trends in elasticities were similar to the previous model ($F_{0.025}$ for all ages) with juvenile survival elasticity increasing in its importance to the population growth rate, adult survival elasticity decreasing slightly and fertility elasticity increasing slightly.

DISCUSSION

Sand tiger shark population status

The decline of the western North Atlantic sand tiger shark population over the past 20 years has been well documented (Musick et al. 1993, Musick et al. 1998, Musick 1999, Castro et al. 1999, NMFS 1998, NMFS 1999, Compagno 2001). This has caused sand tiger sharks to be placed under legal 'protected' status and to be placed on the endangered species candidate list (Musick et al. 2000). This species is also currently listed as vulnerable by the IUCN in its Red List of Threatened Animals. Musick et al.

(2000) stated that the population might be stabilizing under the current NMFS fishery management plan (FMP), but that no recovery is apparent. The results presented here (under the stated conditions used in model simulations) indicate that the western North Atlantic sand tiger shark population may be continuing to decline, and that recovery has not yet occurred.

Musick (1999) stated that one of the two most vexing problems in assessing vulnerability and extinction risk in marine fishes is assessing uncertainty (variability) in estimating vital rates and other population parameters. Only one of the previous attempts to model sand tiger demography incorporated uncertainty (Cortés 2002), and one incorporated fishing mortality, but no uncertainty or density-dependent compensation when fishing mortality was imposed (Goldman 1998). Most importantly, all previous studies used life history parameters based on Branstetter and Musick (1994), which were shown to be inaccurate in Chapter 4 of this dissertation. As such, I incorporated the new estimates of life history parameters and uncertainty into vital rate estimates through Monte Carlo simulation, and examined one possible mechanism for density-dependent compensation when fishing mortality is imposed. As such, the results of the demographic models presented herein are probably more representative of the current status of the sand tiger shark population in the western North Atlantic and of their vulnerability to fishing mortality. However, my model simulation results need to be tested with empirically derived data.

Model simulation assumptions and limitations

Monte Carlo simulation was used because this probabilistic approach allows the inclusion of a range of values that reflect the uncertainty in estimates of demographic

traits (maximum age, age at first reproduction, fecundity and age-specific survivorship). I used distributions for these traits that I thought would reasonably approximate the biology of sand tiger sharks.

Sand tiger sharks have been exploited to varying degrees over the past 25 years (through bycatch and some directed fishing), which may have violated the assumption of a stable age distribution. If exploitation rates have been relatively consistent over the years since achieving protected status, however, it is less likely that the assumption of a stable age distribution was violated. Nonetheless, the predicted stable age distribution provides insight into the general age-specific composition of the population.

Overall, the statistical distributions I used to describe survivorship seemed reasonable, although the lower bounds used may be less realistic for larger individuals (Table 5.1). I dealt with this by setting the distributions for sharks greater than 1.5 m TL as shown in Figure 5.2b, instead of discarding the lowest estimate as was done by Cortés (2002). By doing so, I felt I used a slightly more cautious approach. Cortés (2002) assigned a higher probability to estimates of natural mortality obtained from the Peterson and Wroblewski (1984) method since its results are based on empirical, rather than estimated, parameters and generally gave higher values of survivorship. In this study, the Peterson and Wroblewski (1984) method provided the highest estimates in all model scenarios for sharks above 18 years of age. Assigning estimates of M from their model the highest probability would have lowered vital rate estimates, as values obtained from that model were not the highest for the first 18 age classes. (Ages 18 through 40 only comprised 8.5 % of the predicted stable age distribution – Figure 5.3). The manner in which my survivorship probability distributions were set for sharks three years of age and

greater, gave the highest estimated survivorship value twice the probability of occurring

in model simulations regardless of the method it was calculated from (Figure 5.2b).

Since young animals are likely to have lower survivorship than older animals and are

potentially the most difficult for which to estimate natural mortality, I felt it was a more

cautious approach to use uniform distributions for ages zero through two (< 1.5 m TL).

Density-independent models assume invariability in vital rates over time. While

we know that vital rates do vary over time, it is extremely difficult to collect and continue

to update the biological information required for most shark species. The life table

models used herein appear to be "robust" to deviations of the assumptions of traditional

density-independent population and fisheries models (e.g. invariance of vital rates over

time) (Cortés 2002).

Elasticities and density-dependent compensation

Elasticity analysis for sharks has shown that population growth rates are generally

much more sensitive to perturbations of juvenile and adult survival than to the survival of

age-zero individuals or fecundity (Heppell et al. 1999, Cortés 2002). This is a more

typical pattern for long-lived animals in general whether marine or terrestrial (Heppell et

al. 1999, Heppell et al. 2000b, Cortés 2000), and suggests that the protection of age-zero

animals would be insufficient to aid in the recovery of declining shark populations.

Therefore, management efforts need to focus on juvenile and adult portions of the

population to effectively aid in the recovery of elasmobranch species. While in some

cases examined, juvenile and adult sharks appear to be equally susceptible to increased

mortality (Cortés 2002). My results for sand tiger sharks indicate that juveniles would be

the most important group of individuals, followed by adults, for management to focus on

(Table 5.2). Cortés (2002) produced an elasticity continuum for 38 shark species, which corresponds with the well-known 'r - K' continuum (Musick 1999). My elasticity calculations for sand tiger sharks place them near the lower end of that continuum.

Elasticity analysis provides useful insight into the effects of decreasing the survival of one or more ages or stages of a population. However increases in fecundity or a change in the age at first reproduction could offset the effect of reduced survival of adult ages. The ultimate benefit of elasticity analysis is in its predictive ability - one does not have to wait for a population response (or lack of one) to understand the potential effects of increased mortality on particular ages or groups of ages in the population. This is critical as recovery times of shark populations are likely to be long due to their general life-history characteristics.

Heppell et al. (1999) and Cortés (2002) evaluated the potential for density-dependent compensation by calculating the ratios of mean adult survival elasticity to mean fertility elasticity and of mean juvenile survival elasticity to mean fertility elasticity. For example, a ratio of juvenile survival to fertility elasticities of 2.0 indicates that a 10 % decrease in juvenile survival would have to be compensated for by a 20 % increase in fertility to return to its original 'r'. They deemed that the required compensatory response was not possible if its magnitude exceeded the biological limits of age zero survival (= 1) or fecundity of a given population. For sand tiger sharks, the ratio of mean adult survival elasticity to mean fertility elasticity was 6.98, and the ratio of mean juvenile survival elasticity to mean fertility elasticity was 10.2. Both of these values vastly exceed the potential for this species.

My inclusion of density-dependent compensation in life-table model simulations where fishing mortality was imposed, by using the I_α (net increase in sub-adult survivorship) value generated by the Au and Smith (1997) model, provided fairly reasonable results. However, the amount of predicted compensation in sub-adult survivorship was not enough to keep population growth rates stable when F was imposed, and the 'intrinsic rebound potential' ($r_{F=0.025} = 0.0085$) was not achieved (Table 5.4)[1]. This may be a result of using the rebound potential model in this manner, a lack of the 'intrinsic rebound potential' model's ability to accurately predict the required compensation for this species, or due to the biological parameter inputs for sand tiger sharks used in my models. Additionally, I_α predictions may have fallen short of keeping population statistics stable due to assumptions of that model (e.g. it assumes $r = 0$ to begin with, and that Z is sustainable). Future investigation of the use of the intrinsic rebound potential model in the manner presented here should focus on this aspect. If the I_α predictions were representative of the true potential for sub-adult survivorship to increase, this would mean that sand tiger sharks are even more susceptible to exploitation than previously thought. It appears that 'connecting ' the life-table models used by Cortés (2002) and the intrinsic rebound potential model of Au and Smith (1997) is useful and should be applied to other elasmobranch species to better evaluate the performance of the method. Initial indications (from this study) are that using I_α in this capacity could become a useful tool for future demographic modeling of elasmobranch and other long-lived fishes.

---

[1] Distributing I_α in different ways (e.g. giving entire increase in sub-adult survivorship to age zero, or ages zero through three) produced nearly identical results.

Conclusion

Demographic analysis is extremely useful in evaluating potential population productivity and changes caused by imposing various conditions of fishing mortality (Caughley 1977, Hoeing and Gruber 1990). Continuing advances in modeling techniques for estimating vital rates of long-lived fishes are beginning to reveal more insight into their population growth rates and productivity.

The use of Monte Carlo simulation does not eliminate the need for further data gathering or sensitivity tests (Cortés 2002). Important additional data to gather to enhance predictive power of the models and elasticity analysis used herein include better information on natural mortality (M) and longevity. The ability to obtain refined estimates of natural mortality (M), possibly through tag-recapture data, would be useful for model simulations. The information required in order to enhance demographic modeling of sand tiger sharks will likely be slow in coming as it is difficult to gather, but the pursuit of refined data (and models) is a necessity if we are to better model the demography of all elasmobranch fishes.

The present demographic analysis provides new information that improves our understanding of sand tiger shark population dynamics, and gives fishery managers a more accurate idea of the population's current status and sensitivity to fishing mortality. Elasmobranchs tend to have low productivities relative to other marine fishes (Musick 1999), however there is a relatively wide range among species. My estimates of sand tiger shark population statistics are at the lower (slower growing) end of the continuum Cortés (2002) generated for vital rates of 38 other shark species, and the general r – K continuum. My model simulations suggest that the sand tiger shark population may still

be slowly declining and that it is probably more sensitive to fishing mortality than previously thought. In order to test the model, empirical data on the current F on sand tiger sharks due to bycatch and catch per unit effort trends is needed. Continuing to gather data on sandtiger shark bycatch and further refinement of population parameter estimtes are critical for future assessments of their population status.

Aside from reducing sand tiger shark bycatch as much as possible, the focus of management needs to be placed on ways to preserve the reproductive capacity of the population and allow for the survival of adults in their best-contributing reproductive years. Considering the low reproductive rate of sand tiger sharks, this would correspond to a relatively large range of ages and sizes. Increasing juvenile survivorship via reduced fishing mortality would (obviously) allow more individuals to reach reproductive age, but survival of the first several reproductive ages are critical to the recovery of this population.

Chapter 6

A comparison of growth completion rates of endothermic and ectothermic sharks

In the Introduction Chapter of this dissertation, I put forward a general hypothesis regarding the possible effects of endothermy on life history parameters such as growth completion rate (k). Elevated body temperature in several lamniform shark species is considered to be a highly evolved aspect of their biology that directly relates to their functioning as highly active apex predators in cool temperate and boreal environments (Block et al. 1993, Block and Finnerty 1994, Naylor et al. 1997, Lowe and Goldman 2001, Bernal et al. 2001). The physiological ecology of any species is instrumental not only in understanding its environmental niche, but in providing clues about species' life history parameters that have evolved over time to their current state. Garland and Carter (1994) emphasized the inherent link between physiological ecology and evolution quite eloquently by stating:

> *"Physiological ecology is concerned with the way that physiological traits fit*
> *organisms for the ecological circumstances in which they live, so there is always,*
> *by definition, an implicit evolutionary component to it."*

They further stated that:

> *"The field of physiological ecology is fundamentally evolutionary to the extent*
> *that it considers how organisms came to be the way they are and how they might*
> *change in the future."*

The relative rate of growth is a critical component of every species' life history strategy (Musick 1999). A comparison of growth completion rates (k) is a standard method for examining life history strategies and species limitations, and provides insight

184

into species ecology and vulnerability (Branstetter 1990, Cortés 2000). Considering the link between physiological ecology and evolution, the fact that several teleost and elasmobranch fishes are endothermic and that many of them are commercially fished, it is somewhat surprising that the question of whether endothermic fishes achieve their maximum size at a faster rate than ectothermic fishes has not been addressed. A faster rate of growth can lead to earlier age at maturity, higher intrinsic rates of increase and greater potential for resilience in the face of high exploitation.

Elasmobranch fishes have developed their current life history strategies over the past 400 million years. Relative to most other fishes, life history patterns in elasmobranchs are generally characterized by slow growth rates, long lifespan, late sexual maturity, low fecundity and long gestation times (Musick et al. 2000). Branstetter (1990) examined general trends in life history traits of 27 shark species, grouping sharks based on growth completion rates, litter size and size at birth relative to adult females. Cortés (2000), examined life history patterns and correlations between traits related to body size, reproduction, age, and growth in 164 shark species. Both studies showed similar trends amongst groups of shark species and placed sharks in similar life history categories base on body size, offspring size, k coefficient, longevity and litter size, however no separate comparison of these trends between endotherms and ectotherms were made.

The goal of this dissertation Chapter was to make the first general qualitative comparison of trends in growth completion rates (k; yr^{-1}) of endothermic and ectothermic sharks that achieve similar maximum length and live in similar temperature regimes. I examined general trends of several life history traits relative to the female growth

completion rates of seven ectothermic and seven endothermic shark species (Table 6.1), including multiple entries for some species to represent different geographic locations (Table 6.2). Growth completion rates were compared to female maximum total length (TL), mean pup TL at birth, mean estimates of female longevity, median sea-surface temperature (SST) at which species occur, mean gestation time and litter size (Table 6.2). (Growth completion rates for sexes combined were used when k values for females were unavailable, and are noted accordingly in Table 6.2). Trends in growth completion rates were also compared to the percentage of offspring length to maximum female length (%BL) in order to factor out the effects of body size (Cortés 2000) (Table 6.2). A variety of sources were used to obtain parameter estimates, and are listed in Appendix 3.

Trends in life history traits relative to growth completion rates

Length at birth, maximum length and longevity

Both ectotherms and endotherms showed decreasing trends in maximum TL, longevity and length at birth relative to increasing growth completion rates (Figures 6.1, 6.2 and 6.3). These trends are not surprising as faster growth completion rates are generally associated with shorter lifespan and maximum length achieved, and large adults tend to produce relatively large pups. The trends I observed do not differ from those reported by Branstetter (1990) and Cortés (2000). However, when Cortés (2000) factored out the effect of body size (by comparing k with %BL), the relationship became slightly positive. This occurred for the endotherms I examined, however the ectotherms continued to show a decrease in %BL relative to increasing k (Figure 6.4). The

Table 6.1: Scientific names, common names and general distribution of ectothermic and endothermic shark species examined in comparison of growth completion rates (k).

Ectotherms	Common name	General distribution
Carcharias taurus	Sand tiger shark	Temperate to sub-tropical
Carcharhinus falciformes	Silky shark	Temperate to tropical
Carcharhinus plumbeus	Sandbar shark	Temperate to tropical
Carcharhinus obscurus	Dusky shark	Temperate to tropical
Carcharhinus signatus	Night shark	Warm temperate to tropical
Prionace glauca	Blue shark	Cool temperate to tropical
Cetorhinus maximus	Basking shark	Boreal to cool temperate

Endotherms		
Lamna ditropis	Salmon shark	Boreal to cool temperate
Lamna nasus	Porbeagle shark	Boreal to cool temperate
Isurus oxyrinchus	Shortfin mako shark	Warm temperate to tropical
Carcharodon carcharias	White shark	Cool temperate
Alopias vulpinus	Common thresher shark	Temperate to tropical
Alopias supercilliosus	Bigeye thresher shark	Temperate to tropical*
Alopias pelagicus	Pelagic thresher shark	Temperate to tropical

*Can tolerate temperatures as low as 6 °C (Smith et al. in press)

Table 6.2: Female life history traits used for comparison of ectothermic and endothermic shark species. % BL = 100(mean length at birth/ female maximum length); SST = sea surface temperature. All lengths are cm TL; gestation period is in months.

Ectotherms	k (yr^{-1})	Maximum length	Median SST	Longevity	Mean length at birth	% BL	Gestation period	Maximum litter size
Carcharhinus falciformes (NWGM)	0.153*	305	23	22	81.5	26.72	20	15
Carcharhinus falciformes (SGM)	0.091	308	23	22	100	32.47	12	15
Carcharhinus obscurus (WNA)	0.039	371	23	40	100	26.95	12	14
Carcharhinus plumbeus (WNA1)	0.059	234	23	30	62.5	26.71	10.5	13
Carcharhinus plumbeus (WNA2)	0.086	233	23	30	62.5	26.82	10.5	13
Carcharhinus signatus (WNA)	0.125*†	275	14		70	25.45		
Carcharias taurus (WNA)	0.090	318	20	35	100	31.45	10.5	2
Cetorhinus maximus (All)	0.040*	960	20	32	160	16.67	12	6
Prionace glauca (ENP)	0.251	260	12	20	40	15.38	10.5	40
Prionace glauca (WNA)	0.160	327	12	20	40	12.23	10.5	40
Prionace glauca (WNP)	0.160	280	12	20	40	14.29	10.5	40
Endotherms								
Alopias pelagicus (WNP)	0.085	375	20	29	170	45.33	12	2
Alopias supercilliosus (WNP)	0.090	422	20	20	100	23.70	12	2
Alopias vulpinus (ENP)	0.124	550	19	25	132	24.00	9	4
Carcharodon carcharias (ENP)	0.058*	594	15	45	135	22.73	12	9
Carcharodon carcharias (SWA)	0.065*	594	15	45	135	22.73	12	9
Isurus oxyrinchus (ENP)	0.072*	394	19	28	65	16.50	16.5	12
Lamna ditropis (ENP)	0.170	260	10	25	87	33.46	9	5
Lamna ditropis (WNP)	0.140	260	10	25	87	33.46	9	5
Lamna nasus (WNA)	0.061	365	10	45	67.5	18.49	10	5

* k coefficient is for sexes combined. † median value for range given by Branstetter 1990. NWGM = northwestern Gulf of Mexico; SGM = southern Gulf of Mexico; WNA1 = western North Atlantic 1980-1981; WNA2 = western North Atlantic 1990-1992; ENP = eastern North Pacific; WNP = western North Pacific; SWA = southwestern Atlantic.

FIGURE 6.1: Comparison of growth completion rate (k) and maximum total length in
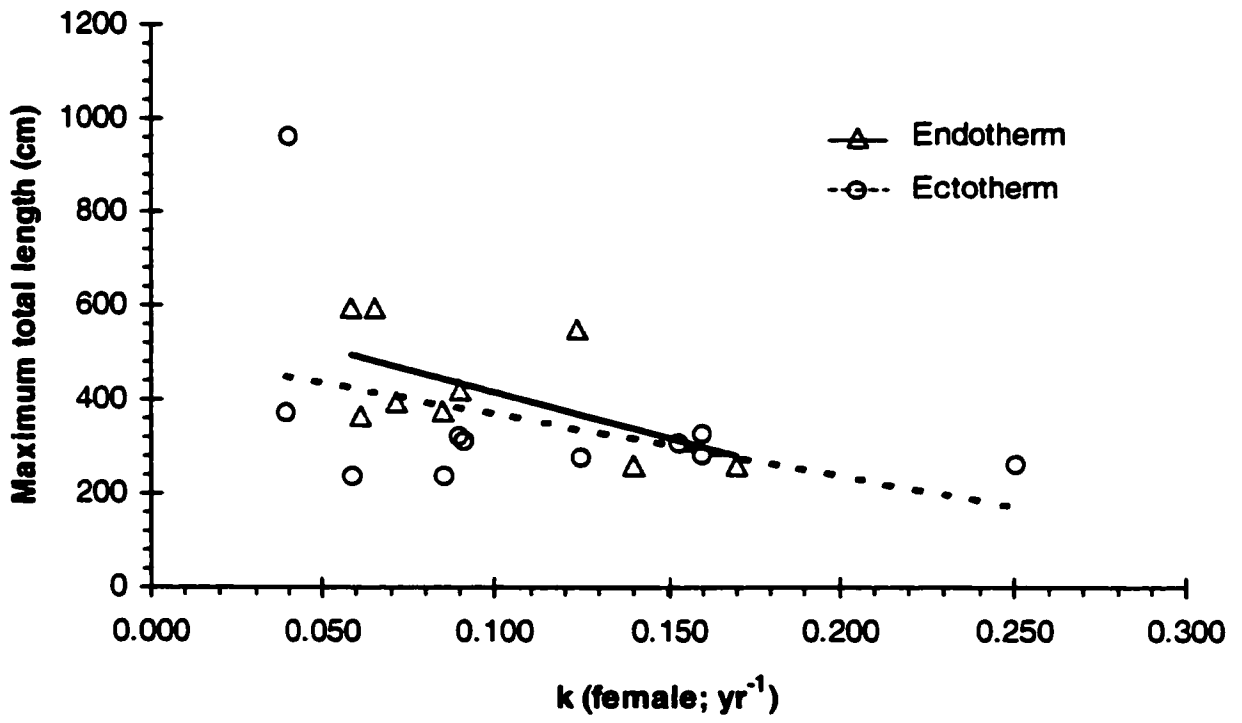
ectothermic and endothermic sharks.

FIGURE 6.2: Comparison of growth completion rate (k) and longevity in ectothermic
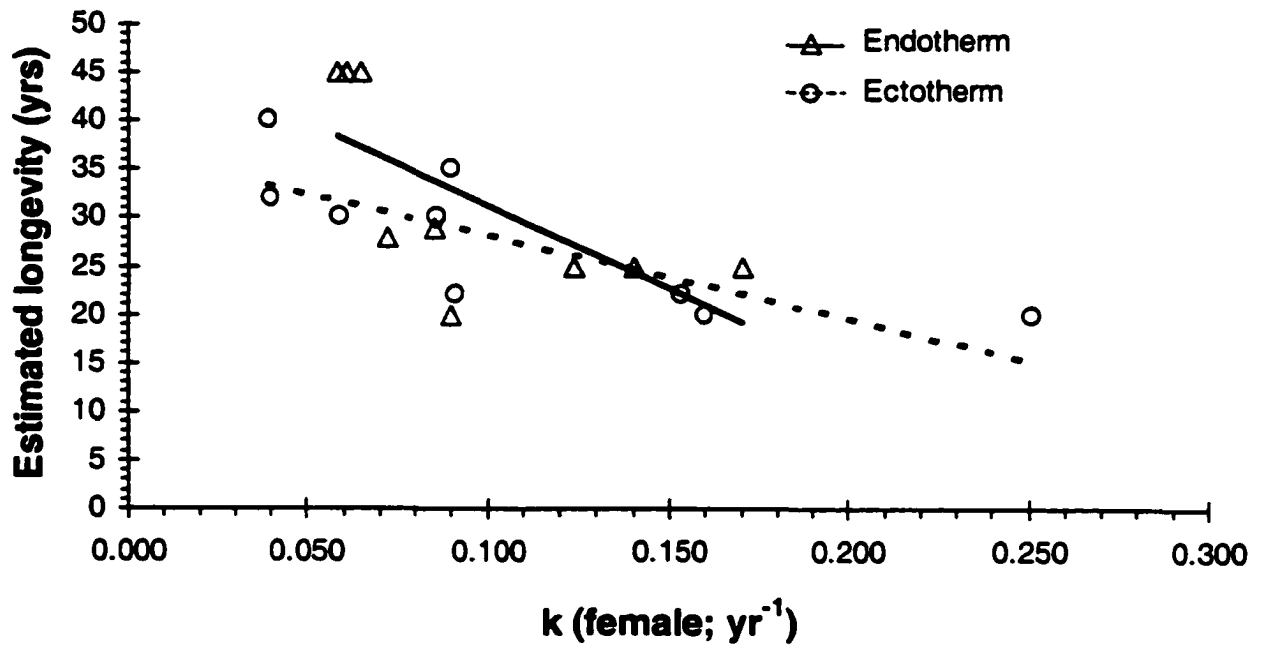
and endothermic sharks.

FIGURE 6.3: Comparison of growth completion rate (k) and mean total length at birth in ectothermic and endothermic sharks.
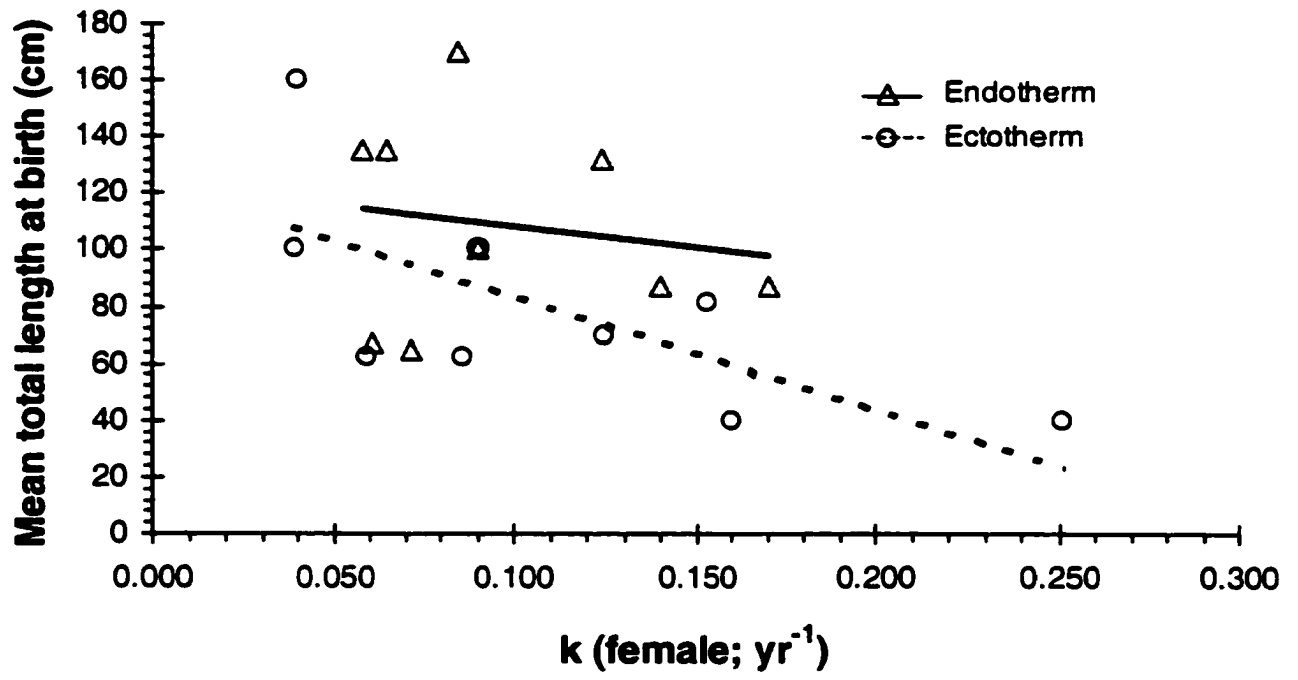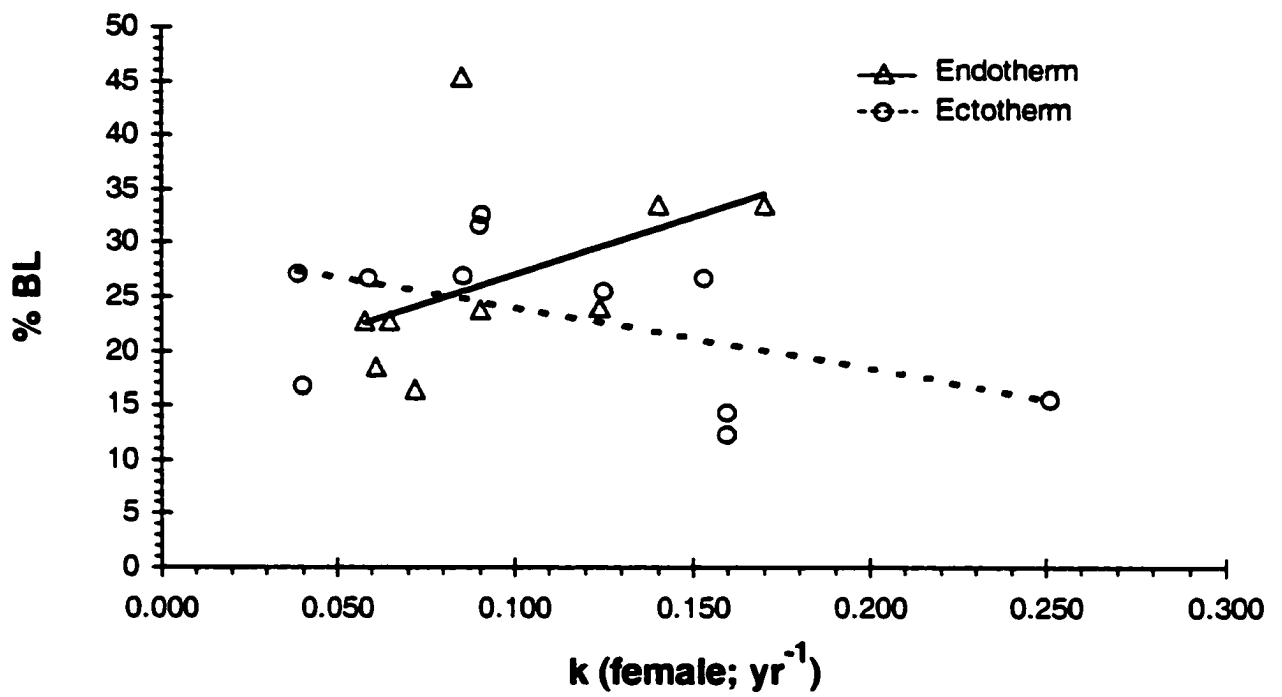
FIGURE 6.4: Comparison of growth completion rate (k) and percentage of offspring

length to maximum female length (%BL) in ectothermic and endothermic sharks.

decreasing trend in %BL relative to the growth completion rates for ectotherms is completely dependent on the blue shark data; when removed, the relationship of %BL to *k* became positive.

SST, gestation period and litter size

Decreasing trends in median SST and gestation period were observed relative to increasing growth completion rates in both ectotherms and endotherms (Figures 6.5 and 6.6). It is interesting that faster growth completion rates were accompanied by lower SST, however if the blue shark and night shark data were removed, the relationship between SST and *k* in ectotherms became positive, which is probably more likely to be the case for temperate and tropical shark species. The interesting result shown in Figure 6.5 is that for ectotherms and endotherms with similar growth completion rates, endotherms typically occurred in cooler water.

Litter size increased with increasing growth completion rates for ectotherms, but decreased slightly for endotherms (Figure 6.7). The large increase in the litter size of ectotherms is driven by blue shark litter size; the increase became very slight when those data were removed. Even so, this comparison shows that endothermic sharks with the fastest growth completion rates tend to have smaller litters than ectothermic sharks with similar growth completion rates.

Possible effects of endothermy

The results of Chapters 1 and 4 of this dissertation further furled my long-standing curiosity regarding the role of endothermy in the life history strategies of lamnid (the so-called mackerel) and alopiid (thresher) sharks. Six of the seven life history traits

FIGURE 6.5: Comparison of growth completion rate (k) and median sea-surface temperature where ectothermic and endothermic sharks occur.
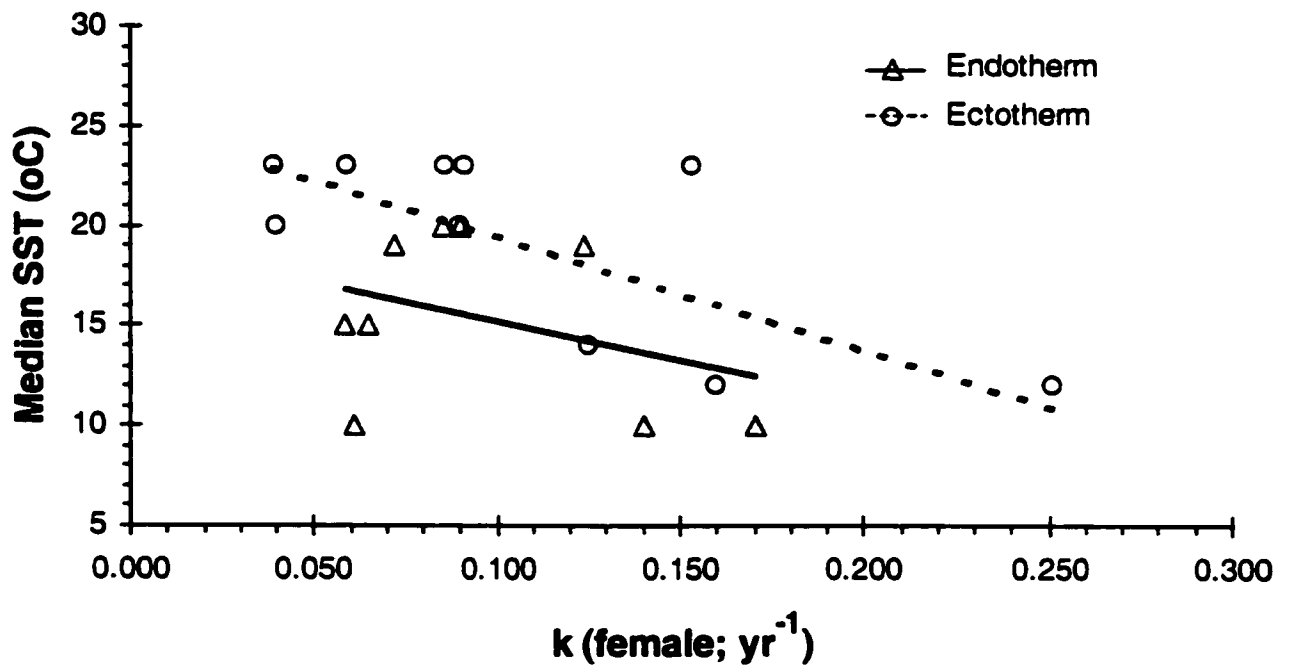
FIGURE 6.6: Comparison of growth completion rate (k) and mean gestation period of
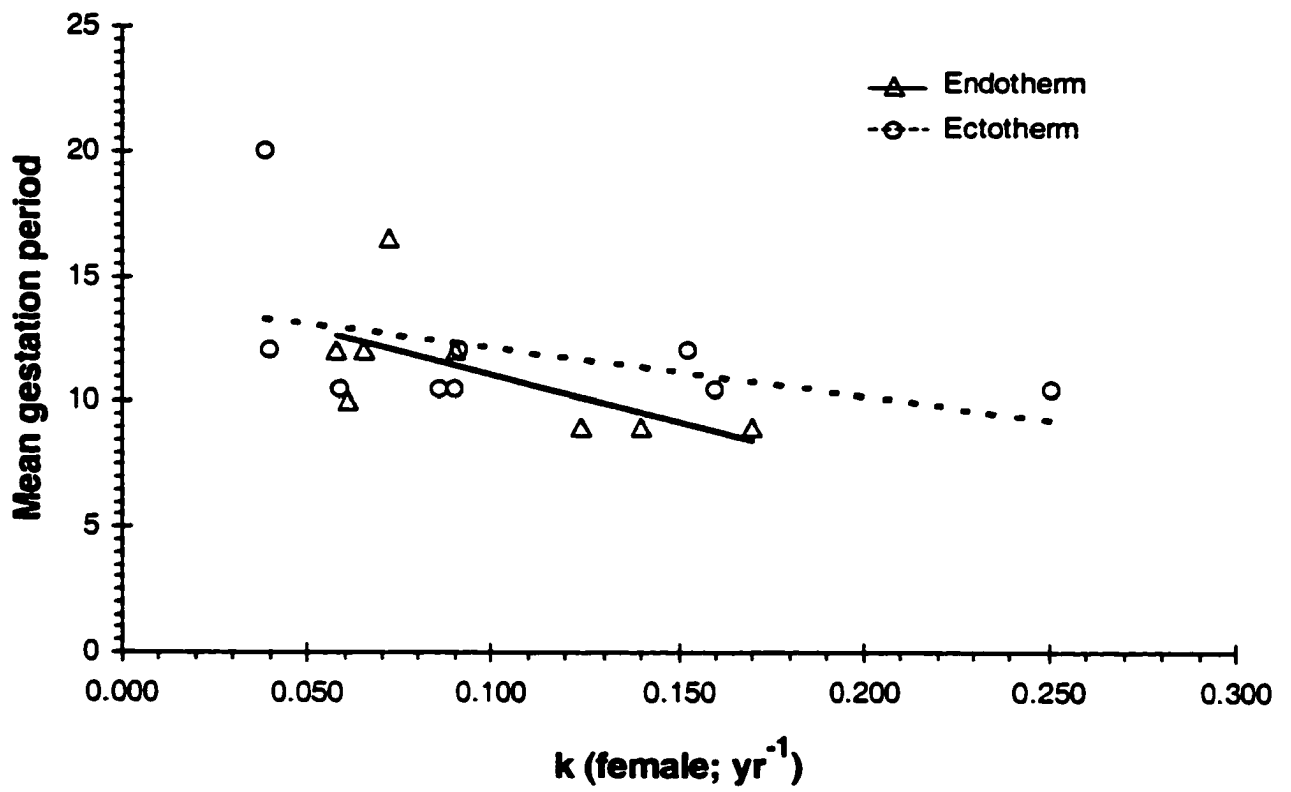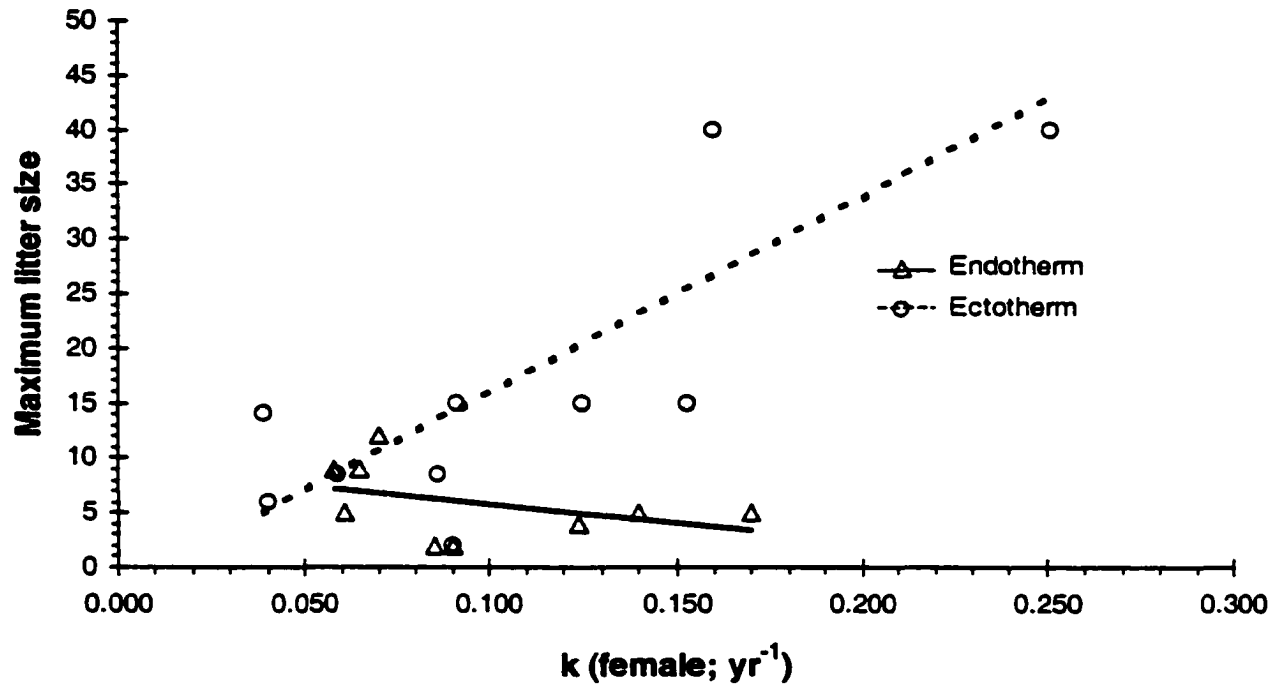
ectothermic and endothermic sharks.

FIGURE 6.7: Comparison of growth completion rate (k) and maximum litter size of

ectothermic and endothermic sharks.

examined relative to growth completions rates provided no indication that endothermic sharks achieve their maximum length at a faster rate than ectothermic sharks. However, the comparison of k with median SST at which species occur indicated that for sharks possessing similar growth completion rates, the endothermic sharks occurred in cooler water temperature regimes. This indicates that endothermy may have played an evolutionary role in maintaining growth completion rates as these species moved into new niches in temperate and boreal seas as global circulation developed during the past 60 million years. The development of global ocean circulation changed the world's oceans from a warm water environment into a much more dynamic system with boreal and temperate environments which were open to 'niche partitioning' (Valentine 1984, Block and Finnerty 1994). The Order Lamniformes can be tracked genetically and through the fossil record to the mid-Cretaceous period (124-140 million years ago) and the families Lamnidae and Alopiidae date back at least 60 million years (Applegate and Espinosa-Arrubarrena 1996, Purdy 1996, Shiria 1996, Martin 1996). As such, the timing of the development of global circulation may be the driving evolutionary pressure behind the development of endothermy in lamnid and alopiid sharks and in maintaining their ability to pursue and capture highly active prey in colder temperature regimes.

The trends presented in this Chapter also indicate that for species with growth completion rates greater than 0.10 yr^{-1}, endotherms tend to have slightly shorter gestation times and produce fewer and larger pups. Endothermy may play a role in the shorter gestation periods in cold-water species, particularly for the porbeagle and salmon sharks. Porbeagle and salmon sharks possess a kidney *rete* not found in the other endothermic sharks (see Chapter 3). This *rete* lies directly above the uteri and would provide a

warmer environment for gestating pups. This has been suggested as a possible contribution to the difference between shortfin mako and salmon shark gestation periods (Mollet et al. 1999) (see Table 6.2).

The data examined herein are obviously sensitive to minor changes in given values for the various life history traits or environmental parameters. As refined growth completion rates for several of the ectothermic and endothermic species become available, further examination of the role endothermy has played in the evolution of life history parameters and overall strategies should be made.

APPENDICES

Appendix 1: Equations for estimating natural mortality (M) used in demographic model.

1) Hoenig (1983);

$$\ln M = 1.46 - 1.01(\ln \omega)$$

where ω = maximum age

2) Pauly (1980);

$$\log M = -0.0066 - 0.279(\log L_\infty) + 0.6543(\log k) + 0.4634(\log T)$$

where L_∞ is the maximum length, k is the growth coefficient (both from the von Bertalanffy growth function) and T is the mean annual water temperature.

3) Chen & Watanabee (1989);

$$M_t = \left(\frac{1}{t_{max} - t} \right) * \left(\ln \frac{e^{k(t_{max})} - e^{kt_o}}{e^{kt} - e^{kt_o}} \right)$$

where t = age, k is the growth coefficient and t_o is the age (or time) when length is theoretically zero (both from the von Bertalanffy growth function).

4) Peterson & Wrobleski (1984);

$$M_w = 1.92(W^{-0.25})$$

where W = weight in kg.

5) Jensen k method (1996);

$$M = 1.50(k)$$

where k is the growth coefficient (from the von Bertalanffy growth function).

6) Jensen age at maturity method (1996);

$$M = 1.65/(\alpha)$$

where α is the age at first reproduction.

Appendix 2: Converting the net increase in I_α from Au and Smith (1997) into the increase in S per sub-adult age class in life history table.

Before fishing (F = 0):

$$S_0 S_1 S_2 ... S_n = I_\alpha \qquad (1)$$

where n = maximum subadult age, I_α = the net increase in sub-adult age classes.
This can be re-written as:

$$\prod_{i=0}^{n} S_i = I_\alpha \qquad (2)$$

After fishing, compensation occurs in the form of increased survivorship of sub-adult age classes, resulting in a new cumulative survival of $I_{\alpha F}$. If the net increase in survival affects all sub-adult age classes equally, then:

$$aS_0 aS_1 aS_2 ... aS_n = I_{\alpha F} \qquad (3)$$

where a = increase in S per sub-adult age class, and n = maximum sub-adult age
It follows that:

$$a^{n+1} \prod_{i=0}^{n} S_i = I_{\alpha F} \qquad (4)$$

then:

$$a^{n+1} = \frac{I_{\alpha F}}{I_\alpha} \qquad (5)$$

therefore:

$$a = {}^{n+1}\!\!\sqrt{\frac{I_{\alpha F}}{I_\alpha}} \qquad (6)$$

Appendix 3: Sources for life history parameter estimates used in Chapter 6. Camhi et al.

1999, Compagno 1984, Cortés 2000 and Compagno 2001 supplemented main sources.

Ectotherms	Main source
Carcharhinus falciformes (NWGM)	Branstetter 1987
Carcharhinus falciformes (SGM)	Cortés 2000
Carcharhinus obscurus (WNA)	Natanson et al. 1995, Romine in prep.
Carcharhinus plumbeus(WNA1)	Sminkey and Musick 1995
Carcharhinus plumbeus(WNA2)	Sminkey and Musick 1995
Carcharhinus signatus(WNA)	Branstetter 1990
Carcharias taurus (WNA)	Goldman 2002
Cetorhinus maximus (All)	Pauly 1978, Cortés 2000
Prionace glauca (ENP)	Cailliet et al. 1983
Prionace glauca (WNA)	Skomal and Natanson in press
Prionace glauca (WNP)	Tanaka et al. 1990

Endotherms	
Alopias pelagicus (WNP)	Lui et al. 1999
Alopias supercilliosus (WNP)	Lui et al. 1998
Alopias vulpinus (ENP)	Cailliet et al. 1983
Carcharodon carcharias(ENP)	Cailliet et al. 1985
Carcharodon carcharias(SWA)	Cliff and Wintner 1999
Isurus oxyrinchus (ENP)	Cailliet et al. 1983
Lamna ditropis (ENP)	Goldman 2002
Lamna ditropis (WNP)	Tanaka 1980
Lamna nasus (WNA)	Natanson et al. 2002

NWGM = northwestern Gulf of Mexico; SGM = southern Gulf of Mexico; WNA1 = western North Atlantic 1980-1981; WNA2 = western North Atlantic 1990-1992; ENP = eastern North Pacific; WNP = western North Pacific; SWA = southwestern Atlantic.

LITERATURE CITED

Anderson, S.D. and K.J. Goldman. 2001. Temperature measurements from salmon sharks, *Lamna ditropis*, in Alaskan waters. Copeia 2001:794-796.

Applegate, S.P. and L. Espinosa-Arrubarrena. 1996. The fossil history of *Carcharodon* and its possible ancestor, *Cretolamna*: A study in tooth identification. Pages 19-36 *In* A.P. Klimley and D.G. Ainley editors, Great White Sharks: The Biology of *Carcharodon carcharias*. Academic Press, San Diego.

Au, D.W. and S.E. Smith. 1997. A demographic method with population density compensation for estimating productivity and yield per recruit of the leopard shark (*Triakis semifasciata*). Can. J. Fish. Aquat. Sci. 54:415-420.

Bernal, D., Dickson, K.A., Shadwick, R.E. and Graham, J.B. 2001. Review: Analysis of the evolutionary convergence for high performance swimming in lamnid sharks and tunas. Comp. Biochem. Physiol. A. 129: 695-726.

Blagoderov, A.I. 1994. Seasonal distribution and some notes on the biology of salmon shark (*Lamna ditropis*) in the northwestern Pacific Ocean. Journal of Ichthyology 34(2):115-121. Originally published in, and translated from, Voprosy Ikhtiologii.

Block, B.A. and J.R. Finnerty. 1994. Endothermy in fishes: A phylogenetic analysis of constraints, predispositions, and selection pressures. Env. Biol. Fish. 40:283-302.

Branstetter, S. and J.A. Musick. 1994. Age and growth estimates for the sand tiger in the Northwestern Atlantic Ocean. Trans. Am. Fish. Soc. 123:242-254.

Branstetter, S. 1990. Early life-history implications of selected carcharhinoid and lamnoid sharks of the northwest Atlantic. Pages 17-28 *In* H.L. Pratt Jr., S.H. Gruber and T. Taniuchi editors, Elasmobranchs as Living Resources: Advances in the Biology, Ecology, Systematics and the Status of the Fisheries. NOAA Tech. Rep. NMFS 90.

Brodeur, R.D. 1988. Zoogeography and trophic ecology of the dominant epipelagic fishes in the northern Pacific. *In* Nemoto, T. and W.G. Percy editors, The biology of the subarctic Pacific. Proceedings of the Japan-United States of America seminar on the biology of micronekton of the subarctic Pacific. Bulletin of Ocean Research Institute, University of Tokyo, No. 26 (Part II):1-27.

Burne, R.H. 1923. Some peculiarities of the blood vascular system of the porbeagle shark, *Lamna cornubica*. Phil. Trans. Roy. Soc. London 212:209-257.

Cailliet, G.M., L.K. Martin, J.T. Harvey, D. Kusher and B.A. Weldon. 1983.

Preliminary studies on the age and growth of blue, *Prionace glauca*, common thresher, *Alopias vulpinus*, and shortfin mako, *Isurus oxyrinchus*, sharks from California waters. Pages 179-188 *In* E.D. Prince and L.M. Pulos editors, Proceedings of the international workshop on age determination of oceanic pelagic fishes: tunas, billfishes, and sharks. NOAA Tech. Rep. NMFS 8.

Camhi, M. 1999. Sharks on the line II: An analysis of Pacific state shark fisheries. National Audubon Society Publication. October 1999, 114 pp.

Campana, S.E. 1990. How reliable are growth back-calculations based on otoliths? Can. J. Fish. Aquat. Sci. 47:2219-2227.

Carey, F.G., J.G. Casey, H.L. Pratt, D. Urquhart and J.E. McCosker. 1985. Temperature, heat production, and heat exchange in lamnid sharks. Southern California Academy of Sciences, Memoirs 9:92-108.

Carey, F.G., J.M. Teal and J.W. Kanwisher. 1981. The visceral temperatures of mackerel sharks (Lamnidae). Physiol. Zool. 54:334-344.

Carlander, K.D. 1969. Handbook of freshwater fishery biology, volume 1. Iowa Univ. Press, Ames.

Casey, J.G. and N.E. Kohler. 1990. Long distance movements of Atlantic sharks from the NMFS cooperative shark tagging program. Pages 87-91 *In* S.H. Gruber editor, Discovering sharks. American Littoral Society, New Jersey.

Castro, J.I., C.M. Woodley, and R.L. Brudek. 1999. A preliminary evaluation of the status of shark species. FAO Fisheries Technical Paper. No. 380. Rome, FAO, 72 p.

Caswell. H. 2001. Matrix population models: construction, analysis, and interpretation. 2nd edition. Sinauer, Sunderland, MA.

Caughley, G. 1977. Analysis of vertebrate populations. Wiley, New York, NY.

Cerrato, R.M. 1990. Interpretable statistical tests for growth comparisons using parameters in the von Bertalanffy equation. Can. J. Fish. Aquat. Sci. 47:1416-1426.

Chen, S.B. and S. Watanabe. 1989. Age dependence of natural mortality coefficient in fish population dynamics. Nippon Suisan Gakkaishi 55(2):205-208.

Compagno, L.J.V. 2001. Sharks of the World. An annotated and illustrated catalogue of shark species known to date. Volume 2. Bullhead, mackerel and carpet sharks (Heterodontiformes, Lamniformes and Orectolobiformes). FAO species catalogue for fishery purposes, No. 1, Vol. 2 Rome, FAO. 269 p.

Compagno, L.J.V. 1990. Shark exploitation and conservation. Pages 391-414 *In* H.L. Pratt Jr., S.H. Gruber and T. Taniuchi, editors, Elasmobranchs as Living

Resources: Advances in the Biology, Ecology, Systematics and the Status of the Fisheries. NOAA Tech. Rep. NMFS 90.

Compagno, L.J.V. 1984. FAO species catalogue. Vol. 4. Sharks of the World. An annotated and illustrated catalogue of shark species known to date. Part 1. Hexanchiformes to Lamniformes. FAO Fisheries Synopsis, (125)4, Pt.1, 249 p.

Cortés, E. 2002. Incorporating uncertainty into demographic modeling: application to shark populations and their conservation. Conserv. Biol. 16(4):1-15.

Cortés, E. 2000. Life history patterns and correlations in sharks. Rev.Fish. Sci. 8(4):299-344.

Cortés, E. 1999. A stochastic stage-based population model of the sandbar sharks in the western North Atlantic. Pages 115-136 *In* J.A. Musick, editor, Life in the slow lane: Ecology and conservation of long-lived marine animals. Symposium 23. American Fisheries Society, Bethesda, MD.

Cortés, E. and G.R. Parsons. 1996. Comparative demography of two populations of the bonnethead shark (*Sphyrna tiburo*). Can. J. Fish. Aquat. Sci. 53::709-718.

De Kroon, H., J. van Groenendael, and J. Ehrlén. 2000. Elasticities: a review of methods and model limitations. Ecology 81:607-618.

Ebert, T.A. 1999. Plant and animal populations: methods in demography. Academic Press, San Diego, CA.

Eschricht, D.F. and J. Müller. 1835a. Über die arteriösen and venösen Wundernetze an der Leber und einen merkwürdigen Bau dieses Organes beim Thunfische, *Thynnus vulgaris*. Physikal. Abhandl. d. K Wissensch. Berlin, pp. 1-32.

Eschricht, D.F. and J. Müller. 1835b. Nachtrag zu der Abhandlung der Herren Eschricht und Müller über die Wundernetze an der Leber des Thunfisches: Über die Wundernetze am Darmkanal des *Squalus vulpes* L., *Alopecias vulpes* Nob. Physikal. Abhandl. d. K Wissensch. Berlin, pp. 325-328.

Evans, G.T., and J.M. Hoenig. 1998. Testing and viewing symmetry in contingency tables, with application to readers of fish ages. Biometrics 54:620-629.

Francis, R.I.C.C. 1990. Back-calculation of fish length: a critical review. J. Fish Biol. 36:883-902.

Fudge, D.S. and E.D. Stevens. 1996. The visceral *retia mirabilia* of tuna and sharks: an annotated translation and discussion of the Eschricht and Müller 1835 paper and related papers. Guelph Ichthyol. Rev. 4:1-92.

Gallucci, V.F., L. Hulbert and B. Wright. 2002a. Shark abundance changes: an unexpected explosion. Abstracts of the 168th Annual Meeting of the American Association for the Advancement of Science, Boston, MA, February 2002.

Gallucci, V.F. and B. Wright. 2002b. Sharks, pinnipeds and ecosystem dynamics. Abstracts of the 168th Annual Meeting of the American Association for the Advancement of Science, Boston, MA, February 2002.

Garland, T. and P.A. Carter. Evolutionary physiology. Annu. Rev. Physiol. 56:579-621.

Gilmore, R.G. 1993. Reproductive biology of lamnoid sharks. Env. Biol. Fish. 38:95-114.

Gilmore, R.G., J.Q. Dodrill and P.A. Linley. 1983. Reproduction and embryonic development of the sand tiger shark, Odontaspis taurus (Rafinesque). Fish. Bull. 81(2):201-225.

Goldman, K.J. and J.A. Musick. In press. Biology of the Salmon Shark, Lamna ditropis. In: Sharks of the Open Ocean. E.K. Pikitch and M. Camhi eds. Blackwell Scientific.

Goldman, K.J. and Human B. 2002. Salmon shark, Lamna ditropis In Fowler, S.L., M. Camhi, G. Burgess, S. Fordham and J. Musick editors, Sharks, rays and chimaeras: the status of the chondrichthyan fishes. IUCN/SSG Shark Specialist Group. IUCN, Gland, Switzerland, and Cambridge, UK.

Goldman, K.J. 2001. Sharks and shark bycatch in Alaska State and Federal Waters. In Pat Livingston editor, Ecosystems Considerations for 2002. North Pacific Fishery Management Council, 605 W. 4th Ave., Suite 306, Anchorage, AK 99501-2252.

Goldman, K.J. 1997. Regulation of body temperature in the white shark, Carcharodon carcharias. Journal of Comparative Physiology B. 167:423-429.

Goldman, K.J., S.D. Anderson, J.E. McCosker and A.P. Klimley. 1996. Temperature, swimming depth, and movements of a white shark at the South Farallon Islands, California. Pages 111-120 In A.P. Klimley and D.G. Ainley editors, Great White Sharks: The Biology of Carcharodon carcharias. Academic Press, San Diego.

Goodman, D. 1982. Optimal life histories, optimal notation, and the value of reproductive value. Amer. Nat. 119(6):803-823.

Gorbatenko, K.M. and Cheblukova L.V. 1990. Environment conditions and fish species composition in the epipelagic zone of the Okhotsk Sea suring summer. Journal of Ichthyology 30, 89-100. Originally published in, and translated from, Voprosy Ikhtiologii 30, 21-30.

Graham, J.B., H. Dewar, N.C. Lai, W.R. Lowell, and S.M. Arce. 1990. Aspects of shark swimming performance determined using a large water tunnel. J. Exp. Biol. 151:175-192.

Gruber, S.H., J.R.C. De Marignac and J.M. Hoeing. 2001. Survival of juvenile lemon sharks at Bimini, Bahamas, estimated by mark-depletion experiments. Trans. Am. Fish. Soc. 130:376-384.

Hamlett, W. C. 1999. Male reproductive system. Pages 444-470 *In* Hamlett, W.C. editor, Sharks, skates and rays: the biology of elasmobranch fishes. Johns Hopkins Press, Baltimore, MD.

Hamlett, W. C. and T.J. Koob. 1999. Female reproductive system. Pages 398-443. *In* Hamlett, W.C. editor, Sharks, skates and rays: the biology of elasmobranch fishes. Johns Hopkins Press, Baltimore, MD.

Heppell, S.S., C. Pfister and H. DeKroon. 2000a. Elasticity analysis in population biology: methods and applications. Ecology 81:605-606.

Heppell, S.S., H. Caswell and L.B. Crowder. 2000b. Life histories and elasticity patterns: perturbation analysis for species with minimal demographic data. Ecology 81:654-665.

Heppell, S.S., L.B. Crowder and T.R. Menzel. 1999. Life table analysis of long-lived marine species, with implications for conservation and management. Pages 137-148 *In* J.A. Musick, editor, Life in the slow lane: Ecology and conservation of long-lived marine animals. Symposium 23. American Fisheries Society, Bethesda, MD.

Heppell, S.S. 1998. Application of life-history theory and population model analysis to turtle conservation. Copeia 1998:367-375.

Hickman, C.P., L.S. Roberts and F.M. Hickman. 1984. Integrated principles of zoology. Seventh edition. Times Mirror/Mosbey College Pub. St. Louis, MO.

Hinton, D.E. 1990. Histological techniques. Pages 191-209 *In* C.B. Schreck and P.B. Moyle editors, Methods for fish biology. American Fisheries Society, Bethesda, MD.

Hochachka, P.W., W.C. Hulbert, and M. Guppy. 1978. The tuna power plant and furnace. Pages 153-181 *In* G.D. Sharp and A.E. Dizon editors, The physiological ecology of tunas, Academic Press, New York.

Hoeing, J.M., M.J. Morgan and C.A. Brown. 1995. Analyzing differences between two age determination methods by tests of symmetry. Can. J. Fish. Aquat. Sci. 52:364-368.

Hoenig, J.M., and S.H. Gruber. 1990. Life-history patterns in elasmobranchs: Implications for fisheries management. Pages 1-16 *In* H.L. Pratt Jr., S.H. Gruber and T. Taniuchi, editors, Elasmobranchs as Living Resources: Advances in the Biology, Ecology, Systematics and the Status of the Fisheries. NOAA Tech. Rep. NMFS 90.

Hoenig, J.M. 1983. Empirical use of longevity data to estimate mortality rates. Fish. Bull. 82:898-903.

Holden, M.J. 1977. Elasmobranchs. Pages 187-214 *In* J.A. Gulland editor, Fish population dynamics. John Wiley and Sons, New York, NY.

Holden, M.J. 1974. Problems in the rational exploitation of elasmobranch populations and some suggested solutions. Pages 117-138 *In* F.R. Jones editor, Sea Fisheries Research. Halstead Press,J. Wiley and Sons, New York.

Iino, R. 1939. Migration of salmon sharks. Suisan Kenkyu-shi 34, 171-173. (In Japanese.)

JAMARC. 1980. The development of the shark resources in the North Pacific Ocean, fiscal years 1979 and 1980. Japan Marine Fishery Resources Center (JAMARC) Kaihatsu News (Development News) No. 11, p. 17-25, August 1980. [English translation #63, by Tamio Otsu, NMFS/SWFC, Honolulu, HI, June 1982.

Jensen, A.L. 1996. Beverton and Holt life history invariants result from optimal tradeoff of reproduction and survival. Can. J. Fish. Aquat. Sci. 53:820-822.

Kimura, D.K. 1980. Likelihood methods for the von Bertalanffy growth curve. Fish. Bull. 77: 765-773.

Kosugi, H. and H. Tsuchisaki. 1950. On the longline fishing of salmon sharks in the Japan Sea off Hokkaido. Hokusuisi Geppo, 17(1):14-20. In Japanese.

Krebbs, C.J. 1985. Ecology: the experimental analysis of distribution and abundance. 3rd edition. Harper and Row Pub., New York, NY.

Lai, N.C., K.E. Korsmeyer, S. Katz, D.B. Holts, L.M. Laughlin and J.B. Graham. 1997. Hemodynamics and blood properties of the shortfin mako shark (*Isurus oxyrinchus*). Copeia 1997:424-428.

Last, P.R. and J.D. Stevens. 1994. Sharks and Rays of Australia. CSIRO Division of Fisheries, Australia, 513 p.

Lawless, J.F. 1982. Statistical models and methods for lifetime data. Wiley, New York, NY.

Lowe, C.G. and K.J. Goldman. 2001. Thermal and bioenergetics of elasmobranchs: bridging the gap. In: T.C. Tricas and S.H. Gruber (eds.) The Behavior and Sensory Biology of Sharks and Rays: State of the Art and Future Direction. American Elasmobranch Society Symposium, Special Volume in Honor of Dr. D.R. Nelson. Env. Biol. Fish. 60:251-266.

Liu, K, C. Chen., Liao, T. and Joung, S. 1999. Age, growth, and reproduction of the pelagic thresher shark *Alopias pelagicus* in the northwestern Pacific. Copeia 1999(1):68-74.

Liu, K, Chiang, P., and Chen, C. 1998. Age and growth estimates of the bigeye thresher shark, *Alopias superciliosus*, in northeastern Taiwan waters. Fish. Bull.96:482-491.

Martin, A.P. 1996. Systematics of the Lamnidae and the origination time of *Carcharodon carcharias* inferred from the comparative analysis of mitochondrial

DNA sequences. Pages 49-53 *In* A.P. Klimley and D.G. Ainley editors, Great White Sharks: The Biology of *Carcharodon carcharias*. Academic Press, San Diego.

Mathsoft Inc. 2000. S-Plus 2000 Professional Release 1. Mathsoft Inc., Seattle, WA.

McCosker, J.E. 1987. The white shark, *Carcharodon carcharias*, has a warm stomach. Copeia (1):195-197.

McKinnell, S. and M.P. Seki. 1998. Shark bycatch in the Japanese high seas squid driftnet fishery in the North Pacific Ocean. Fish. Res. 39:127-138.

McKinnell, S. and B. Waddell. 1993. Associations of species caught in the Japanese large scale pelagic squid driftnet fishery in the central North Pacific Ocean: 1988-1990. Int. North Pac. Fish. Comm. Bull. 53(2):91-109.

Media Cybernetics. 1999. Optimus, version 6.5. Media Cybernetics, Silver Spring, MD.

Mollet, H.F. and G.M. Cailliet. 2002. Comparative populations demography of elasmobranchs using life history tables, Leslie matrices and stage-based models. Mar. Freshwater Res. 53:503-516.

Mollet, H.F., G. Cliff, H.L. Pratt Jr. and J.D. Stevens. 2000. Reproductive biology of the female shortfin mako, *Isurus oxyrinchus* Rafinesque, 1810, with comments on the embryonic development of lamnoids. Fish. Bull. 98:299-318.

Musick, J.A. M.M. Harbin, S.A. Berkeley, G.H. Burgess, A.M. Eklund, L. Findley, R.G. Gilmore, J.T. Golden, D.S. Ha, G.R. Huntsman, J.C. McGovern, S.J. Parker, S.G. Poss, E. Sala, T.W. Schmidt, G.R. Sedberry, H. Weeks and S.G. Wright. 2000. Marine, estuarine, and diadromous fish stocks at risk of extinction in North America (exclusive of Pacific salmonids). Fisheries 25(11):6-30.

Musick, J.A. 1999. Ecology and conservation of long-lived marine animals. Pages 1-10 *In* J.A. Musick editor, Life in the slow lane: Ecology and conservation of long-lived marine animals. American Fisheries Society Symposium 23, Bethesda, MD.

Musick, J.A., J. Gelsleichter, R.D. Grubbs and K.J. Goldman. 1998. Virginia Institute of Marine Science Shark Ecology Program, J.A. Musick, J. Gelsleichter, R.D. Grubbs, and K.J. Goldman, editors. Appendix SB-IV-13 *in* Report of the 1998 Shark Evaluation Workshop. NOAA/NMFS, Panama City, FL.

Musick, J.A., S. Branstetter and J.A. Colvocoresses. 1993. Trends in shark abundance from 1974-1991 for the Chesapeake Bight region of the U.S. mid-Atlantic coast. NOAA Tech. Rep. NMFS 115:1-18.

Nagasawa, K. 1998. Predation by salmon sharks (*Lamna ditropis*) on Pacific salmon (Oncorhynchus spp.) in the North Pacific Ocean. Bulletin of the North Pacific Anadromous Fish Commission, No. 1, 419-433.

Nakano, H. and Nagasawa K. 1996. Distribution of pelagic elasmobranchs caught by salmon research gillnets in the North Pacific. Fisheries Science 62(5), 860-865.

Nakano, H. and Nagasawa K. 1994. Distribution of the salmon shark (*Lamna ditropis*) in the North Pacific Ocean and Bering Sea. Salmon Report Series, No. 37, 226-237. National Research Institute of Far Seas Fisheries, Shimizu Japan.

Naylor, G.J.P., A.P. Martin, E.G. Mattison and W.M. Brown. 1997. Interrelationships of Lamniform sharks: Testing phylogenetic hypotheses with sequence data. Pages 199-217 *In* Kocher, T.D. and C. Atepien editors, Molecular systematics of fishes. Academic Press, San Diego, CA.

Neave, F. and Hanavan M.G. 1960. Seasonal distribution of some epipelagic fishes in the Gulf of Alaska region. Journal of the Fisheries Research Board of Canada 17(2), 221-233.

NMFS. 1999. Final fishery management plan for Atlantic tunas, swordfish and sharks. NOAA/NMFS, U.S. Dept. of Commerce. April 1999, Silver Spring, MD.

NMFS. 1998. Report of the 1998 Shark Evaluation Workshop. NOAA/NMFS, Panama City, FL.

Pauly, D. 1980. On the interrelationships between natural mortality, growth parameters, and mean environmental temperature in 175 fish stocks. J. de Counceil International pour l'exploration de la Mer. 39:175-192.

Paust, B. and R. Smith. 1989. Salmon shark manual: the development of a commercial salmon shark, *Lamna ditropis*, fishery in the North Pacific. University of Alaska Sea Grant College Program, Report 96-01, revised 1989.

Peterson, I. and J.S. Wroblewski. 1984. Mortality rates of fishes in the pelagic ecosystem. Can. J. Fish. Aquat. Sci. 41:1117-1120.

Pratt, H.L. Jr. 1993. The storage of spermatozoa in the oviducal glands of western North Atlantic sharks. Env. Biol. Fish. 38:139-149.

Pratt, H.L. Jr. 1988. Elasmobranch gonad structure: a description and survey. Copeia 1988:719-729.

Pratt, H.L. Jr. and S. Tanaka. 1994. Sperm storage in male elasmobranchs: a description and survey. J. Morphol. 219:297-308.

Pratt, H.L. Jr. and J.G. Casey. 1983. Age and growth of the shortfin mako, *Isurus oxyrinchus*, using four methods. Can. J. Fish. Aquat. Sci. 40:1944-1957.

Purdy, R.W. 1996. Paleoecology of fossil white sharks. Pages 67-79 *In* A.P. Klimley and D.G. Ainley editors, Great White Sharks: The Biology of *Carcharodon carcharias*. Academic Press, San Diego.

Quinn. T. J. and R. B. Deriso. 1999. Quantitative fish dynamics. Oxford University Press. New York, NY.

Ricker, W.E. 1992. Back-calculation of fish lengths based on proportionality between scale and length increments. Can. J. Fish. Aquat. Sci. 49:1018-1026.

Robinson, S.M.C. and G.S. Jamieson 1984. Report on a Canadian commercial fishery for flying squid using drifting gill nets off the coast of British Columbia. Can. Industry Rep. Fish. and Aquatic Sci. 150:25pp.

Roff, D.A. 1982. The evolution of life histories: theory and analysis. Chapman and Hall, New York, NY.

Sano, O. 1962. The investigation of salmon sharks as a predator on salmon in the North Pacific, 1960. Bulletin of the Hokkaido Regional Fisheries Research Laboratory, Fisheries Agency, No. 22, 68-82. (In Japanese.)

SAS Institute Inc. 1999. Version 8.0. Statistical Analysis Systems Institute, Inc., Cary, NC.

Shirai, S. 1996. Phylogenetic interrelationships of neoselachians (Chondrichthyes: Euselachii). Pages 9-34 In Stiassney, M.L.J., L.R. Parenti and G.D. Johnson editors, Interrelationships of Fishes. Academic Press, San Diego, CA.

Sminkey, T.R. and J.A. Musick. 1995. Age and growth of the sandbar shark, *Carcharhinus plumbeus*, before and after population depletion. Copeia 1995:871-883.

Smith, S.E., D.W. Au and C Show. 1998. Intrinsic rebound potentials of 26 species of Pacific sharks. Mar. Freshwater Res. 49: 633-678.

Smith R.L. and D. Rhodes. 1983. Body temperature of the salmon shark, *Lamna ditropis*. Journal of the Marine Biology Association of the U.K. 63:243-244.

Strasburg, D.W. 1958. Distribution, abundance, and habits of pelagic sharks in the central Pacific Ocean. U.S. Fisheries Bulletin 58, 335-361.

Tanaka, S. 1980. Biological investigation of Lamna ditropis in the north-western waters of the North Pacific. In: Report of investigation on sharks as a new marine resource (1979). Published by: Japan Marine Fishery Resource Research Center, Tokyo [English abstract, translation by Nakaya].

Valentine, J.W. 1984. Climate and evolution in the shallow sea. Pages 265-277 In P. Brenchley editor, Fossils and Climate. John Wiley and Sons Ltd.

Walker, T.I. 1998. Can shark resources be harvested sustainably? A question revisited with a review of shark fisheries. Mar. Freshwater Res. 49:553-572.

Walker, T.I. 1992. Fishery simulation model for sharks applied to the gummy shark, *Mustelus antarcticus* Gunther, from Southern Australian waters. Aust. J. Mar. Freshwater Res. 43:195-212.

Wintner, S.B. and G. Cliff. Age and growth determination of the white shark, *Carcharodon carcharias*, from the east coast of South Africa. Fish. Bull. 97:153-169.

Wourms, J.P. 1977. Reproduction and development in chondrichthyan fishes. Amer. Zool. 17:379-410.

VITA

Kenneth James Goldman

Born January 25, 1963 in Denver, Colorado. Graduated from Manuel High School,

Denver, Colorado in 1981. Started undergraduate education at Metro State University,

Denver Colorado, 1986, transferred to San Francisco State University (SFSU), San

Francisco, in 1989. Graduated from SFSU Magna Cum Laude with Bachelor of Science

degree with emphasis on Marine Biology and Limnology in 1993. Entered Master of

Arts program at SFSU in 1993, graduated with M.A. in Biology in 1996. Entered the

doctoral program at the Virginia Institute of Marine Science, College of William and

Mary in 1996. Defended Ph.D. in August 2002. Became a postdoctoral fellow and part-

time lecturer at California State University, Long Beach in August 2002.